COALESCENCE OF SECONDARY DISPERSIONS

IN FIBROUS BEDS

by

NAEL GEORGE SHALHOUB

A thesis submitted to the University of Aston in Birmingham
for the degree of Doctor of Philosophy

DEPARTMENT OF CHEMICAL ENGINEERING,
THE UNIVERSITY OF ASTON IN BIRMINGHAM. October 1975.

TO MY MOTHER AND FATHER

SUMMARY

A study has been made of the coalescence of secondary dispersions in a fibrous bed. The literature pertaining to the formation, hydrodynamic behaviour and methods of separation of droplets less than one hundred micrometres in diameter has been reviewed with particular reference to fibrous bed coalescers. The main operating parameters were identified as inlet drop size distribution, phase ratio, superficial velocity and the thickness and voidage of the bed.

A recirculatory rig with interchangeable fibrous bed pads was designed and operated with toluene-water dispersions generated by a combination of centrifugal pumps. Inlet drop sizes were analysed using a Coulter Counter and outlet drops were sized photographically. A novel technique, involving conductivity measurements at different planes in the bed, was developed to measure hold up distribution.

Single phase flow and two phase flow pressure drops were correlated by a Blake-Kozeny type equation. Exit drop size was independent of inlet drop size distribution and phase ratio but a function of superficial velocity and packing thickness. Average bed hold up was independent of inlet drop size distribution and phase ratio, but decreased with increase in superficial velocity. Hold up was not evenly distributed in the bed, the highest value occurred at the inlet followed by a sharp drop at approximately 1.2×10^{-2} m. Hold up remained constant throughout the rest of the bed until the exit plane, where it increased.

From the results, a mechanism is postulated involving:

(a) Capture of the inlet drops followed by interdrop coalescence until an equilibrium value is reached.

(b) Equilibrium size droplets flowing as rivulets through the intermediate portion of the bed, and

(c) Each rivulet forms droplets at the exit face, which detach by a 'drip point' mechanism.

Key words: 'Coalescence' and 'Fibrous beds'

ACKNOWLEDGEMENTS

The author wishes to express his sincere thanks and gratitude to:

Professor G.V. Jeffreys,

for providing the facilities for this research and for his helpful guidance, encouragement and personal interest in the supervision of this project.

Dr. C.J. Mumford,

for his constant advice and interest throughout each phase of this study.

The University of Aston in Birmingham,

for awarding me a Studentship to pursue this research.

The members of the Technical Staff and Photographic Section of the Department of Chemical Engineering.

Special thanks are extended to Miss R. Lyons for assistance in checking the manuscript, and Miss N. Freeman for typing the thesis with exceptional competence.

LIST OF CONTENTS

CHAPTER 1

INTRODUCTION

Droplet dispersions resulting from the mixing of immiscible, or partially miscible, liquid-liquid systems are widely encountered industrially. Examples occur in liquid-liquid extraction, the contamination of aviation fuel by water and in the desalting and de-watering of crude oil. Effluent water from factories also commonly contains an oil phase. In the absence of stabilizers, these dispersions can be defined as:

(a) Primary Dispersions which are arbitrarily characterised by droplets of mean diameter greater than 100×10^{-6} m. In such dispersions, the droplets will settle under gravity due to buoyancy and given sufficient time, they collect at a phase boundary where drop-drop and drop-interface coalescence occurs.

or

(b) Secondary Dispersions: Such dispersions are cloudy in appearance and are often referred to as hazes. These consist of microscopic droplets of diameter generally less than 100×10^{-6}m. They may result from powerful agitation in mixers or pumps or in a variety of other ways, e.g. 'critical temperature emulsification', super-saturated vapour condensation or alternate heating and cooling. The separation of these dispersions by simple settling is very slow, and may take days or even weeks; settling rates of 0.23×10^{-6} m s^{-1} are common. Although there can be no clear boundary between primary and secondary dispersions in terms of drop size, because system physical properties and phase impurities affect separation rates, secondary dispersions are conventionally taken as droplets below 100×10^{-6} m in diameter.

It is often necessary, in the interests of ecology, safety or economics to separate these dispersions. The separation of primary dispersions does not in general present any serious problems. However with secondary dispersions it is necessary to increase the settling rates. A major method involves coalescence by flow through a fibrous bed. This may be the most attractive since it is efficient, inexpensive and continuous. The bed does not function as a filter since it operates under steady state conditions and the drops are not retained within the bed. Droplets are held on the fibres where they can grow by coalescence until a size is reached after which they are released to settle rapidly under gravity. Since the bed does not act as a sieve, the pore size of the bed does not have to be equal to the inlet drop size.

Unfortunately, at the present time there is no accepted theory to explain the coalescence mechanism within a fibrous bed and design is by trial and error. Therefore in this study an attempt has been made to identify the coalescence mechanisms involved by means of experimental work and analysis of a model system. In addition the conflicting claims as to major design and operating parameters, viz, inlet drop size, phase ratio, dispersion superficial velocity and bed thickness have been critically examined.

CHAPTER 2

METHODS OF SEPARATION

Various methods are used to coalesce secondary dispersions into large drops so that the dispersed phase can ultimately be separated by gravity settling. These include the addition of chemical coagulants, the use of an alternating electrical field, heat treatment, centrifugation and contact with solid surfaces. These are reviewed below.

2.1 ADDITION OF CHEMICALS

Chemical additives may assist in any of the following ways:

(a) By inversion of the phases, to convert a more readily coalesced material into the dispersed phase.

(b) By neutralisation of surface charges.

or

(c) By dissolution of the protective film surrounding each droplet.

Oil-in-water emulsions may be broken by slightly acidifying the mixture and then coagulating with aluminium or calcium salts[5]. A different technique, albeit restricted to a polar dispersed phase, involves the addition of further dispersed phase, roughly equivalent in volume to four times the emulsion volume[6]. This is reported to aid the removal of water droplets from benzene, but not the reverse. However the addition of hydrochloric acid renders both phases polar and a benzene-in-water system can then be separated by the addition of excess benzene. The glycerine-nitrobenzene system is exceptional in that although both components are polar dispersed nitrobenzene cannot be recovered by dilution.

Hayes et al[1] have described the addition of demulsifying agents which enable crude petroleum to be desalted prior to refining. Waterman[7] also described the effect of surface active agents which migrated to the oil-water interface, ruptured the skin and/or displaced the stablizer back

into the oil. The added molecule was of such dimensions, in such limited concentration and so arranged at the interface that film quality and thickness were drastically changed. The synthetic material caused the natural skin to recede from part or all of the interface forming a thin film which could be broken by the attractive intermolecular forces at very close distances.

One disadvantage of chemical additives is the possibility of the liquid system becoming contaminated. Care is therefore needed when adding these substances. Furthermore, the presence of surfactants, which reduce the interfacial tension between the liquids in the emulsion, could cause harmful effects not only be producing finer droplets, but also by forming surface coatings on coalescer elements, thus preventing them from functioning correctly[4].

This method also suffers from the disadvantages of high cost and technical and practical limitations in its application. Reproducibility of breaking rate could only be obtained with a high degree of control. Results varied, dependent upon traces of impurities, slight differences in amounts of impurities, the quantity of air bubbles drawn into the system during agitation, and with variation in the type and intensity of agitation. Clearly it would be impossible to control all these variables in industrial scale operations.

2.2 CENTRIFUGATION

Substitution of centrifugal for gravitational force can promote rapid continuous sedimentation of the dispersed phase. Therefore centrifuges are used extensively in refineries and on board ship, either for complete removal of a contaminant including fine solid particles or to increase the rate of separation of two liquids with a low density

difference, high viscosity of the continuous phase, or a small drop size.

Two main types are available:

(a) The Hollow-Bowl centrifuge, which has the advantage of simplicity and ease of cleaning. It consists of a long tube of relatively small diameter, for example 0.12 m, which revolves at high speeds of 250 revs s^{-1} or more. This generates large centrifugal forces with a high ratio of travel to settling distance[9].

(b) The Disc-Bowl centrifuge: This contains a number of conical discs which rotate with the bowl. These are designed to reduce the settling distance and for cases when the light liquid is dispersed. The centrifugal force is applied to a film of the liquid less than 0.13×10^{-2} m thick. The nature of the liquid to be centrifuged determines the spacing between the discs, but the total length of travel for the liquid in this space may be 200 to 250 times the film thickness, e.g. up to 20×10^{-2} to 25×10^{-2} m. Recent designs permit operation under pressures up to 1.0×10^{6} Nm^{-2} [10].

The efficiency of any centrifugal separator may be improved by a reduction in the liquid flow rate to the bowl, thus increasing the mean residence time. The U.S. Navy developed a unit for the purification of JP-5 jet fuel in order to prevent engine failure. Since this fuel had a higher specific gravity and viscosity than aviation gasoline, problems arose in the removal of water and solids.

Centrifuges are relatively expensive machines with both high capital and operating costs. Consequently their use has been restricted to military applications such as the purification of jet fuel. They are used in ordinary chemical processes only when low residence time is

essential or when phase separation is difficult; examples therefore arise in pharmaceutical and radiological processes.

2.3 ELECTROSTATIC COALESCERS

Electrostatic coalescers are used mainly in the petroleum industry in the purification of crude oil from its connate sediments and corrosion inducing salts such as $MgCl_2$, thus reducing corrosion and fouling of distillation equipment. Catalyst poisons such as sodium, iron and arsenic are removed by electrostatic precipitation of the crude oil into which about 5% fresh water has been dispersed, i.e. desalting[12]. Electrostatic coalescers have been used to increase the purity of Uranium extract by reducing the entrainment of aqueous liquid[13] and in mixer-settlers to separate emulsions formed in liquid/liquid systems[16].

The emulsion is passed through a settling vessel containing two or more electrodes arranged as vertical parallel plates; one is grounded to the vessel wall and the other insulated from the vessel and suspended into the flowing liquid. If the top phase in the settler can act as a conductor, insulation of the electrodes is necessary. Otherwise non-insulating electrodes may be used. Alternating current fields of 78.74 to 157.48 kVm^{-1} are common and the rapid movement of the droplets thus produced may contribute to the collision rate[9]. Direct currents at much lower voltages are less commonly used.

Two mechanisms promote the separation of dispersions in liquids of low conductivity due to the applied electrical field[7,11]:

(a) Dipole Coalescence

Forces between particles due to the acquisition of an induced dipole in an a.c. or d.c. field. These occur at high concentrations of the

dispersed phase but cease at concentrations below 0.1% for a single stage unit, due to a decrease in efficiency as the population of uncoalesced droplets decreases.

(b) Electrofining

Forces resulting from the interactions between a unidirectional applied field and particles having a net charge.

The first mechanism is more general since it results from the application of either an alternating or a unidirectional field. Hence the particle may carry an induced dipole even though it has a net charge and is responsive by electrophoresis. Generally systems whose conductivity is greater than 10^{-10} ohm^{-1}, such as crude oil, coalesce in an a.c. field just as well as in a d.c. field. This suggests that dipole coalescence is the predominant mechanism.

Pearce[15] found that when water dispersed in a nonconducting continuous phase stabilized by ions was subjected to an electrical field, the droplets became polarized and aligned into chains along the lines of force. The attractive coalescing force, F', between two aligned drops of equal size is thus given by [11]:

$$F' = 6KE'^2 r^2 (r/d_o)^4 \quad \ldots\ldots\ldots\ldots\ldots\ldots\ldots \quad 2.3.1$$

The effect of drop radius may be illustrated by considering drops of 0.250×10^{-6} m which coalesce to 0.25×10^{-2}m before they fall from the field under gravity. The force of coalescence due to an increase in r^2 is 10^8 times that at the start. Clearly therefore, the electrostatic field is a versatile and effective means of separating one type of liquid from another.

For a given field strength there is a limitation on the size to

which the drops may coalesce. This is due to the tendency of electrically charged drops to redisperse, forming smaller stable drops[14]. The condition necessary for stability is given by[11]:

$$E_{cr} \leq k(\sigma/r)^{\frac{1}{2}} \quad \ldots\ldots\ldots\ldots\ldots\ldots\ldots\ldots \quad 2.3.2$$

To avoid such effects it is necessary to reduce the coalescing gradient as drop size increases.

Recently there has been great interest in electrical devices capable of coalescing water, but these suffer from disadvantages such as high capital and operating costs.

2.4 CONTACT WITH SOLID SURFACES

This phenomena is best considered in two sections, viz, surface coalescers; in which coalescence occurs on the surface of a membrane and depth coalescers in which coalescence occurs within the porous material.

2.4.1 Surface Coalescers

Surface coalescence is sometimes referred to as 'Interfacial Tension Separation', or 'Stripping', since any porous membrane is pervious to the flow of any liquid under certain conditions, provided the membrane capillary is larger than the liquid's molecular size. Conversely, any porous media is impervious to the flow of any liquid under certain other conditions. Whether a porous membrane is pervious or impervious to the flow of a particular liquid depends primarily on the following conditions:

(a) The interfacial tension value between the two liquids.

(b) The size of the maximum opening in the pervious membrane.

(c) The degree of wetting, non-wetting or preferential wetting of the membrane by the two liquids. This is discussed in more detail in Section 3.5.

(d) The pressure drop across the membrane. If the operating pressure exceeds a critical value, the membrane ruptures, causing incomplete separation.

The maximum safe operating pressure for any given liquid-liquid separatory system, across a system of circular capillaries of a known maximum capillary radius, can be calculated on the basis that the force which tends to cause rupture of the membrane is a product of the pressure P and the effective capillary cross-sectional area A'. The force resisting rupture is a product of the interfacial tension value σ and the circumference of the opening C'. Thus $\sigma C' = PA'$. For a circular opening of radius r', then $2\pi r' \sigma = \pi r'^2 P$ or $P = 2\sigma/r'$. Figure 2.1 outlines the relationship between the maximum capillary radius, the rupture pressure and the interfacial tension value of the liquids.

An example is a porous membrane which allows the passage of one of the immiscible phases through its capillaries but simultaneously repels the passage of the other liquid. Not only must it be wetted by the liquid passing through it, but this must be preferential so that the other phase will never displace it. In this case the membrane retains the dispersed phase drops on its surface where coalescence occurs to produce drops of equilibrium size, i.e. capable of removal due to buoyancy effects.

If both immiscible phases wet the solid surface and are initially in contact with it, one will tend to displace the other, owing to its greater specific molecular attraction. Then that solid is preferentially

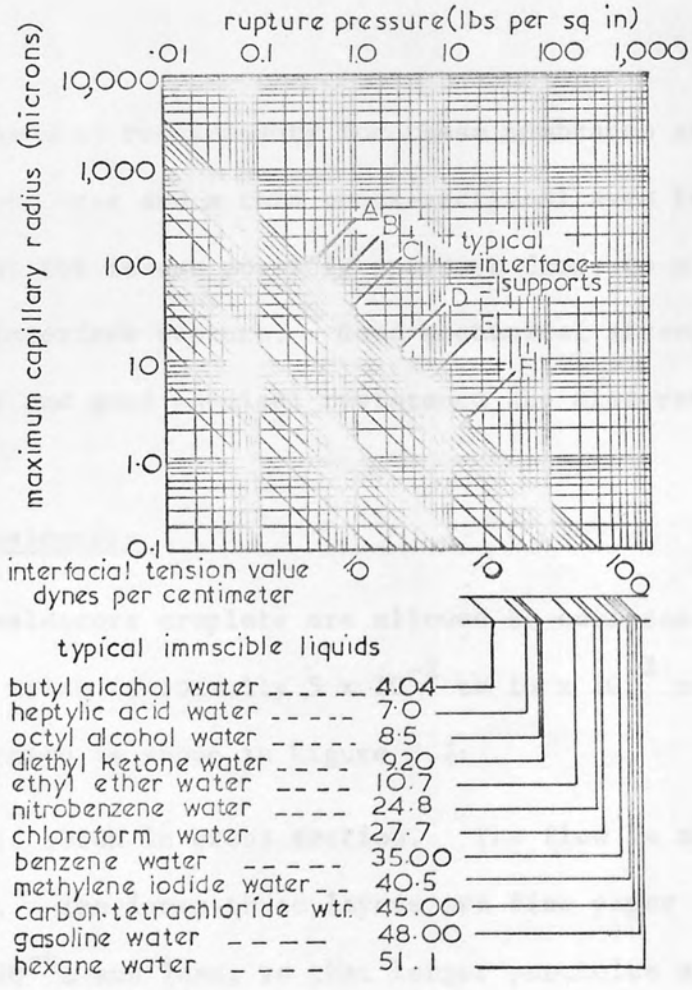

Fig . 2.1 Relationship between max. capillary radius. rupture pressure , and interfacial tension value of the liquids(17.)

wetted by the more strongly attracted liquid. Thus media selection depends upon the liquid to be separated, i.e. the media could be hydrophobic or hydrophilic, providing the continuous phase wets the media. Silicon treated cellulose fibres are often used to separate water dispersed in organic liquids; these allow the organic liquid to pass through while repelling the water. Fine wire mesh coated with Teflon is also hydrophobic.

Finally, the main requirements for these membranes are a high percentage of open area and a thin cross-sectional area to enable a high flow rate at the lowest possible pressure drop, to minimize the possibility of interface rupture. Good mechanical strength, a smooth external surface and good chemical resistance are also required.

2.4.2 Depth coalescers

In depth coalescers droplets are allowed to coalesce within the porous material which is normally 5×10^{-2} to 10×10^{-2} m thick. A typical construction is shown in Figure 2.2.

The media is shown in cross section. The flow is normally from centre outwards. The inner three layers are fine paper of increasing fineness, 20×10^{-6}m and less, so that larger particles are stopped on the first layer of relatively coarse paper, leaving fine particles to be stopped by the finer media. This increases element life by preventing the blockage of finer media by the coarse particles. Usually one layer is resin impregnated to give strength to the assembly. The outer two layers are normally of fibreglass in which coalescence of the dispersed phase takes place until large drops leave the assembly and settle under gravity. Depth coalescence mechanisms are discussed in more detail in Chapter 5.

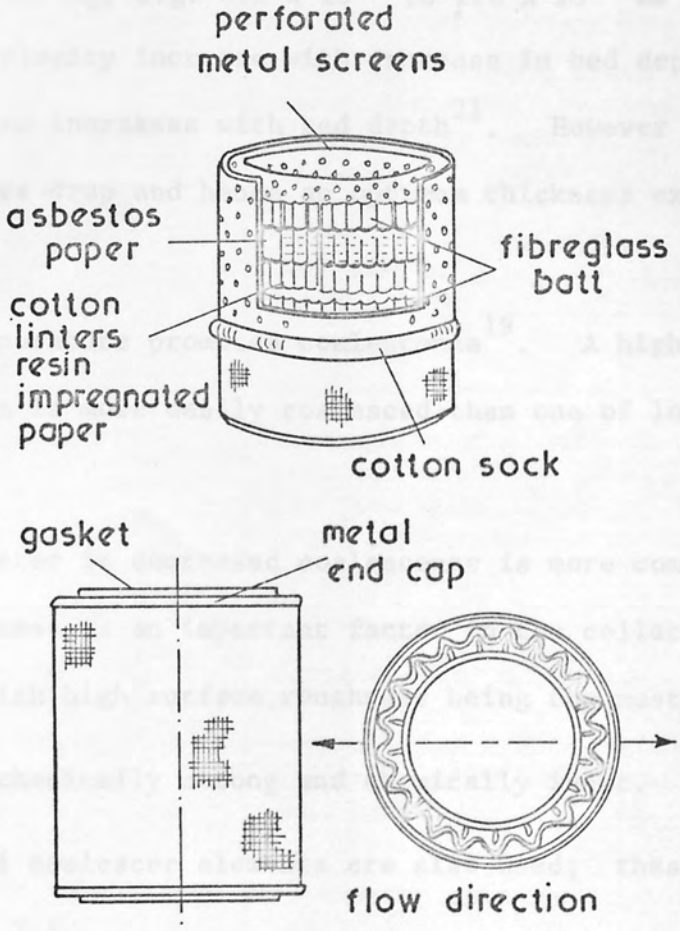

Fig.2.2 The various layers of a depth coalescer element (3.27)

The basic requirements of a coalescer element are as follows:

(a) The bed must be closely packed and possess a high surface area to volume ratio.

(b) The bed must be wetted by the dispersed phase.
This is contradicted by some authors.

(c) The superficial velocity must be between a minimum and a maximum for a given packing, e.g. 0.1×10^{-2} to 1.8×10^{-2} ms^{-1} [20].
The maximum velocity increases with increase in bed depth. Coalescence efficiency also increases with bed depth[21]. However this leads to a high pressure drop and hence an optimum thickness exists for each application.

(d) Increased temperature promotes coalescence[19]. A high interfacial tension system is more easily coalesced than one of low interfacial tension[20].

(e) As fibre diameter is decreased coalescence is more complete[20,21].
Surface roughness is an important factor in the collection process, fine fibres with high surface roughness being the most efficient.

(f) It must be mechanically strong and chemically inert.

Other forms of coalescer elements are also used; these are described in Table 2.1.

For more efficient separation, especially for decontamination of jet fuels, a multi-element separator has been designed incorporating both a depth coalescer and a surface coalescer. Other vessels containing two stage separators in vertical or horizontal arrangement have also been designed as in Figure 2.3[2,17,18,27,28].

Recently a magnetic separator has been developed in which the oil phase is rendered magnetically responsive by adding an oil soluble,

TABLE 2.1

COALESCER ELEMENTS

BED	APPLICATION	REF.
A pebble bed filter, 5×10^{-2} m in diameter, 18×10^{-2} m deep using 0.16×10^{-2} to 0.32×10^{-2} m pebbles.	Separation of 1000 p.p.m. fuel oil-water emulsion, 80% of which was finer than 254×10^{-6} m in diameter. Only 20 p.p.m. escaped in the treated effluent	22 23
Excelsior tanks	Treating Colombia crude oil-water emulsions, removed about 85% of water content.	24
'Alundum', or glass wool	Water-in-oil emulsion. Bed must be preferentially water wetted in the presence of oil.	25
Steel Wool	Separation of traces of caustic soda dispersed in gasoline after the Sweetening Process. (Extraction of mercaptans by sodium or potassium hydroxide solution)	26
Fibre glass, polyester, polypropylene, knitted steel, polytetrafluoroethylene felt. Also a mixed bed of fibre glass and polyester felt.	Separation of 1000 p.p.m. water-in-gasoil emulsion, droplet size 5×10^{-6} m in diameter. The mixed bed proved most efficient.	30
A granular mixture of dissimilar metals such as iron and aluminium or of carbon with a metal.	Separation of 1100 p.p.m. oil-in-water as well as water-in-oil emulsions. Only 50 p.p.m. escaped in the effluent.	31

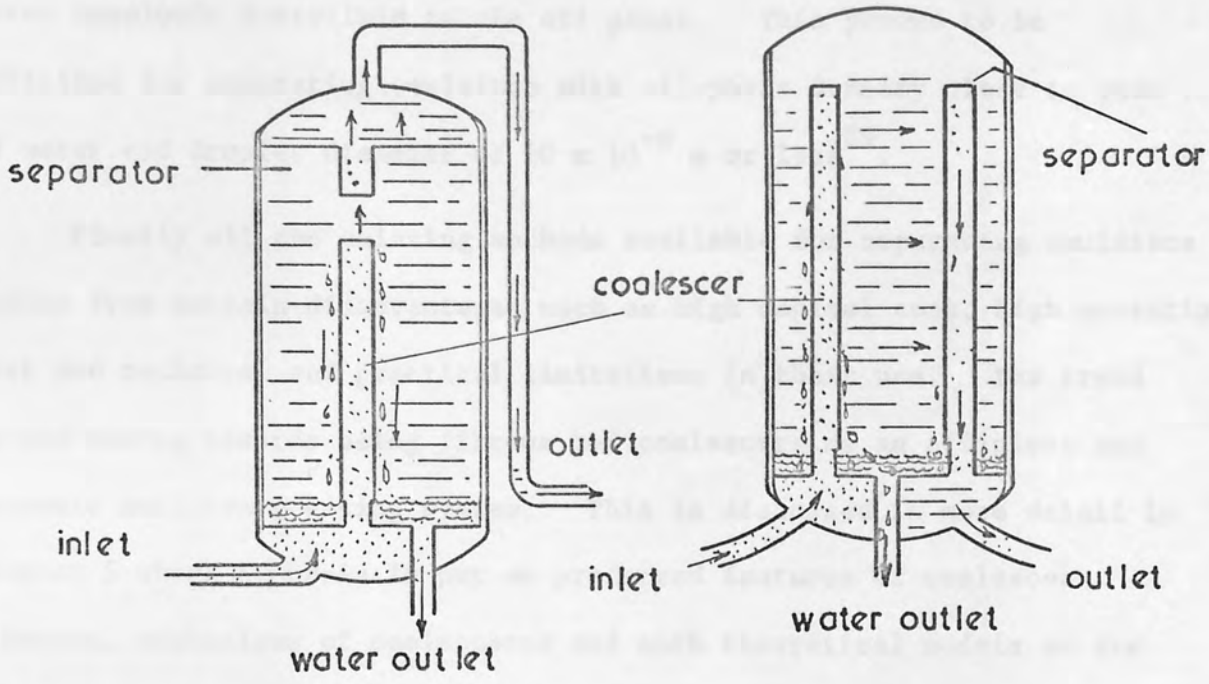

Vertical arrangement of coalescer and separator

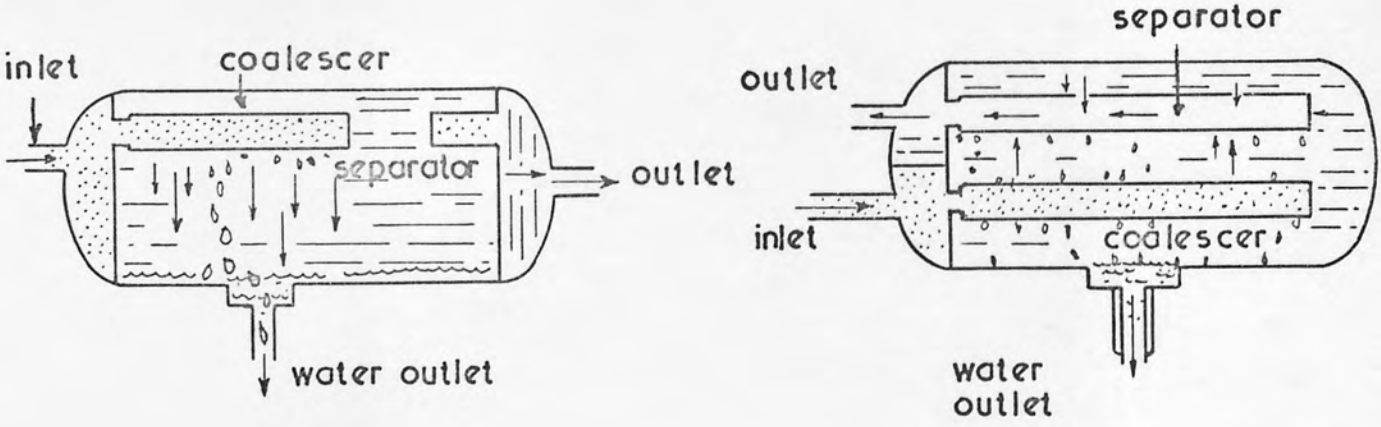

Horizontal arrangement of coalescer and separator

Fig . 2.3 Coalescer and separator arrangements.

water insoluble ferrofluid to the oil phase. This proved to be efficient for separating emulsions with oil-phase density close to that of water and droplet diameter of 10×10^{-6} m or less[29].

Finally all the existing methods available for separating emulsions suffer from certain disadvantages such as high capital cost, high operating cost and technical and practical limitations in their use. The trend is now moving towards using fibrous bed coalescers as an efficient and economic emulsion breaking system. This is discussed in more detail in Chapter 5 where emphasis is put on preferred features of coalescer elements, mechanisms of coalescence and such theoretical models as are available for design.

CHAPTER 3

COALESCENCE PROCESSES

The transfer of a solute between two liquid phases is the basis of all liquid-liquid extraction processes. Mass transfer rate is normally enhanced by increasing the interfacial area and turbulence, and this is usually brought about by dispersing one phase in the other in the form of liquid droplets. When mass transfer is complete the drops must be separated to form a bulk phase. This involves allowing them to settle into a packed dispersion where interdrop coalescence may occur, and finally coalesce at the bulk interface.

In order to control coalescence in any particular system, it is necessary to understand the fundamental mechanisms involved. Thus when a drop approaches an interface a film of the continuous phase is trapped between the drop and the interface. This film drains, until it becomes very thin and ultimately ruptures allowing the drop to pass into its homo-phase. A similar process occurs in drop-drop coalescence and during coalescence in packed beds. The present work is concerned with droplets in the mean size range 26×10^{-6} to 36×10^{-6} m - the so called secondary dispersions. Because of the sphericity and stability of such drops the coalescence mechanisms will differ in some respects from those of drops in the range above 1×10^{-3} m for which most data are available. However, since the smaller drops grow to primary drops within the bed it is worthwhile reviewing the literature on coalescence of the larger drops.

3.1 DROP-INTERFACE COALESCENCE

This was found to occur in five stages[32,45,59] :

(a) Drop arrival at the interface.

(b) Drop and interface deformation.

(c) Continuous-phase film drainage from between the drop and the interface.

(d) Film rupture.

(e) Drop content deposition into the interface.

It is generally agreed that stages (a) and (b) occur immeasurably fast, while stage (e) requires about 0.06 to 0.08 seconds. Therefore the coalescence time could be taken as stages (c) and (d) and is of the order of several seconds or more dependent upon the factors discussed in Section 3.2.

In all investigations a distribution of coalescence times has been reported and for any given system the distribution of times was approximately Gaussian. Therefore numerous determinations were necessary to determine a mean coalescence time, t_m, or half-life rest time, $t_{\frac{1}{2}}$, defined as the time taken for half the number of drops in the population to coalesce. Gillespie and Rideal[33] obtained their results from samples of 100 to 200 drops whilst Jeffreys and Hawksley[34] employed an all glass apparatus and found that reproducible mean results could be obtained from 70 to 100 drops under carefully controlled conditions. More recently Hodgson[35] has refined the technique further to reduce the number of measurements to 30. $t_{\frac{1}{2}}$ is generally more reproducible than t_m and the ratio $t_m/t_{\frac{1}{2}}$ is in the range 1.01 to 1.27[36].

Another phenomenon observed by most investigators is 'step-wise' coalescence in which a drop residing at the interface coalesces partially with the release of a smaller drop which in turn coalesces and produces an even smaller drop. As many as eight stages have been reported[37]. This was first reported by Ward and Cox[38] during froth floatation studies but its mechanism was only explained later by other workers[34,36,37] using high speed photography. It has been suggested that this phenomenon is responsible for the production of a secondary haze or fog in certain types of settling equipment, thus causing entrainment and loss of efficiency. However other methods of haze formation are discussed in Chapter 7.

Whilst a number of correlations are available for coalescence time,

generally in terms of the ratio of number of drops not coalescing in time t to the total number of drops assessed, controversy has arisen over their validity[44,46-48]. This may be because pure systems were used in some studies[34] whilst in others surfactants[40] or electrolytes[42] were present which are known to reduce the interfacial tension of the system. The reproducibility of experimental results was also poor, possibly because the effect of any parameter is not constant either for all immiscible liquid-liquid systems or for the different experimental techniques used. These correlations are not in any event applicable to coalescence in packed beds since they have been proposed for a single drop at an interface, that is neglecting the effect of the presence of other drops and of the solid surfaces.

3.2 FACTORS AFFECTING COALESCENCE

Since the rate determining step for coalescence of a drop at an interface is drainage and rupture of the continuous phase film, factors affecting this control the coalescence process. These are summarised in Table 3.2.

Different investigators agree that temperature gradient, vibrational effects, the presence of a third component and applied electrical field promote coalescence but do not agree on the effects of drop size, distance of fall and density difference. This may be due to the variety of experimental conditions under which the variable was investigated, or the system could have been contaminated. Observations made by Hitit[63] showed that impurities have a far more significant effect on coalescence time than any of the factors discussed. Reproducibility of his results was affected by a jelly-like scum generated by sunlight that formed at the interface; this was reduced by shielding the materials studied from

TABLE 3.2

FACTORS AFFECTING COALESCENCE TIME

No.	Variable (increasing)	Effect on coalescence time	Explanation in terms of effect on continuous film drainage rate	References	Comments
(1)	Drop size	(i) Increases $t_{\frac{1}{2}} \propto d^n$ n varied with conditions	More of the continuous phase film	33,36,37,39, 40,42,43,54, 56.	In stepwise coalescence smaller size daughter drops have a longer life at the interface than the original larger drops. (39, 45, 54)
		(ii) Independent of drop size		57,58	
(2)	Distance of fall	(i) Increases $t \propto H^n$ where n is const. depending upon drop size or $n = 11 \times 10^{-5} \left(\frac{\rho^2}{\mu_c^{0.5}}\right)^{0.91}$	Drop 'bounces' and film is replaced.	34,36	Discrepancy of results was due to apparatus dimension and particularly the dimension of the cup that receives the drop. (36,59)
		(ii) Independent of distance travelled.		43	
		(iii) Either increases or decreases.	Depending on thermal or mechanical disturbances produced.	57	
(3)	Curvature of interface towards drop:				
	(a) concave	Increases	More continuous phase in film	43,49,59	
	(b) convex	Decreases	Less continuous phase in film		
(4)	Interfacial tension	Decreases	More rigid drop, force causing drainage acts on smaller area.	40,57	
(5)	Viscosity Ratio $\frac{\mu_c}{\mu_d}$	Decreases	Either less continuous phase film or higher drainage rate.	37,40,42,57	
(6)	Phase $\Delta\rho$	Increases $\Delta\rho^n$ n = 1.2,0.32,0.25	More drop deformation, more continuous phase film.	37,39,45,49, 57	
(7)	Temperature	Decreases $t_{\frac{1}{2}} \propto \left(\frac{T}{25}\right)^{-0.7} \mu_d^{0.5}$ (13)	Increases μ ratio.	33,34,37,39 40,41,43	Overall coalescence time, however as distinct from first step time, may on occasions show an increase with increase in temperature because of transition from single step to stepwise coalescence
(8)	Temperature gradients	Decreases	Film distorts.	40,43	
(9)	Vibrational effects	Decreases	Assists in film rupture.	33,40,43,57	
(10)	Electrostatic effects	Decreases	Increase in effective gravitational force.	33,37,40,42	Causes formation of twin secondary drops (36,39).
(11)	Applied Electric fields	(i) Decreases	Increase in effective gravitational field.	54,60	The efficiencies of electrostatic coalescers are dependent on this fact.
		(ii) Independent		61	
(12)	Presence of a third component				
	(a) Surfactants	Increases $t_m \propto c_1^n$ $0.3 < n < 0.45$	'Skin' formation around the drop, film drainage inhibited.	43,62	
	(b) Mass transfer into drop	Increases	Sets up interfacial tension gradients which oppose film flow.	36,37,39,45 64,65	Coalescence times are almost independent of solute concentration only primary step being affected for transfer from the drop. (45)
	(c) Mass transfer out of drop	Decreases	Sets up interfacial tension gradients which assist flow of film.	36,37,39,45 64,65	
(13)	Impurities	Varies in an unpredictable way.		63	All researchers found it necessary to clean the interface, otherwise reproducible results were unobtainable.

direct sunlight. Most of the studies mentioned have been of drop-interface coalescence but the same factors will affect drop-drop coalescence as well as coalescence in packed beds. Generally it has been accepted that the separation efficiency in fibrous bed coalescers increases with increase in interfacial tension, increase in temperature and decrease in dispersed phase viscosity. These will be discussed in more detail in Section 5.1.

3.3 SINGLE DROP COALESCENCE MODELS

The drainage times of the continuous phase film trapped between the drop and the interface are similar to the rest times measured in the work reviewed earlier. Therefore many investigators[33,39,42,50-54] have attempted to compare experimentally determined coalescence times with theoretical models based upon drainage of this continuous phase film.

The drainage rate depends upon:

(a) Film thickness.

(b) Shape of the drop at the interface.

(c) Physical properties of the system.

(d) Forces involved in the drainage process.

Therefore attempts have been made to determine the actual film profiles experimentally and to express them in a mathematical form to verify the models. In these models either a constant or varying film thickness was envisaged dependent upon the shape of the boundary surfaces of the film. They may be classified as uniform and non-uniform film models but are outside the scope of this work[55].

3.4 DROP-DROP COALESCENCE

In non-wetted packings, the coalescence of primary dispersions

proceeds mainly via the drop-drop mechanism. Some evidence, as discussed in Chapter 5, indicates that this is partly so in the coalescence of secondary dispersions in fibrous beds. Therefore factors, mostly determined under simulated conditions, affecting drop-drop coalescence have been considered.

Matejicek et al[66] investigated the effects of surfactant, temperature of the system and size of the dispersed phase drop. The drops, situated one above the other in the continuous phase, were acted upon only by buoyancy. Coalescence time results indicated that drop-drop coalescence was slower than the drop-interface type. Coalescence time increased with decrease in drop diameter and with increase in surfactant concentration but decreased with increase in temperature. In the second part of their analysis[67] a model was presented and compared with their experimental results.

Scheele and Leng[68] studied the factors which determine whether two colliding drops will coalesce or rebound for 3.4×10^{-3} m diameter anisole drops in water. The apparatus was designed to control drop size, impact velocity and collision angle. From analysis of high speed photographs, they found that for relative approach velocities of 1.9×10^{-2} to 11.2×10^{-2} m s^{-1}, the apparent drop contact time was less than 0.07 seconds. The drops oscillated and the probability of coalescence during this short time interval was a function of the phase and the amplitude of the drop oscillations at the moment of contact. For coalescence to occur, the phase angle was between 0^{o} and 127^{o} and for bouncing, the angle was between 150^{o} and 345^{o}. No obvious relation existed between coalescence probability and impact velocity, and many low velocity coalescences and high velocity bounces were observed. Applying the classical parallel disc-rigid interface model to describe film thinning, they concluded that

it failed to predict fast enough thinning rates to enable rupture. Thus any model describing film thinning must allow for mobility of the interfaces.

Using two drops of n-butyl benzoate in water, placed in a watch glass, Kintner[69] observed the same events as for a drop coalescing on a flat interface. By dyeing one drop he observed that slight mixing occurred after the coalescence was complete. Mc Cay and Mason[70] formed a drop in an immiscible organic phase and allowed it to rest on a flat non-wettable surface of lucite. A second drop with 1% acetone was allowed to fall gently on to it. The acetone produced instantaneous coalescence. It was demonstrated that when the ratio of drop diameter was greater than 3.5, partial coalescence took place; below this no secondary drop was formed. When the ratio was larger than 12, the surface of the larger drop was undisturbed by the coalescence and the mechanism was similar to that for partial coalescence at an interface.

Robinson and Hartland[71] studied the approach of two or more drops towards an interface, and towards each other, using high viscosity liquids in a two dimensional bed. The arc length of the profile was measured and observations were made of one drop resting at an interface and of two or more drops resting on this one in a vertical column.

Theoretical studies were made, based on the idea of film thinning and rupture. Models[59,72,73] were derived, but these are outside the scope of the present work.

In conclusion, the coalescence of droplets in secondary dispersions within fibrous beds appears to proceed partly via a drop-drop coalescence mechanism. Droplets must approach and adhere to the fibre and reside there long enough for coalescence with an adjacent drop to take place. Thus all the parameters discussed above must be considered in conjuction

with hydrodynamics of flow and collection within the packed bed outlined in Chapter 5.

3.5 DROPS COALESCING ON SOLID SURFACES

When a primary drop, i.e. a drop greater than 100×10^{-6} m in diameter, is in contact with a clean solid surface, it may:-

(a) Spread, forming a thin film over the solid surface.

or

(b) Remain as a stable drop. Such behaviour is conveniently defined by the contact angle θ. This is the angle between the tangent to the drop, measured at the junction of the drop and the solid surface, and the surface of the solid. The angle is measured into the drop as shown in Figure 3a. Several of the methods available for measuring contact angle, have been described by Osipow[74] and Bikerman[75]. When θ is zero, complete 'wetting' of the solid by the liquid is implied, i.e. a liquid film is formed on the solid surface. A value for θ of 180^{o} though never encountered in practice, would correspond to complete 'non-wetting'.

The contact angle θ can be measured with an accuracy of $\pm 0.3^{o}$ [74]. Unfortunately, determinations of θ in supposedly identical systems have frequently given grossly different results. Several factors could account for the poor reproducibility, but the hysteresis of wetting is one of the most important. This phenomenon may be demonstrated with one drop when the solid support is tilted as illustrated in Figure 3b. According to Harkins[76] if equilibrium is attained, there can only be one value of the contact angle between a given solid and liquid. He attributed hysteresis to improper surface preparation and poor measurement techniques. Certainly both hysteresis and inconsistent preparation occur frequently in experimentation

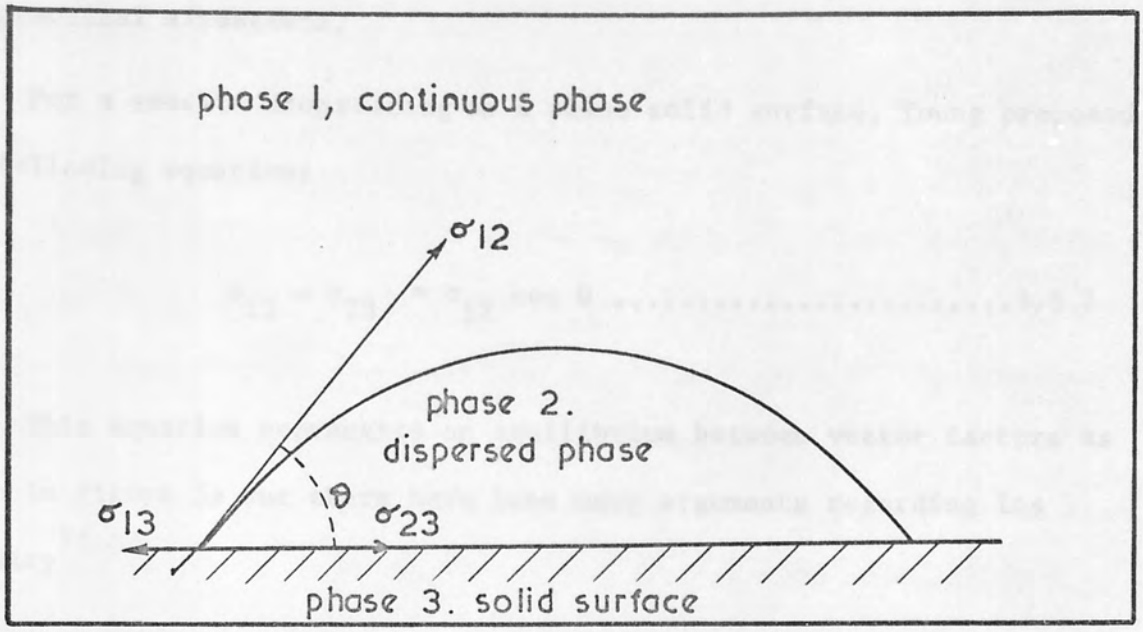

Fig. 3a. The contact angle of a sessile drop at a solid / liquid / liquid boundary

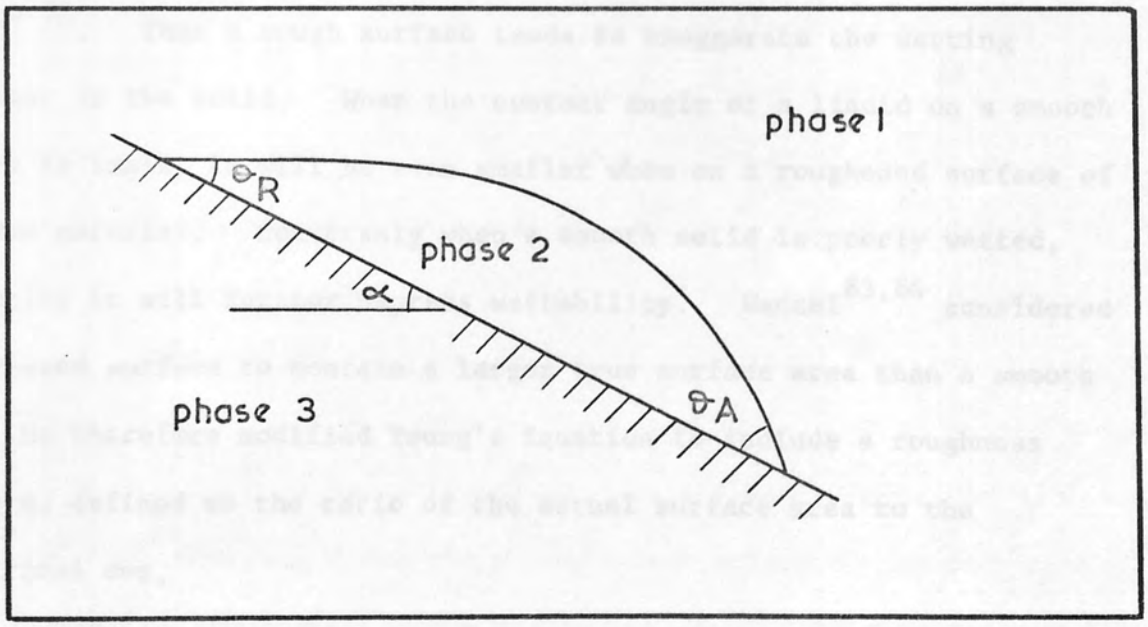

Fig. 3b Advancing and receding contact angles demonstrated by the form of a drop on a tilted solid surface

and practical situations.

For a sessile drop resting on a plane solid surface, Young proposed the following equation:

$$\sigma_{13} - \sigma_{23} = \sigma_{12} \cos \theta \quad \ldots\ldots\ldots\ldots\ldots\ldots\ldots\ldots 3.5.1$$

This equation represents an equilibrium between vector factors as shown in Figure 3a but there have been many arguments regarding its validity[77-82].

3.6 FACTORS AFFECTING CONTACT ANGLE

3.6.1 Surface Roughness

Every groove, valley or scratch on a solid surface acts as a capillary in which liquid flows as long as $\theta < 90^{o}$ or retreats when $\theta > 90^{o}$ [75]. Thus a rough surface tends to exaggerate the wetting behaviour of the solid. When the contact angle of a liquid on a smooth surface is small, it will be even smaller when on a roughened surface of the same material. Conversely when a smooth solid is poorly wetted, roughening it will further depress wettability. Wenzel[83,84] considered a roughened surface to contain a larger true surface area than a smooth one. He therefore modified Young's Equation to include a roughness factor x, defined as the ratio of the actual surface area to the geometrical one,

$$x(\sigma_{13} - \sigma_{23}) = \sigma_{12} \cos \theta' \quad \ldots\ldots\ldots\ldots\ldots\ldots\ldots\ldots 3.6.1$$

where θ' is the contact angle on the roughened surface. x is always greater than unity except on an ideally smooth surface when it is equal

to unity.

$$\therefore \quad x \cos \theta = \cos \theta' \qquad \text{.....3.6.2}$$

Though the Wenzel equation is widely accepted, Shepard and Bartell[85,86] found that it failed to satisfactorily correlate their results. Further, θ depended upon whether the interface at the periphery of the drop was roughened. It was observed that if the drop rested on a roughened surface but the solid-liquid-vapour interface extended onto a smooth area of the surface, the contact angle was the same as that measured on a smooth surface.

3.6.2 Temperature

Physical properties of a system vary with temperature and therefore the stability of the drops of any given system is temperature dependent. Since the surface tension of almost all pure liquids decreases with an increase in temperature, the contact angle will also decrease[87]. If any mixing between the liquid and the solid occurs, θ would tend to be smaller the greater the mutual interpenetration. Since in general, higher temperatures favour intermixing, $(\frac{d\theta}{dT})$ should also be negative in these systems. As the variation is small, Davies and Rideal[88] equate $(\frac{d\theta}{dT}) = -0.06^{o}$/deg C on high energy surfaces and Harkins et al[89] equate it to $(\frac{d\theta}{dT}) = 0.06^{o}$/deg C on low energy surfaces. Finally Ponter et al[90] equate $(\frac{d\theta}{dT}) = -0.1^{o}$/deg C for water drops on a smooth copper surface under isothermal conditions.

3.6.3 Time

Using the system water/cellulose/air, Borgin[91] found that the contact angle fell from 30^{o} to 11^{o} after 600 to 900 seconds after which it became

stable for periods up to 24 hours. This initial decrease in contact angle was probably due to the water penetrating the cellulose mass.

An initial rapid increase in contact angle followed by a slow increase was reported by Elliot and Leese[92] using air bubbles to impinge upon a paraffin wax surface immersed under water, or aqueous solutions of long chain alcohols. They asserted that the increase in contact angle was the result of an increase in σ_{12} and possibly σ_{23}, due to desorption of the solute molecules in excess of the equilibrium value prescribed by the Gibbs adsorption isotherm.

3.6.4 Interfacial Velocity

From a study in which the rate of motion of a water/air interface over paraffin wax varied, Yarnold and Mason[93] reported that for very low velocities of 0.27×10^{-4} ms^{-1} or less, very little change occurred in the advancing angle but the receding angle fell with increasing rate of recession. This supports Ablett's[94] results which show the absence of a velocity effect below about 0.17×10^{-4} ms^{-1} for the advancing angle.

3.6.5 Addition of a Third Component

Much of the published data deals with the liquid/vapour situation. Little work has been done on the wettability of a solid surface by a liquid when submerged in a second immiscible liquid[95,96,97]. Furthermore, the effect of adding a third component has received little attention.

Harkins[76] found that the addition of n-butyl alcohol to water to form an 0.818 molar solution reduced the contact angle of water on paraffin from 111° to 55.3°. Solutions of n-butyl amine, n-butyric

acid, n-acetic acid and sodium n-butyrate have the same general effect.

More recently Juma[98] using the three phase system toluene/acetone/water on various solid surfaces showed a substantial change in wettability of both high energy e.g. stainless steel and low energy e.g. p.t.f.e. surfaces. As the acetone concentration increased, the contact angle decreased and became zero at 59% acetone for both the aqueous phase on stainless steel and the organic phase on p.t.f.e. This was related to a decrease in interfacial tension.

The importance of 'wetting' of packings when primary drops are coalesced in packed beds is discussed in Chapter 4. In the case of secondary drops, there is no established theory explaining this effect, but fibre roughness is extremely important. This is discussed in more detail in Chapter 5.

The information presented above reviews some of the work on drop coalescence. Other important work, viz, the coalescence behaviour of a monolayer of drops at an interface and the coalescence of dispersion bands in vertical and horizontal settlers has been reviewed elsewhere[55,63]. These are not relevant to this work and have not been considered.

CHAPTER 4

COALESCENCE OF PRIMARY DISPERSIONS IN PACKED BEDS

The coalescence and phase separation of dispersions in packed beds depends on whether a primary or secondary dispersion is to be treated. The mechanisms of coalescence, and hence the design criteria differ. However, since secondary dispersions coalesce within the bed to form primary dispersions and some analogies may exist between the two, particularly as regards outlet mechanisms, the coalescence of primary dispersions in packed beds consisting of conventional ring packings or knitted mesh packings has been reviewed.

4.1 DROPLET BEHAVIOUR IN CONVENTIONAL PACKINGS

Droplet behaviour in packed liquid-liquid extraction columns was studied by Pratt et al[99-104] using large drops and packings preferentially wetted by the continuous phase. In this situation, unlike in phase separation, there are three components and generally the phases are in countercurrent flow. Furthermore the void size is always larger than the mean drop size. Nevertheless the results obtained in the absence of mass transfer are relevant.

Using a 5.0×10^{-2} m column containing packings greater than the critical size d_p defined as:

$$d_p = 2.42 \left(\frac{\sigma}{\Delta\rho\, g}\right)^{0.5} \qquad \text{.....4.1.1}$$

the Sauter mean diameter of exit drops was predicted by[99,100]:

$$\frac{d_{vs}\,\Delta\rho\sigma}{\mu_c^{\,2}} = 1.42\left(\frac{\Delta\rho\sigma^3}{\mu_c^{\,4} g}\right)^{0.475} \left(\frac{V_o \varepsilon X}{V_d}\right) \qquad \text{.....4.1.2}$$

where the symbols are as defined in the Nomenclature. By approximating the exponent to 0.5, this expression can be simplified with a slight loss

in accuracy to:

$$d_{vs} = 0.92 \left(\frac{\sigma}{\Delta\rho g}\right)^{0.5} \left(\frac{V_o \varepsilon X}{V_d}\right) \quad \text{.....4.1.3}$$

At substantially zero flow rates:

$$d^o_{vs} = 0.92 \left(\frac{\sigma}{\Delta\rho g}\right)^{0.5} \quad \text{.....4.1.4}$$

In equation 4.1.3, V_o can be determined experimentally from

$$\frac{V_d}{X} + \frac{V_c}{1-X} = \varepsilon V_o (1-X) \quad \text{.....4.1.5}$$

by plotting $V_d + \left(\frac{X}{1-X}\right) V_c$ vrs $X(1-X)$ on arithmetic co-ordinates to give a straight line passing through the origin with a slope of εV_o. A graphical correlation was presented to predict V_o from packing and system physical properties, together with a nomogram relating V_o and the phase flow rates to the hold up[102].

Thornton et al[109] investigated the exit drop size of toluene drops dispersed in water in a column packed with Raschig rings. They found that the equilibrium drop size was achieved after passage through several feet of packing and the change in drop diameter with packing height was represented by:

$$d_{vs} = d_{vs(eq)} + 0.27 \exp - (0.0157h) \quad \text{.....4.1.6}$$

where $d_{vs(eq)}$ was the equilibrium value of the Sauter mean diameter. The effect of each packing section was assumed to be additive but this was later considered to be invalid since droplets within the packing travel at

velocities less than their terminal velocities. Thornton suggested 80% while Thomas[110] claimed 50% to be a more realistic velocity by analogy with knitted mesh packings.

An impact-breakdown mechanism was postulated for the approach to equilibrium drop size [111]. Provided the packing is larger than the critical size d_p, defined by equation 4.1.1, the drops rise within the interstices of the bed and are arrested by collisions with the packing elements. Dissipation of energy occurs which may break the droplet, thus decreasing its mean diameter with packing height. Alternatively a coalescence process occurs with the droplets being retained to coalesce repeatedly until they are large enough to redisperse. As packing size decreases, the coalescence mechanism predominates, particularly when the packings are less than the critical drop size.

To simulate droplet collision with the packing elements, Thornton et al[112] examined the impact of single drops, moving through a continuous phase at their terminal velocity, with fixed baffles. A critical drop size existed above which breakdown of the drop occurred on impact; otherwise the drop was deformed and deflected by the baffle. The critical drop size d_{cr} produced by a symmetrical collision yielding two equal size drops could be correlated although, in practice, asymmetrical collisions would result in a drop size distribution. Furthermore the collision velocity is a function of the dispersed phase hold up and the continuous phase velocity,

$$V = \phi V_t - \frac{V_c}{\varepsilon(1-X)} \qquad \text{.....4.1.7}$$

where ϕ is a factor to allow for the restricted drop rise. Using the values of d^o_{vs} from equation 4.1.4 over a limited range of physical

properties and flow rates:

$$d^{o}_{vs} = 0.5\, d_{cr} \quad \ldots\ldots\ldots\ldots\ldots\ldots\ldots\ldots\ldots\ldots 4.1.8$$

There are a considerable amount of data concerning other phenomena in packed columns, e.g. 'flooding'. This limiting flow condition is a function of the liquid system, its flow rate and the particular packing. Clearly a knowledge of 'flooding' is critical for coalescer design and a number of graphical correlations for 'flooding' data have been published[103,104,114-116]. It must be reiterated that all the above work was with continuous phase wetted packings which is not the optimum for phase separation; this is discussed in Section 4.2.

4.2 DROPLET BEHAVIOUR IN KNITTED MESH PACKED BEDS

Knitted mesh packed beds comprise an open woven wire mesh having 90% to 99% voidage. They may be manufactured from either a single material e.g. stainless steel or polymer, or a mixed material of stainless steel and polymer. Honeykamp et al[118] used knitted mesh packings preferentially wetted by the continuous phase in a Scheibel column. They concluded that the exit drop size was independent of inlet drop size as well as continuous and dispersed phase flow rates. However, packing height was important. A 'characteristic' drop size was produced similar to that found in conventional packings. High voidage packings showed similar flow characteristics to conventional packings greater than d_p.

From studies covering a range of packing voidages 97.5% - 98.75% it has been concluded that the working range increased with increase in voidage and that the limiting flow was dependent upon inlet drop size[119,120]. Large inlet drops, 7.5×10^{-3} m, were restricted at the inlet of the packing and

tended to form a coalesced layer resulting in a reduction of the limiting flow rates. Smaller drops, 3.5×10^{-3} m, accumulated as drops below the packing, their number increasing with flow rate. All of this work was with packings preferentially wetted by the continuous phase. Juma[98] later confirmed that the coalescence efficiency on solid surfaces was higher for dispersed phase wetted packings. To demonstrate this Davies and Jeffreys[121] studied the motion of drops through perforated plates of high and low surface energy materials. For drops which wetted the surface there was an increase in drop volume of up to ten times.

Extending this approach to packings two distinct coalescence mechanisms have been identified dependent upon the degree of 'wetting', with respect to the dispersed phase[110,121]:

(a) 'Non-wetted' packings: The drops remain discrete and coalescence occurs by collisions between drops held in an interstice. Subsequent drops follow the same flow path through the packing[127]. In this case the interdrop coalescence mechanism, discussed in Section 3.4, predominates. The droplets approach an equilibrium drop size, in the manner described for conventional packings[112] but this is attained in a smaller height[110]. For voidages below 95%, the drops are locked in the interstices and cannot move until struck by other drops. Frequent interdrop coalescence occurs resulting in the formation of larger drops. Clearly with increase in voidage, the mechanical holding effect is reduced and the droplet behaviour approaches that reported by Thornton[109].

(b) 'Wetted'packings : The entering drops coalesce on the packing surfaces to form a continuous film into which other drops coalesce. The film drains through the bed under the influence of gravity and enlarged drops detach at the exit. At low flow rates and high

voidages, 95% - 99%, a 'drip point' exit mechanism prevails, sometimes with the formation of secondary drops detrimental to efficient operation. At high flow rates and lower voidages, 'jetting' prevails in which the dispersed phase leaves the bed in a continuous stream. Since drop/interface coalescence predominates the factors which control this mode of coalescence determine the coalescence efficiency of the packing. A limited comparison yielded[110]:

$$\frac{d^o_{vs} \text{ 'wetted' knitted mesh}}{d^o_{vs} \text{ 'non-wetted' Raschig Rings}} = \frac{2.44\left(\frac{\sigma}{\Delta\rho g}\right)^{0.5}}{0.92\left(\frac{\sigma}{\Delta\rho g}\right)^{0.5}} = 2.65 \quad \ldots\ldots\ldots 4.2.1$$

$$\frac{d^o_{vs} \text{ 'wetted' knitted mesh}}{d^o_{vs} \text{ 'non-wetted' knitted mesh}} = \frac{2.44\left(\frac{\sigma}{\Delta\rho g}\right)^{0.5}}{0.92\left(\frac{\sigma}{\Delta\rho g}\right)^{0.5}} = 2.65 \quad \ldots\ldots\ldots 4.2.2$$

For efficient coalescer performance, with 'wetted' packings, it was suggested that the system should preferably be operated in the 'drip point' region. However packed coalescers can be operated in the 'jetting' region[122] and indeed most liquid-liquid separators do operate under these conditions. If the phase boundary is positioned near the packing outlet, jet break up does not cause any problems. With restriction of operation to 'drip point' detachment, the packing capacity would be very low and possibly uneconomical for use in separators.

An interesting phenomenon was discovered at the junction between the 'wetting' and 'non-wetting' zones in a 5.0×10^{-2} m vertical gravity settler, part of the walls of which was treated by Dichloro-Dimethyl Silane to render it hydrophobic. Substantially more coalescence

occurred at the junctions than in the column[123,124]. This effect was reproduced and exaggerated by constructing a knitted mesh packing made from alternative threads of stainless steel, a high surface energy material, and a polymer such as polypropylene or p.t.f.e., a low surface energy material. This mixed packing was evaluated in the separation of kerosene-water dispersions using a variable ratio of stainless steel to polymer, 3:1 to 1:3. Coalescence was complete irrespective of which phase was dispersed. Also higher throughputs and increased flooding velocities were obtained than in identical packings knitted of a single material[123]. Separation was achieved at flow rates up to 0.92 ms^{-1}[126]. However, outside the range 3:1 to 1:3, the packing efficiency decreased for one or the other of the phases dispersed, whilst generally optimum results could be obtained with 1:1 ratio of the materials[122].

To study the coalescence mechanism, a matrix of square mesh of stainless steel and polypropylene was constructed and immersed in a dispersion of water in kerosene. Droplets were retained at the junction where they grew into streams and left the packing. The 'non-wettable' fibre retained the drop whilst the 'wettable' fibre encouraged coalescence until a continuous film was formed[123]. The advantage of a mixed packing is its ability to separate both oil-in-water and water-in-oil dispersions; that is, it comprises a universal packing[125].

A common criticism of knitted mesh packings is their sensitivity to particulate matter present in industrial process streams. This may not affect their performance however, and can in some cases be removed by backflushing or washing through with water[126].

In all the above studies the packing void size distribution was not known. Consequently to define the packing geometry and identify

the parameters controlling drop coalescence within 'not-wetted' packings, Wilkinson[127] constructed a packed bed of mono-sized glass ballotini. He identified two mechanisms:

(a) A drop retention mechanism within the bed.

and

(b) A release mechanism at the exit of the bed.

Statistical analysis of the results indicated that packing thickness, dispersed phase flow rate, preferential surface treatment and inlet drop size had a minor effect on exit drop size. However, the size of the packing element at the exit section of the bed was important. Thus these should be as large as possible but compatible with the size predicted by the drop retention model presented.

In conclusion, different coalescing aid arrangements have been proposed to reduce the overall size of industrial gravity settlers[110]. This has been taken further by the use of mixed knitted mesh packings which increased the settler loading by a factor of 10 times that achieved under gravity settling without increasing entrainment values[126].

CHAPTER 5

COALESCENCE OF SECONDARY DISPERSIONS IN FIBROUS BEDS

There are numerous methods available for separation of secondary dispersions, but in this study discussion is restricted to coalescence in fibrous beds. Therefore preferred features of coalescer elements, coalescence mechanisms and mathematical models of fibrous beds coalescers will now be discussed.

5.1 PREFERRED FEATURES OF A COALESCER ELEMENT

The feasibility of fibre glass coalescence beds for crude oil desalting was studied by Burtis and Kirkbride[19]. They found that improved separation efficiencies were obtained by:

(a) Decreasing the superficial velocity in the range 0.66×10^{-2} to 0.027×10^{-2} ms^{-1}.

(b) Decreasing the water-to-oil ratio in the range 0.3 : 1 to 0.2 : 1.

(c) Increasing the temperature; 275^{o} F was the optimum temperature. Temperatures above 350^{o} F were not practical due to the high pressure required to prevent vaporization.

(d) Increasing fibre packing density from 144.2 to 240.3 kg m^{-3}.

(e) Increasing the bed thickness; 12.7×10^{-2} m was adequate for an approximate concentration of 30 P.P.M. salt in oil. These workers and Hayes et al[1], who conducted a crude oil desalting demonstration using fibre glass in a full scale refinery unit for a period of 58 weeks, concluded that desalting by glass fibre beds was commercially attractive.

Critical Velocity

From a study using water-in-oil emulsions Voyutskii et al[105] claimed that water separation only occurred below a certain critical

velocity; below this velocity coalescence depended upon total fibre contacting surface rather than on pore size. Guedsen[107] separated petroleum fractions dispersed in water using a mixed fibrous bed of cotton and glass wool and also identified a critical separation velocity below which complete separation was possible. Effluent water content, as determined by titration, was found to increase with either increase in superficial velocity or decrease in total surface when separating water-in-oil dispersions using a fibre glass bed[108].

Farley and Valentin[8] investigated the coalescence of high viscosity oils, with viscosities of 3.5 to 20.0 Ns m^{-2}, with application to ballast water treatment. The oils were dispersed in water by pumping. A number of beds were used including porous porcelain, activated alumina and fibre glass as water wetted solids, and polypropylene, polystyrene and steel gauze as oil wetted solids. Effluent oil content was determined by light absorption following extraction with chloroform. As would be expected it increased with increase in superficial velocity, decrease in bed thickness and decrease in oil viscosity. It was considered more efficient to split the total packing thickness into two beds in series, with an intermediate oil take off, the second bed having twice the thickness of the first.

Sareen et al[20] observed visually the performance of single fibres (cotton, polypropylene, glass and p.t.f.e.) and mixed fibres (cotton-glass fibre bed and cotton-Dynel fibre bed) in coalescing several oil-in-water emulsions. The superficial velocity was varied from 0.1×10^{-2} to 1.8×10^{-2} ms^{-1} and the dispersed phase viscosity from 1.4×10^{-3} to 137×10^{-3} Nsm^{-2}; dispersed phase concentration was in the range 2% to 5% by volume. Coalescence performance improved with decrease in fibre diameter and increase in

bed length, but there was a practical limit to the maximum bed depth. While residence time in the bed increased, the coalescence was better but there was a corresponding increase in pressure drop. Furthermore, redispersion of the coalesced drops occurred due to channels being formed within the bed. Coalescence performance decreased with increase in dispersed phase viscosity but then became constant at values above 90×10^{-3} Ns m^{-2}. A critical separating velocity was also identified. Photomicrographs of exit drops indicated that a drop would break away from the fibre after attaining an equilibrium size; when the superficial velocity was higher than the critical velocity a retained drop was carried away before attaining the equilibrium size. These results were later confirmed by Davies and Jeffreys[121].

Essentially 100% oil separation efficiency was achieved by Langdon et al[113] at a superficial velocity of 1×10^{-2} ms^{-1} using a coalescer made from phenol-formaldehyde coated glass fibre 3.2×10^{-6} m in diameter. Both inlet and effluent oil content were determined by a light reflectance technique. The pressure drop during the run increased from 13.8×10^{3} to 172.4×10^{3} Nm^{-2} due to oil accumulation in the bed and, to a lesser extent, to mechanical degradation of the fibres. The possibility of solids contamination was ruled out. Because of the differential increase in pressure, efficiencies were in fact determined under unsteady-state conditions. If solid contaminants were present, they would be deposited in the bed causing a gradual but permanent decrease in voidage. This cannot be avoided and replacement or intermittent back washing of the bed would eventually become necessary. Thus the bed ought not to be used as a filter as suggested by Hazlett[128]. More recently, Euzen et al[30], confining the variables studied to fibre material, fibre diameter, packing thickness and superficial velocity,

concluded that a composite packing of thin fibre glass wool followed by a coarse packing of polyester felt was the most efficient for the removal of water from oil. Pressure drop was accurately predicted by:

$$\Delta P = k' x (L \times V')^{0.86} \quad \ldots\ldots\ldots\ldots\ldots\ldots\ldots\ldots\ldots\ldots 5.1.1$$

Unfortunately this correlation is of limited use since it applies only to the specific system studied. Furthermore, other variables such as packing voidage and fibre diameter, were assumed constant.

To simulate the flow through fibrous beds, Vinson and Churchill[117] used photo-etched screens to separate a 0.05% oil-in-water emulsion with an average drop size of 3×10^{-6} m. The emulsion was prepared using a homogenizer and drop size estimated by a light scattering technique. Coalescence efficiency decreased with increase in superficial velocity, from 0.025×10^{-2} to 2.08×10^{-2} ms^{-1}, increase in screen filament width, from 8.5×10^{-6} to 31.4×10^{-6} m, and increase in aqueous phase viscosity from 0.9×10^{-3} to 9.4×10^{13} Ns m^{-2}. A correlation developed for drop removal with filtration variables is discussed in more detail in Section 5.3.3.

Preferential Wettability

Whether or not the packing should be preferentially wetted by the dispersed phase has been the subject of much discussion. Voyutskii et al[105] concluded that for best performance the fibre should be sufficiently 'water-wetted' to coalesce the water, but not so 'wetted' as to become clogged by the accumulation of water. The appearance of a secondary dispersion in the effluent was attributed to excess water wetting. In a second study[106] a mixed packing of viscose and wool fibres exhibited improved coalescence performance compared with single fibre material.

Sareen et al[20], using a photomicrographic technique, concluded that preferential wetting was not the controlling factor since drops that adhered to the fibre did not wet it. The results were justified by the relative surface roughness of the fibres used. A similar conclusion was reached by Davies and Jeffreys[121]. Since droplet sizes were much smaller than the equilibrium drop size, droplets that adhered to the packing would be spherical regardless of material. However, surface roughness was considered extremely important.

For coalescence to take place, Burtis and Kirkbride[19] concluded that the packing must be preferentially wetted by the dispersed phase. Hazlett[128] accepted this principle to explain the attachment mechanism.

Farley and Valentin[8] concluded that water wetted packings were far superior to oil wetted ones for the separation of oil from water. The latter held the drops too tightly and did not allow coalesced drops to leave the packing; this resulted in their finally being broken up into clouds of small droplets by the water stream.

Langdon et al[129] considered the separation performance of a packing to be mainly determined by its wetting properties. An improved element with well defined and stable wetting characteristics could be achieved by using a packed bed composed of two materials, one essentially hydrophobic and the other essentially hydrophilic.

From this brief review of previous work on fibre wetting phenomena it is clear that there is a lack of understanding as to the effect of the nature of the coalescing media on the coalescence process. The consensus is however that preferential 'wetting' of the packing by the dispersed phase is not critical, but surface roughness is extremely important. Suggestions that improved coalescer performance achieved by dipping the bed in the dispersed phase, i.e. 'priming', is due to prewetting effects

are unproven. The phenomenon is more probably due to filling up the 'active sites' in the bed, i.e. increasing the hold up of the dispersed phase which is a major factor affecting the ultimate effectiveness of the coalescer.

System Properties

As would be anticipated system interfacial tension is important in the operation of a coalescer element. Generally, the higher the interfacial tension, the easier is the separation. Values as low as 20×10^{-3} Nm $^{-1}$ can be separated satisfactorily, but below this value separation becomes increasingly difficult[27]. Rose[152] confirmed this from a study of nine different water-organic dispersions. Sareen et al[20] found that, during the separation of oil in water emulsions, for an interfacial tension value of 20×10^{-3} Nm $^{-1}$ incomplete coalescence was observed for water soluble surfactants while coalescence was complete with oil soluble surfactants for values as low as 3.52×10^{-3} Nm^{-1}.

Some theories have been presented as to how surfactants poison coalescer elements. Bartle[27] suggested adsorption of the surfactant by the element. This would cause re-emulsification of the dispersed phase present on the media. Osterman[4] suggested there was adherence of the surfactant to the media thus allowing the emulsion to pass through unaffected due to the change in fibre wettability. Lindenhofen[130] disproved the above theories experimentally and suggested that the surfactant film at the oil-water interface, water dispersed, may present a mechanical or electrical barrier to the coalescence of water droplets in the media. Flushing the element with Iso-propyl alcohol improved its coalescence performance and lowered its pressure drop. More recently[131] he suggested that commercial coalescers, which normally have a cotton outer wrapping or 'sock', malfunction due to the sock's

adsorption of surfactant from the continous phase when dispersed phase, i.e. water wetted, causing a high surfactant concentration at the release point. By coating the sock with a fluorocarbon resin a hydrophobic surface was produced and this operated normally even if poisoning was attempted. These results support the theory first presented by Hazlett[132] that poisoning is caused by interference with the detachment process at the point of release of the coalesced water drops from the sock.

From a study of the effect of the sodium sulphonate surfactant on fibrous bed coalescence, Hazlett[132] concluded that doubling the surfactant concentration from 0.5 P.P.M. to 1.0 P.P.M. influenced the coalescence phenomena to a greater extent than a 30 fold change in velocity. The additive did not affect the approach or attachment processes but only affected droplet release. Thus instead of the drops growing into balloon-shaped globules and detaching from the same site by rupture of the neck, they were extended by the force of the continuous phase film into thin fingers, which oscillated normal to the flow and released drops from the tip as shown in Figure 5.2.2.

With continuous phase soluble surfactants, a reduction in interfacial tension from 40×10^{-3} to 10×10^{-3} Nm^{-1} reduces the thermodynamic instability of dispersions and stable emulsions can readily be formed. At values of 0.1×10^{-3} Nm^{-1} droplets break up spontaneously to form a stable emulsion[76]; such an emulsion cannot be coalesced in a fibrous bed. Even in very low concentrations surfactants affect the interfacial tension. In larger concentrations, however, the drops are completely covered with a 'skin'. For dilute surfactants, the drop surface is not completely covered and size distribution change may occur due to drop interactions. For higher concentrations, the coverage becomes complete and the drops are

isolated causing a distribution highly resistant to change. However for primary drops falling through a continuous phase at low Reynolds numbers the surfactant is swept to the rear of the drop by the tangential velocity on the surface forming a 'dust cap'[153]. No comparable work has been published for secondary drops.

5.2 COALESCENCE MECHANISMS

An extensive literature survey indicates that there is no accepted theory as to the mechanisms involved in the coalescence of micro size drops during passage through a fibrous bed.

Burtis and Kirkbride[19] considered rupture of the continuous phase film between the drops when flowing through the small passages to be a factor as well as preferential wetting of the packing by the dispersed phase. Subsequently Voyutskii et al[106] proposed the following steps for the coalescence process:

(a) Collision of the droplets with bed fibres.

(b) Adhesion of the droplets to the fibres.

(c) Coalescence of the micron sized droplets.

(d) Adhesion of the coalesced drops to the fibre surface.

(e) Trickling down of the coalesced drops from the bed.

Sareen et al[20] later proposed the following mechanisms:

(a) Inertial Impaction: Droplets with the same relative mass as the continuous phase follow the streamlines around any obstructions in the stream. If flow is turbulent and vortices occur, the drops can be brought to a fluid interface even though the density difference is low. Provided the density of the dispersed phase is less than that of the continuous phase, this mechanism does

not inhibit droplet approach to the fibre or to any other drop.

(b) Direct Interception: Droplets of finite diameter will tend to touch the cylindrical fibre at a distance $\frac{d}{2}$ from the packing surface.

(c) Brownian Movement: Continuous movement of the droplets in the dispersion due to impacts by the surrounding medium molecules. This is only applicable to droplets in the submicron range.

(d) Electrostatic Movement: Droplets carrying opposite electrostatic charges attract each other. This is likely to occur in water-in-oil emulsions.

(e) Rupture in Capillaries: For film thinning and rupture to occur one of the drops must be held in the bed. Photomicrographic studies have shown that coalescence does not occur between freely moving drops following contact as they are carried through the bed.

Three other possible mechanisms were considered by Bartle[27]:

(a) Pore Catchment: A drop is arrested if the drop radius is slightly larger than the pore radius. Consequently approaching drops will tend to coalesce with the arrested drop as shown in Figure 5.2.1a. This may be typical of behaviour encountered at a screen or wire gauze.

(b) Flow Path Intersections: Due to inertial forces, large drops do not tend to follow streamlines as easily as small ones. Different size droplets travelling in a tortuous path will therefore intersect, with the possibility of collision and subsequent interdrop coalescence at each path intersection, as shown in Figure 5.2.1b. This is likely to occur in fibrous bed coalescers.

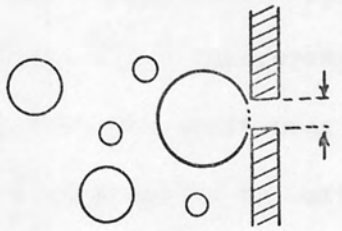

a. pore catchment

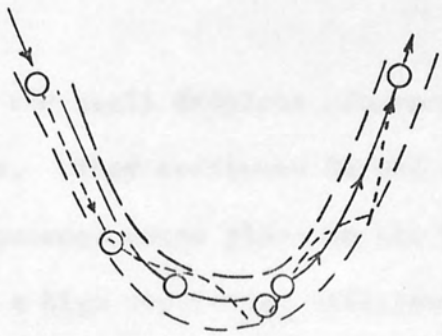

b. flow path interception

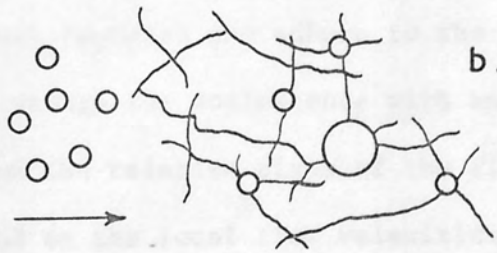

c. impingement

Fig. 5.2.1 Mechanisms of coalescence of a secondary dispersion

(c) Impingement: If the packing is hydrophilic, water droplets will cling to the fibre and move along the fibres in the direction of pressure gradient until they arrive at either a fibre intersection, or a pore too small to pass through. Here the droplets are constrained until joined by other drops. When the droplet formed by coalescence builds up to a sufficient size, it will break away from the fibre intersection under the influence of the viscous drag caused by the continuous phase flowing round it. This mechanism was also proposed by Curtis[133] for the separation of water from oil and is shown in Fig. 5.2.1c.

Davies and Jeffreys[121] stated that the small droplets adhere to the surface where coalescence takes place. They confirmed Sareen et al's[20] conclusion that no interdrop coalescence takes place in the bulk phase flowing through the packing. For a high separation efficiency droplets must approach and adhere to the packing surface and reside there long enough for coalescence with an adjacent drop to take place. Depending on the relative sizes of the fibres, capillary spaces and droplets and on the local flow velocities droplets arrive at the surface either by direct interception or, in the case of submicron drops, by Brownian movement. Electrostatic charges may also affect the migration of small drops to a surface in water-in-oil dispersions. This mechanism is discussed in more detail in Section 5.3.1.

The mechanism of coalescence was divided by Hazlett[128] into three stages, viz, the approach of a drop to a fibre or a drop attached to a fibre, the attachment of a drop to a fibre or a droplet already attached to a fibre, and the release of an enlarged drop from a fibre.

(a) Approach: This mechanism was subdivided into direct interception, diffusion and inertial impaction. Electrostatic movement and

the effects of gravity were neglected since Vinson[117] proved these phenomena to be insignificant for the approach mechanism with fine mesh screens, although Sareen et al[20] and Davies and Jeffreys[121] considered electrostatic phenomenon participated in the coalescence process. Hazlett derived mathematical expressions for the efficiencies of these processes, as given in Section 5.3.2.

(b) Attachment: For this process to be effective the dispersed phase must displace the continuous phase from the packing and preferentially wet it.

(c) Release: Following attachment threads of the dispersed phase flow through the coalescer to the exit of the bed where individual drops are released. Their size is affected by flow velocity, surfactant content and fibre diameter. Hazlett's mechanism is discussed in more detail in Section 5.3.2.

More recently[134] Hazlett also defined the mechanism as collection, passage through the bed and release.

(a) Collection: This involves approach, film drainage and film rupture. Since experimental work indicated complete collection of the drops at depths less than those used in practice, this step is not normally a critical factor in fibrous bed performance.

(b) Passage through the bed: The droplets collected by the bed are not immediately released; a considerable number are collected until an equilibrium value is reached dependent upon phase ratio, flow velocity and surfactant content. Droplets are not equally distributed throughout the bed, and the majority are retained in the entry zone. Once the equilibrium value is exceeded, droplets move into the flow channels and pass through the remainder of the

bed[135]. By using cine photography in a transparent coalescer cell, Brown[136] showed that the dispersed phase passed through the intermediate portion of the bed using the same channel repeatedly. The threads pulsed and varied in diameter and flow rate with time. In many cases threads were discontinuous, but when flow restarted the same channels were utilised.

(c) Release: In an ideal situation, one thread feeds a droplet at the downstream face of the bed. A balloon-shaped drop then grows until the hydrodynamic forces exceed the interfacial forces. The rupture occurs at the balloon's neck, the size of the released drop being dependent upon flow velocity and interfacial tension. The presence of surfactants alters the release process, so that jets break up into uniform small drops due to Rayleigh instabilities. Another type of release mechanism is pointing, in which fingers of collected droplets project beyond the bed face. These fingers taper to a point, vibrate and kick small drops from the tip. Langdon[129] and Lindenhofen[131] reported a graping release pattern. This is found at high dispersed phase concentrations or with certain additives. Fibres preferentially wetted by the dispersed phase tend to encourage graping. The various possible droplet release patterns are shown in Figure 5.2.2.

5.3 MODELS OF FIBROUS BED COALESCERS

Until 1969, the design of coalescing devices employing solid contact was largely empirical. Later some mathematical models were derived to assist in the design of fibrous bed coalescers. These are reviewed below.

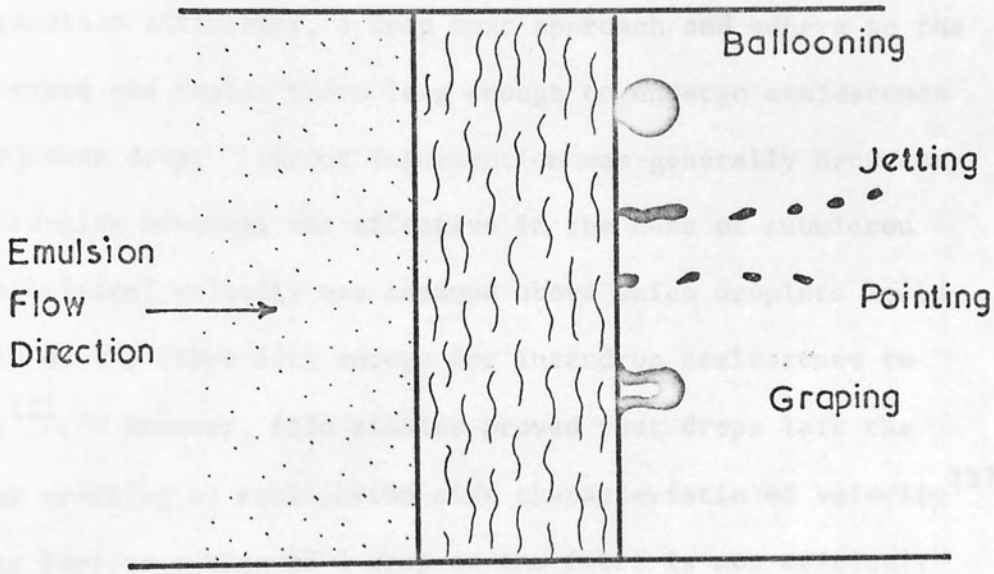

Fig . 5.2.2. Types of droplet release mechanism

Mechanisms within bed and of flow through it unknown

5.3.1 Davies and Jeffreys Model

This was the first qualitative description of the operation of a fibrous bed coalescer. As already explained the mechanism for secondary dispersion separation in fibrous beds is different to that for primary dispersions discussed in Chapter 4. With secondary dispersions, preferential wetting of the bed by the dispersed phase is not critical, but surface roughness is extremely important. For a high separation efficiency, a drop must approach and adhere to the packing surface and reside there long enough to undergo coalescence with an adjacent drop. Direct interception was generally necessary, although Brownian movement was effective in the case of submicron drops. A critical velocity was assumed above which droplets would not be held on the fibre long enough for interdrop coalescence to take place[121]. However, film studies proved that drops left the fibre after reaching an equilibrium size characteristic of velocity[137] so that the residence time of a drop on the fibre is not critical. However, if the superficial velocity is too high, drops leaving the fibre would be too small due to the viscous forces being greater than the force of adhesion.

5.3.2 Hazlett's Model

As was mentioned in Section 5.2, Hazlett[128] divided his coalescence mechanism into approach, attachment and release. The approach process was also subdivided into direct interception, diffusion and inertial impaction. Direct interception was the most important step. Diffusion may assist direct interception for submicron drops while inertial impaction was insignificant.

Direct Interception: Under laminar flow conditions, existing in fibrous bed coalescers, a fluid passing a submerged cylinder such as glass

fibre will follow streamlines shown in Fig. 5.3. Droplet w_1 will be intercepted when it reaches position w_2, but droplet w_3 will not be intercepted even at the closest approach w_4. It will however be intercepted if it follows a streamline closer to the fibre centre. Using Langmuir[138] equation to evaluate the interception process:

$$E_s = \frac{1}{2(2 - \ln Re)}\left(2(1 + R) \ln (1 + R) - (1 + R) + \frac{1}{1 + R}\right) \quad \ldots\ 5.3.2.1$$

This equation predicts an increase in efficiency with increase in velocity, which is contrary to experimental observations[8,19,117,139]. However, it may be possible to relate single fibre efficiency to bed efficiency from a consideration of the total projected area of fibres in the bed. Differences exist between the two systems because in a packed bed fibres are orientated at different angles to the flow causing different collection efficiencies; there is also a pressure drop due to hold up within the bed. With a single fibre in a fixed position there is no pressure drop due to hold up and there is no variation in collection efficiencies.

From the proposed attachment process, Hazlett suggested that fibre wetting by the dispersed phase is critical, i.e. that the drop must spread on the fibre. For this to occur, a continuous phase film between the drop and the fibre must thin to a certain minimum thickness before it ruptures. Film rupture is also critical between a small drop approaching an already attached drop. In fact the process will be more complicated since both interfaces are deformable and the film between them must be ruptured for coalescence to occur.

Describing the release process, it was assumed that the enlarged drops bridge to a fibre downstream to which they attach before release

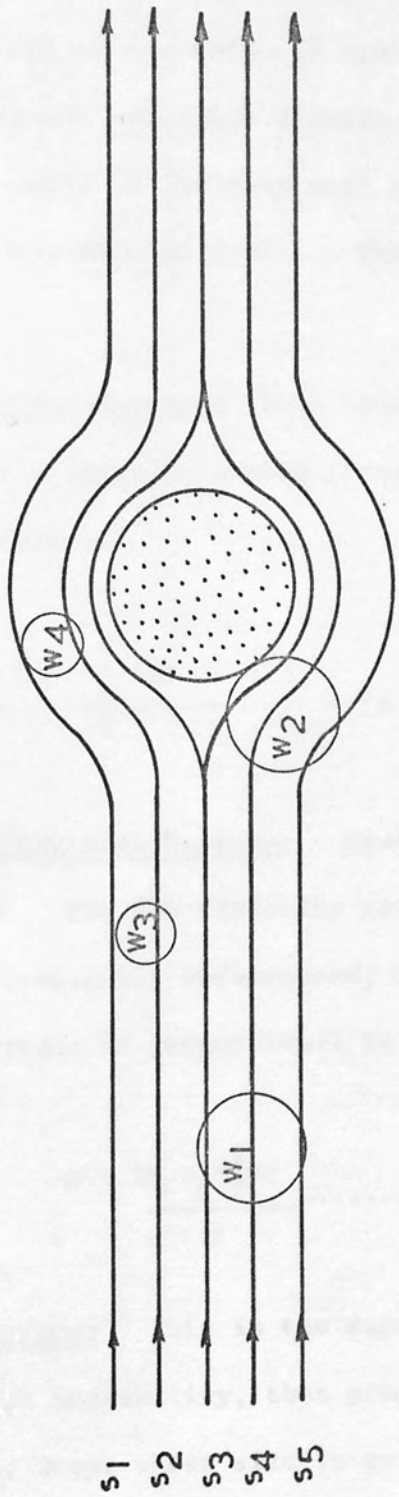

Fig. 5.3. Flow patterns for direct interception.

from the first fibre. Also the coalesced drops do not move through the bed as discrete drops, rather, the dispersed phase passes as threads through the bed until released as individual drops from the downstream face. The size of the released drop depends upon flow velocity, surfactant content and fibre diameter. Before release can occur, the hydrodynamic force on the drop must be greater than the adhesive force between the drop and the fibre. Three possible release mechanisms are presented:

(a) Drop-Volume Rupture: This equates the drag force exerted on the drop with the restraining force of the interfacial tension. This yields:

$$\frac{C \rho_c V'^2 \pi \left(\frac{1}{4} (d)^2 - a^2 \right)}{2} = 2\pi a \sigma \quad \text{.....5.3.2.2}$$

(b) Drop Elongation Rupture: Caused by the moving fluid surrounding a drop. For the viscosity ratio of the drop to the continuous phase frequently encountered, 0.5 to 1.0, the elongation at small distortions is proportional to a dimensionless number F

$$F = \frac{2G \mu_c (\frac{1}{2})d}{\sigma} \quad \text{.....5.3.2.3}$$

(c) Jet Rupture: This is the rupture of an extended jet due to Rayleigh instability, thus producing a series of uniform but smaller drops whose size is governed by interfacial tension and nozzle size. This is the more realistic release mechanism but unfortunately no equation is presented to describe this process. Thus Hazlett's model is of limited use for designing a fibrous bed coalescer.

5.3.3. Vinson and Churchill Model

This model[117] is based on the principle that the probability of a drop colliding with a fibre is normally large in comparison with the probability that it will collide and coalesce with another drop in the flowing stream. If the drop is retained on collision, it will move along the fibre onto another fibre and coalesce with other retained drops. Bitten[140] proved this idea to be invalid. Studying coalescence of water-in-oil emulsions on a single fibre, droplets appeared to grow by the acquisition of free water from the main stream rather than from the surface of the fibre; the coalescence of adjacent drops was very slow and often required as much as 1.8×10^3 s or more to occur.

Retention of a drop depends either upon its physical entrapment or upon its ability to wet a fibre preferentially. The model further assumes that the approach of a drop to a filament is due to direct interception. Continuous phase film thinning is attributed to normal stresses generated by the flow and Van-der-Waals attraction. Brownian movement was assumed negligible since it is only effective for sub-micron size drops. When the film ruptures, the drop makes physical contact with the filament and flattens on it. The probability that a drop will remain on the filament long enough to unite with other drops depends upon drop-filament adhesion as well as wettability. With good wettability, the filaments serve as low energy surfaces along which the flattened drop can move and unite with other drops. The larger the sum of the adhesion force and the wetting force, the larger the globule can grow before release. When adhesion is strong, cohesion failures may occur and only part of the drop will be released. When this occurs, the dispersed phase will be attenuated to sheets or threads downstream of the filament by fluid forces. Under this

condition the released drop size depends upon the sheet or thread thickness, that is upon the amount of attenuation.

Although an equation was given to represent the separation performance of fibrous beds, this was not based on the model but simply the best fit for data obtained experimentally for the system studied using photo-etched screens to simulate fibrous beds. The equation was:

$$\text{Fractional Removal} \quad f = -0.089 + 0.128(U_o d_f \mu_c)^{-0.4} \quad \ldots\ldots \quad 5.3.3.1$$

Therefore, there is no theoretical basis for using this equation for fibrous bed coalescer design.

5.3.4 Spielman and Goren Model:

This model[141,142,143] assumes that as liquid-liquid dispersions pass through the fibrous bed, the suspended droplets are transported to the solid where they are trapped and coalesce into a previously captured bulk of liquid. Under the action of hydrodynamic, gravitational and capillary forces, the coalesced liquid drains through the packing. At steady state operation, the coalesced liquid leaves the bed at the same volumetric flow rate as suspended drops are coalesced within the bed. Two other assumptions are made, viz, that the dispersed phase volume fraction in the aqueous phase is very small, i.e. 0.1%, and that the viscosity of the oil is not too large compared with that of the continuous phase.

Using water and air filtration theory to describe particle capture by the bed, and soil physics and petroleum reservoir engineering to describe the flow of coalesced liquid within the bed[141,142], they suggested that each immiscible liquid flows within fixed microscopic

channels with the non-wetting liquid flowing inside. During the two phase flow within the voids, each phase flows at its own local pressure, local pressure difference between the phases being the capillary pressure. Each channel can be described by a Darcy's Law.

Magnitude estimates indicated that direct interception was the main coalescence mechanism while Brownian diffusion, gravity settling and impaction were negligible. However it was observed experimentally[143] that the dependence of the filter coefficient λ on drop diameter, fibre diameter and flow condition, was in contradiction to the classical interception theory. This led to a re-examination of the concepts underlying the theory of collection by interception and to the development of a rigorous treatment of collection by convection and London Van-der-Waals attraction. The final equations developed were:

(a) For oil non-wetted beds:

$$\frac{\lambda d_f^3}{d^2} = 0.29 \left(\frac{A d_f^2}{\mu_c V' d^4}\right)^{0.25} \quad \text{..... 5.3.4.1}$$

(b) For oil wetted beds:

$$\frac{\lambda d_f^3}{d^2} = 0.08 \left(\frac{A d_f^2}{\mu_c V' d^4}\right)^{0.2} \quad \text{..... 5.3.4.2}$$

The constants and exponents were determined from the data.

These equations are not based on the model but upon the capture of a drop by a fibre rather than by other coalesced drops. Also since a considerable amount of data are required to determine the exponent, these equations are of limited help in designing a fibrous bed coalescer.

5.3.5 Sherony and Kintner Model:

Sherony was the first to develop a model for fibrous bed coalescence and to use it to derive a design equation[144]. The basic assumption is that coalescence occurs between a drop in the stream and a drop attached to the fibre. Adhering to the fibres is a population of drops with a size distribution of some subset of the size distribution in the main stream. Therefore, this model is confined to a sufficiently small concentration of dispersed phase in the entering emulsion that it does not form a continuum in the bed.

Only a certain percentage of the collisions between a moving and a held drop leads to coalescence because of the finite time required for film drainage as discussed in Chapter 3. Using an experimental technique Sherony found this quantity to be about 41%; this was velocity dependent. If the rest time is very long, the flowing stream will sweep the approaching drop away from the stationary drop and coalescence will never take place. Following coalescence the enlarged drop is released and a new drop equal in size to the one first retained takes its place. However this can only be true in the presence of a monodispersion.

Using a combination of aerosol filtration and the kinetic theory of gases, a model was developed which took into account coalescence by different mechanisms. These were:

(a) Impaction: This was divided into impaction by inertial transport of the drop in the stream to the fibre and impaction by interception of the drop with the fibre.

(b) Brownian Diffusion: This can take place between two drops in the stream or between a drop in the stream and a drop on the fibre.

(c) Turbulent Coalescence: Drops which have associated in pairs are squeezed through the capillary passages of the bed and eventually coalesce. From a photomicrographic study[137] of fibrous bed coalescence, these doublets were observed to be formed by eddies created by the presence of the fibres.

As a first order of magnitude they calculated that the collision frequency due to the impaction mechanism was about 150 times higher than turbulent collision and 10,000 times as high as Brownian diffusion. Thus only the impaction mechanism was considered in their final model, leading to the design equation:

$$\left(\frac{\text{Outlet}}{\text{Inlet}}\right) \text{ Particle No. densities} = \exp\left(\frac{-3(1-\varepsilon)S(1+d_{10}/d_f)}{4d_f(1-S)} \times \eta_c L\right) \quad \ldots\ldots\ldots\ldots\ldots 5.3.5.1$$

The model predicts that a smaller fibre diameter, thicker bed and a larger mean inlet drop size, all result in a higher degree of coalescence. This is in agreement with experimental results[21]. In the model derivation, the dispersed phase was assumed to be held-up and uniformly distributed throughout the bed thickness, but Bitten et al[135] have shown that hold up changes with bed thickness. The bed inlet possessed the highest degree of hold up, 2.0 to 3.0 Kg of water/ Kg of fibre, followed by a sharp drop to 0.4 to 0.7 Kg of water/Kg of fibre, at approximately 1.6×10^{-3} m bed thickness. The water retained throughout the rest of the bed did not vary appreciably until the exit side of the bed where it increased.

Furthermore, the coalescence efficiency η_c was subdivided into:

$$\eta_c = \alpha \beta$$

β was found experimentally to be approximately 41%; this would clearly

depend upon the system properties and the superficial velocity. A model for α was derived based on the efficiency of aerosol filters. Calculations indicated that η_c increased with increase in velocity, in agreement with aerosol theory and Hazlett's model[128]. However this is contrary to experimental results obtained with fibrous bed coalescers[8,19,117,139]. Clearly therefore the coalescence efficiency predicted from aerosol filtration theory is not applicable to fibrous bed coalescence and a more accurate theory is needed for predicting efficiency.

5.3.6 Rosenfeld and Wasan Model:

This model[145] may be summarised as follows:
The droplets flow with the continuous phase through the bed. If a droplet comes close to a fibre it will strike it. There is then a probability that the drop will attach to the fibre, thus creating a distribution of held drops. These could be struck by other drops from the main stream and coalesce. Coalescence proceeds until an equilibrium drop size is reached after which the drop is pulled away from the fibre by the fluid drag.

In order to derive a design equation, the following assumptions were made:

(a) So as not to affect the continuous phase flow, the droplets must be small and the emulsion dilute. Spielman and Goren[143] found that pressure drop is independent of drop size, thus the droplets do not affect the continuous phase flow.

(b) Coalescence in the bed is of the interdrop type, that is, the bed hold up is small and there is no continuum of dispersed phase.

(c) Approach to a fibre is mainly by the interception mechanism. London Van-der-Waals forces have been shown to be negligible[146]. This has been accepted by a number of investigators[20,128,144,147].

(d) For any particular system, there is a constant probability that a drop will attach to a fibre or coalesce when it strikes a fibre or a retained drop.

(e) Drops grow by coalescence of a retained drop with drops from the free stream. Essentially there is no coalescence between two drops in the field stream, as was observed by Sareen et al[20] and Bitten[140]. Also if a drop on one fibre were to coalesce with another drop on a different fibre, the effect would be the same as when the first drop detaches from the fibre before coalescing with the other drop. This assumption has been accepted by Sareen et al[20] and Davies and Jeffreys[121].

(f) The drop detaches from the fibre after reaching a critical size. This has also been verified by Sareen et al[20].

(g) Each drop can be considered independently of the overall distribution. Spielman and Goren[142] found that for dilute emulsions, e.g. 0.1% concentration, provided the dispersed phase viscosity is not too large compared with that of the continuous phase, the coalescence efficiency for any given drop size is independent of the size distribution.

After formulation and solving a set of equations, the final theoretical design equation was:

$$\lambda = (8\,\beta(1-\varepsilon)\,d/\pi^2\varepsilon\,(1-S)\,d_f^{\,2}) \times \left(\frac{2d_{fe}+d}{d_{fe}+d}\right) \quad \text{.....5.3.6.1}$$

Comparison of equation 5.3.6.1 with Spielman's experimental data[139,145,148]

showed that it is only valid at low velocities, less than 1.5×10^{-3} ms^{-1} for $\beta = 0.24$, where the turbulence in the bed is insignificant. At larger velocities, the effect of turbulence grows until the equation is no longer valid; a purely empirical extension of the above equation is made to fit the data. This leads to:

$$\lambda = (8\beta(1-\varepsilon)\, d/\pi^2 \varepsilon\, (1-S)\, d_f^{\,2}) \times (V'_{cr}/V')^{0.5} \times \left(\frac{2d_{fe}+d}{d_{fe}+d}\right) \quad \ldots\ldots \quad 5.3.6.2$$

Velocity ranges and some critical velocities obtained from data of various workers are presented in Table 5.3.1. Clearly this theoretical model is not adequate for designing a coalescer element operating in these ranges.

In conclusion a number of shortcomings are apparent in previous work which has in any event been mainly confined to overall measurements, or qualitative observations of separation performance without reference to the effect of inlet drop size. When drop size has been specified, the range has been narrow and measurement techniques have been of limited reliability. Few generally applicable principles have been established to assist in the design and scale up of liquid-liquid coalescers and selection is by trial and error. This is not entirely surprising in view of the interactions between operating parameters summarised in Table 5.3.2.

TABLE 5.3.1

SUPERFICIAL VELOCITY RANGES AND CRITICAL VELOCITIES

Investigator and Reference	Min. Velocity $ms^{-1}\left(x\ 10^{-2}\right)$	Max. Velocity $ms^{-1}\left(x\ 10^{-2}\right)$	Critical Velocity $ms^{-1}\left(x\ 10^{-2}\right)$
Cordes (149)	0.010	1.10	> 1.0
Spielman (139)	0.014	1.70	0.15
Vinson (150)	0.025	2.08	< 0.025
Burtis and Kirkbride (19)	0.027	0.66	0.50
Sareen et al (20)	0.1	1.80	
Langdon et al (113)	0.071	0.508	
Sherony (151)	0.269	4.87	
Farley and Valentine (8)	0.311	0.78	
Hazlett (132)	0.35	25.0	
Hazlett and Carhart (134)	0.83	25.0	
Bitten and Fochtman (135)	1.02	3.05	

TABLE 5.3.2

LIST OF VARIABLES

Variables	1. Inlet drop size distribution 2. Phase ratio of continuous to dispersed phase 3. Superficial velocity of dispersion 4. Choice of dispersed phase 5. Choice of continuous phase 6. Oil-in-water or Water-in-oil emulsions
System Properties	σ, μ_c, μ_d, ρ_c, ρ_d, Temp., Wettability represented by contact angle
Bed Properties	1. Fibre diameter 2. Fibre material 3. Bed thickness 4. Bed voidage
Measured Variables	1. One phase and two phase flow pressure drops 2. Inlet and outlet drop size distribution 3. Type of coalescence medium

CHAPTER 6

ANALYTICAL METHODS FOR MICRO-DISPERSIONS

The determination of droplet sizes is an important step in the study of micro-dispersions. If the dispersion is monodisperse the problem is relatively simple, and only a small number of drops need be counted. In all practical cases however, the dispersion is polydisperse, and must be characterised in terms of a drop size distribution.

Various methods of measurement are available including:

(a) Optical methods such as microscopy, using manual or automatic scanning[155].

(b) Reflectance[156].

(c) Light Scattering[157].

Alternatively, use may be made of sophisticated equipment such as:

(d) The Coulter-Counter[158].

(e) Lasers[159] to produce a hologram.

6.1 MICROSCOPY

Microscopy is the simplest but the most tedious method. A diluted sample of the emulsion is placed in the small depression in a glass slide. The various size ranges are then determined by matching against a calibrated graticule situated in the eye-piece of the microscope. Not less than 300 droplets should be classified[160]; alternatively photographs may be taken for sizing later. By the attachment of a prism to the eye-piece, the image can be projected onto a screen for greater magnification. Clearly there must be adequate contrast; i.e. sufficient difference in refractive index between the droplets and the continuum.

With optical microscopy only a sample is required for analysis.

The light microscope is applied most efficiently in the range 0.25×10^{-6} to 20×10^{-6} m. The lower limit is imposed by the resolving power of the microscope; the upper limit is determined by the thickness of the particle in relation to the depth of field of the optical system. Obviously the sample must be representative, i.e. care must be taken that small droplets are not carried away. Furthermore the method of slide mounting is critical since in a suspension larger droplets may settle rapidly and not be in focus thus giving an uneven droplet count. Accuracy is dependent on the rigourousness of counting and sizing; the number of droplets counted depends on the total number representative of the mother sample. Dispersions with uniform size distribution require less droplets to be counted than those with a broad size distribution.

Several methods have been proposed to eliminate the tedium of visual counting using automatic scanning[155]. However since these techniques are lengthy, especially with manual counting, they were not adopted in the present work in which numerous samples were required for monitoring the inlet emulsion during each experiment.

6.2 REFLECTANCE:

A linear relationship has been found between the percentage reflectance of coloured emulsions and droplet size data determined microscopically[156]. For droplet sizes in the range 1×10^{-6} m to 30×10^{-6} m, the percentage reflectance R' increased as droplet diameter decreased. The equation proposed was:

$$\log R' = -b \log D_s + \log e \quad \text{.....6.2.1}$$

Since

$$D_s = \frac{6\,\phi'}{A_s} \quad \text{.....6.2.2}$$

Therefore $$R' = \frac{eA_s^b}{(6\emptyset')^b} \quad \ldots\ldots\ldots\ldots\ldots\ldots\ldots\ldots 6.2.3$$

That is, the percentage reflectance was proportional to some power of the interfacial area.

This technique gives only an average particle size and special equipment is required[161-163]. It was not considered here since drop size distribution measurements are essential when studying mechanisms of coalescence.

6.3 LIGHT SCATTERING

Light scattering can be divided into three classes dependent upon the size of the droplet relative to the wavelength of the incident light and its refractive index relative to that of the continuum[157].

(a) Rayleigh Scattering: Droplets less than one tenth of the wavelength of the incident light in diameter, i.e. about 0.05×10^{-6} m.

(b) Debye Scattering: Droplet size is not small relative to the wavelength of the incident light and refractive index of the dispersed phase is within 10% of that of the continuum.

(c) Mie Scattering: For large droplets of high relative refractive index. This is more applicable to this study.

The main deterrent to the use of the Mie theory of light scattering is its complexity. Furthermore it is only valid for monodispersed systems or for determining an average drop size for a narrow distribution. The effects of polydispersed systems and multi-scattering are ill-defined.

6.4 THE COULTER COUNTER

The Coulter Counter is an analytical equipment used for measuring

the size distribution of solid particles or immiscible droplets in a dispersion, the continuous phase of which is a liquid of low resistivity, by measurement of a resistance change between two electrodes. A schematic diagram of the principle of operation is shown in Figure 6.4.1. Unfortunately its application is limited to oil-in-water emulsions since the sample must be diluted with an electrolyte before examination. The diluted dispersion is stirred throughout the course of the test to ensure that the oil droplets are uniformly dispersed and may be stabilized to avoid changes. The electrolytes used include 0.9% sodium chloride solution and 2% calcium chloride solution; a complete list is given in reference (158).

A glass tube of special design which contains an electrode is introduced into the beaker containing the diluted sample and a second electrode is placed in the beaker. The top of the tube is connected by a stopcock to a vacuum pump and via a side arm to a mercury manometer. Near its base, the tube has a small aperture through which the droplets can flow when the stopcock is opened. Flow is initiated by a controlled vacuum. Simultaneously, the mercury moves up the right hand limb of the manometer. If the stopcock is closed, the mercury returns to its original equilibrium position. The initial motion of the mercury when the stopcock is closed activates the counting mechanism which records the relative number of drops in a given volume of dispersion.

As each droplet passes through the aperture, it displaces a volume of electrolyte equivalent to its own volume. Since the conductivity of oil droplets is very much lower than that of the aqueous phase the resistance between the electrodes changes momentarily. This change in resistance as each droplet passes through the aperture produces a voltage pulse of short duration the magnitude of which is

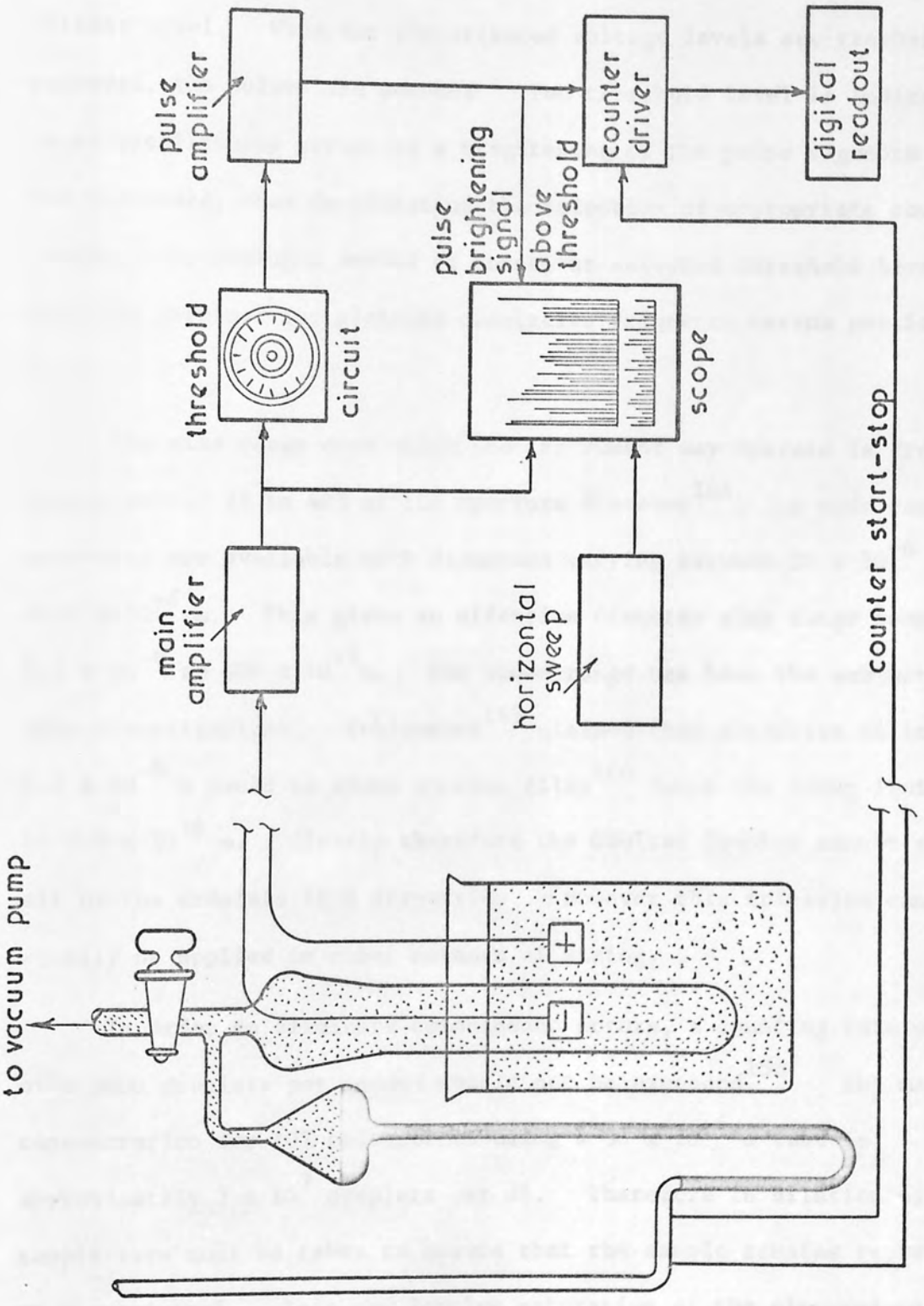

Fig. 6.4.1 Schematic diagram of coulter principle

dependent upon drop size. Each pulse is electronically amplified and fed to one of a series of threshold circuits each with an adjustable voltage level. When the pre-selected voltage levels are reached, or exceeded, the pulses are counted. The threshold level is indicated on an oscilloscope screen by a brightening of the pulse segments above the threshold, thus facilitating the selection of appropriate counting levels. By taking a series of counts at selected threshold levels, data are obtained for plotting cumulative frequency versus particle size.

The size range over which the instrument may operate is from approximately 2% to 40% of the aperture diameter[164]. A wide range of apertures are available with diameters varying between 30×10^{-6} to 1000×10^{-6} m. This gives an effective diameter size range from 0.6×10^{-6} to 400×10^{-6}m. The lower range has been the subject of many investigations. Kubitschek[165] claimed that particles as low as 0.2×10^{-6} m could be sized whereas Allen[166] found the lower limit to be 0.8×10^{-6} m. Clearly therefore the Coulter Counter cannot size all of the droplets in a dispersion. However this criticism can equally be applied to other methods of sizing.

In order to eliminate coincidence errors, a counting rate of over 5000 droplets per second should not be exceeded[158]. The maximum concentration for 10% coincidence using a 30×10^{-6} m tube is approximately 3×10^{7} droplets per ml. Therefore in dilution of the sample care must be taken to ensure that the sample remains representative of the original. This may involve saturation of the electrolyte and rigorous temperature control.

Of the various methods mentioned,this was considered to be most suitable since a large number of drops could be counted to give an

accurate size distribution with minimum statistical error. Most sources of error, discussed in Appendix A, can be eliminated by an established operating technique.

6.5 HOLOGRAPHY

Systems for recording holograms can be classified into Fraunhofer (Far Field) or Fresnel (Near Field) dependent upon the relative distance of the object from the film plane in which the hologram is recorded. Holograms used for particle size analysis are invariably far field[159].

Holography involves two steps:

(a) The recording of a hologram, by illuminating a volume of the dispersion with the collimated light from a pulsed ruby laser, using a camera.

(b) The recreation of the original scene, after developing the hologram, by illumination with a continuous He-Ne gas laser.

The reconstructed volume is a perfect model of the original with uniform magnification throughout and all objects located at their appropriate X, Y and Z co-ordinates.

Holography can be used for particle size analysis in aqueous or non-aqueous solutions under dynamic conditions. Pulsed laser holograms can be recorded in a 20×10^{-9} s exposure time to freeze the action of fluid flow. This extremely short exposure time can record 50×10^{-6} m droplets moving at velocities up to 100 m s^{-1}. This technique is under development for secondary dispersion size measurement in a separate study by Austin[167].

Other methods are available for particle size analysis, these include centrifugation, sieving and sedimentation[155]. Small angle X-ray

scattering[168] can also be used for particles of low refractive index. These are beyond the scope of this work and have not been considered in detail.

CHAPTER 7

EXPERIMENTAL WORK

An apparatus was constructed to coalesce oil water dispersions of variable drop size by passing the dispersion through a glass fibre media of uniform fibre diameter. Provision was made for variation of bed thickness, bed voidage, phase ratio and superficial velocity.

To identify the mechanisms of separation a novel design, involving conductivity measurements at different planes in the bed, was developed.

7.1 SUSPENSION PREPARATION

To evaluate the performance of a fibrous bed coalescer, it was essential to be able to form a reproducible secondary dispersion and therefore consideration was given to the following methods:

(a) Mechanical techniques such as jet break-up and the spinning disc. These are generally only appropriate for forming droplets larger than one hundred micrometres, thus making such techniques outside the scope of this work.

(b) A supersaturated condensation technique. This was used by Spielman[139] to produce a dispersion of mono-sized drops by dispersing a jet of an oil-acetone solution into larger volumes of water. The oil, being insoluble in the water, precipitated out due to supersaturation to produce a suspension of drops less than half a micrometre in diameter. Mean droplet diameters in the range one to seven micrometres were achieved by controlled coalescence after adding an empirically determined quantity of HNO_3. This technique was not suitable for the present study because it required careful control of HNO_3 concentration and a continuous supply of dispersion was desired.

(c) Precipitation of a hydrocarbon suspension by controlled heating

or cooling of a saturated aqueous solution. This method was tested experimentally using a solution of butanol in water in a one hundred millilitre capacity flask. The solution was cooled to 0^{o} C using an ice bath. This increased the hydrocarbon solubility in the water. Heating the solution to 20^{o} C using a constant temperature bath produced a dispersion which was analysed using the Coulter Counter as described in Appendix A. A mean drop size of thirteen micrometres was produced. However the need for careful control of the temperature to within $\pm$ 0.1^{o} C made this method impracticable for continuous operation.

(d) Dispersion under high shear conditions was used by Vinson[150] and Sherony[151]. Vinson[150] produced a dispersion in which most of the drops were between two and three micrometres in diameter using a homogenizer, that is by forcing the mixture through a small orifice under very high pressures. In typical operating conditions the liquids were forced through a small orifice of 10^{-8} m^{2} in area at pressures of about 34.5×10^{6} Nm^{-2}. Sherony[151] used an agitation technique with varying speeds from 13.2 to 26.7 revs s^{-1}.

Therefore, for ease of operation, a variable speed No. 12 stainless steel centrifugal pump with a recycle loop was used. Earlier work in this department [154] had shown the reliability and validity of this technique. Test runs were performed and reproducible drop size distributions in the range 1.4×10^{-6} to 56×10^{-6} m were obtained. The pump speed was varied in the range 33.3 to 86.7 revs s^{-1} and the drop size distribution was found to vary with pump speed as discussed in Section 8.2.

7.2 APPARATUS

A flow diagram of the apparatus is shown in Figure 7.1 and a

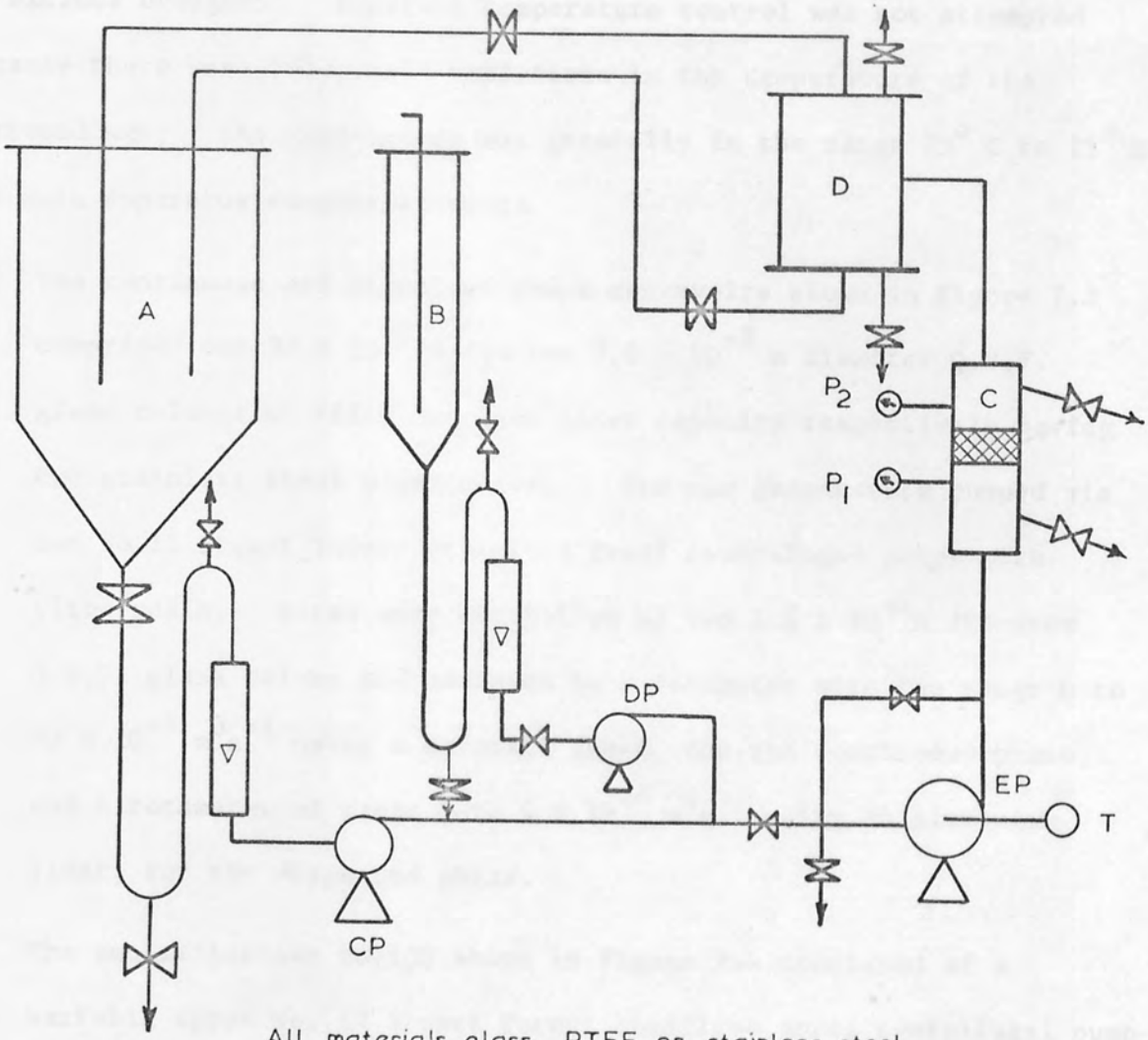

All materials glass, PTFE or stainless steel

A = Continuous phase reservoir

B = Dispersed phase reservoir

C = Coalescence cell

D = Settler

T = Tachometer

CP = Continuous phase pump

DP = Dispersed phase pump

EP = Emulsification pump (variable speed)

P_1 & P_2 = Pressure gauges

Fig . 7.1 Schematic diagram of flow system

photograph of the arrangement shown in Figure 7.2. The apparatus was installed in a hardboard cabinet affixed to a metal framework in order to exclude draughts. Accurate temperature control was not attempted because there were only small variations in the temperature of the surroundings; the temperature was generally in the range 23^{o} C to 25^{o} C. The main apparatus components were:

(a) The continuous and dispersed phase reservoirs shown in Figure 7.3 comprised one 30×10^{-2} m and one 7.6×10^{-2} m diameter Q.V.F. glass columns of fifty and five litre capacity respectively having two stainless steel plate covers. The two phases were pumped via two No.12 Stuart Turner stainless steel centrifugal pumps with viton seals. Rates were controlled by two 1.5×10^{-2}m diameter Q.V.F. glass valves and measured by a rotameter with the range 0 to 40×10^{-6} m^3s^{-1} using a Koronite float, for the continuous phase, and a rotameter of range 0 to 4×10^{-6} m^3s^{-1} using an Aluminium float, for the dispersed phase.

(b) The emulsification device shown in Figure 7.4 consisted of a variable speed No. 12 Stuart Turner stainless steel centrifugal pump with a recycle loop. The pump had a viton seal and its speed was measured using a hand tachometer.

(c) The coalescence device: Two interchangeable coalescence devices were used, one for droplet and pressure drop studies and the other for studying mechanisms within the fibrous beds. These are described in detail in Section 7.3.

(d) The settler shown in Figure 7.4 was made up of a six inch diameter Q.V.F. T-piece having a stainless steel plate at each end with upper and lower flanges for continuous phase recycle streams to be used separately; dependent upon its relative density to that of

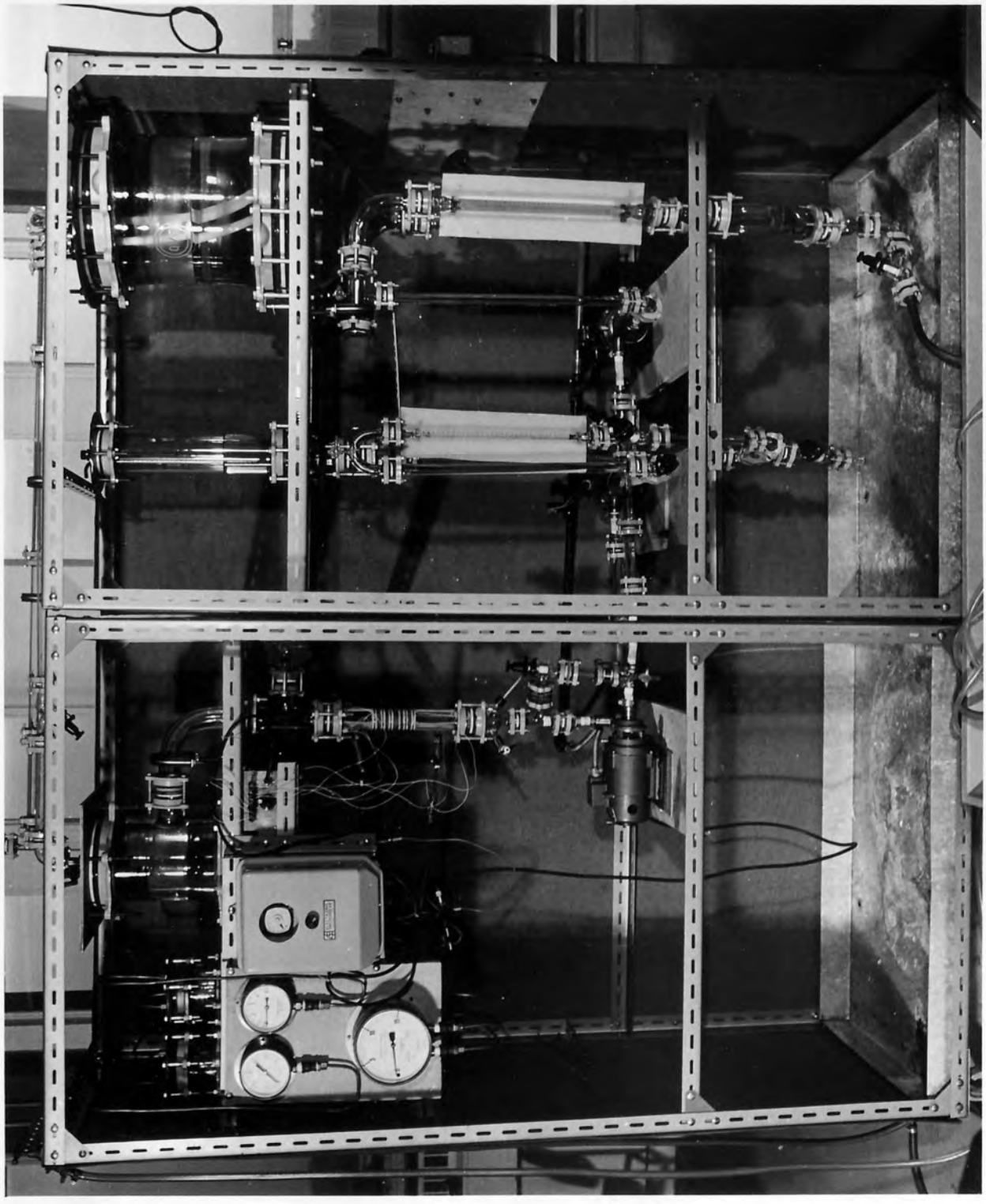

Fig. 7. 2. General arrangement of equipment

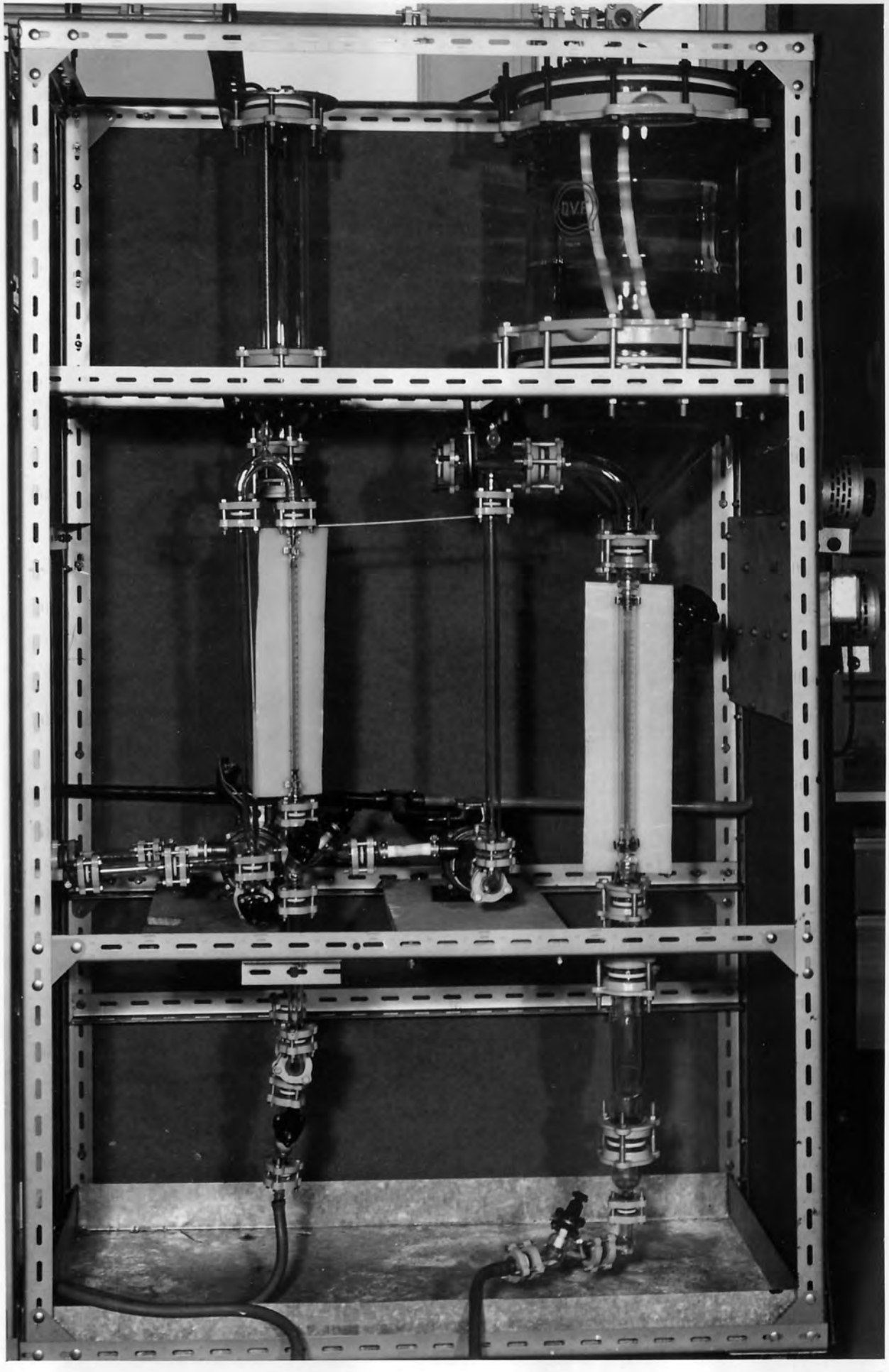

Fig. 7.3. Arrangement of continuous and dispersed phase reservoirs

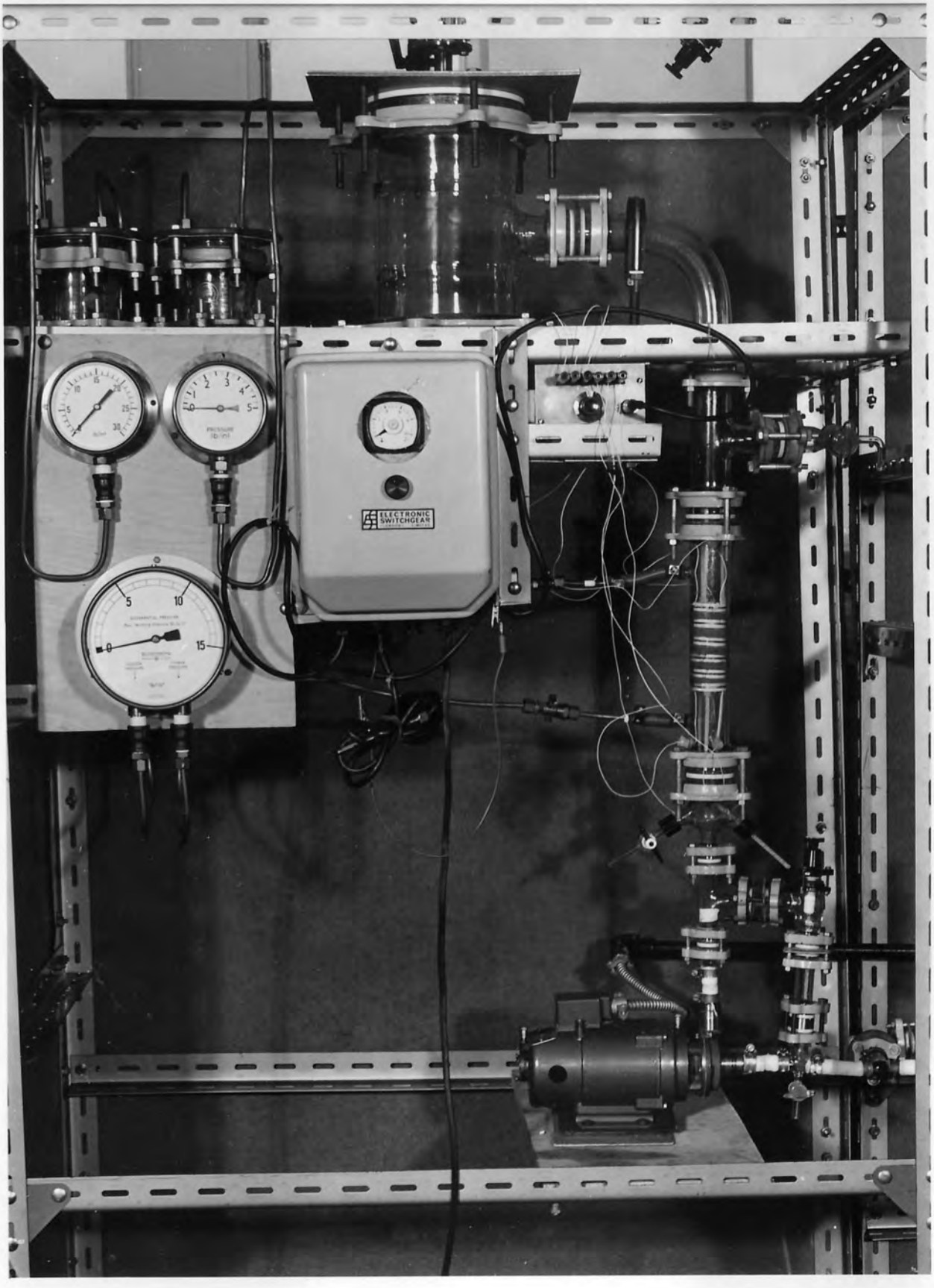

Fig. 7. 4. Dispersion generation loop
(pressure gauges and conductivity meter mounted on left side)

the dispersed phase.

The apparatus was effectively isolated from sources of external contamination and consisted primarily of Q.V.F. glass, stainless steel and short connecting sections of half inch diameter p.t.f.e. tubing. The p.t.f.e. tubing of the quality used had been shown to be inert to the phases processed[127].

7.3 THE COALESCENCE DEVICE

Each coalescence device consisted of a one and a half inch i.d. twelve inches long Q.V.F. glass section flanged at both ends. Two pressure tapping points were drilled into the glass wall approximately six centimetres from each end. Two glass sampling valves were provided as shown for inlet and exit drop size analysis. Pressure drop across the bed was determined using two pressure gauges in the range 0 to 2.1 x 10^5 Nm^{-2}, at the high pressure end, 0 to 3.4 x 10^4 Nm^{-2}, at the low pressure end, and a differential pressure gauge in the range 0 to 1.03 x 10^5 Nm^{-2} to check on the measurements. These were connected via two reservoirs which prevented the process liquids entering the gauges; this prevented damage to the gauges and acted as a 'shock absorber'; that is, to damp out minor fluctuations and give a stable reading.

Two methods were used to study the coalescence of secondary dispersions in fibrous beds:

(a) Inlet drop size and outlet drop size observations: Variation of exit drop size and pressure drop across the bed with operating variables, viz inlet drop size, phase ratio, superficial velocity and bed thickness was investigated.

A special packing holder was designed and care was taken to ensure that no obstructions existed inside the packing in order to avoid

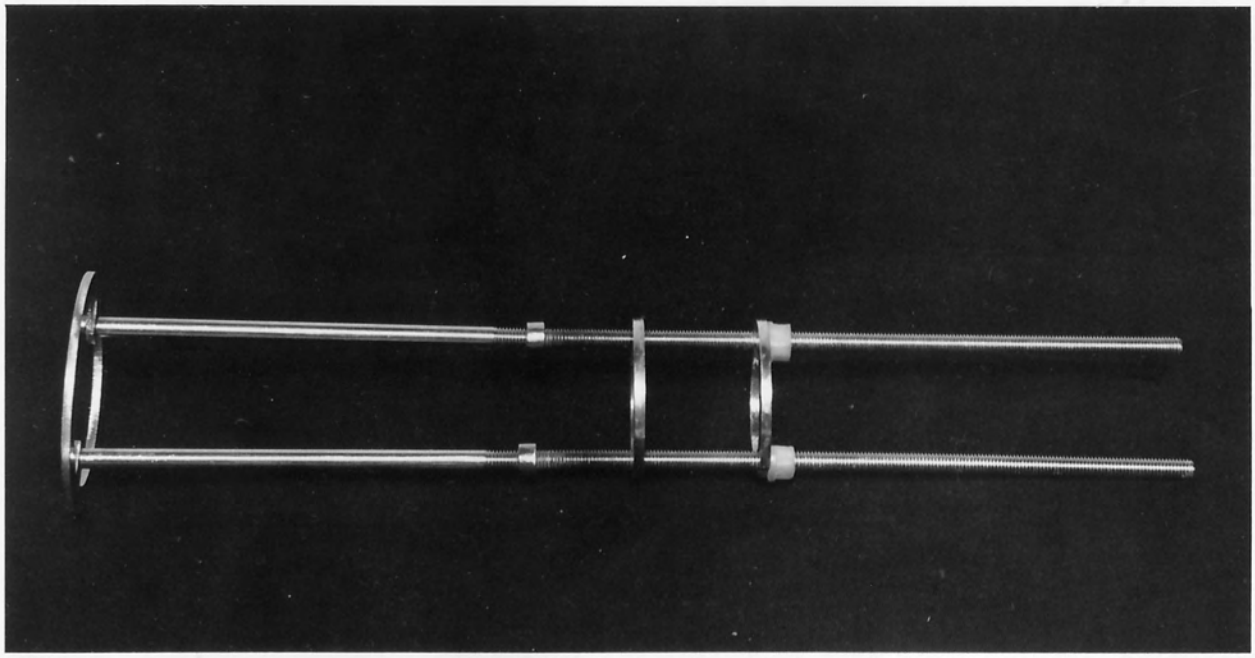

Fig. 7.5. Stainless steel packing holder

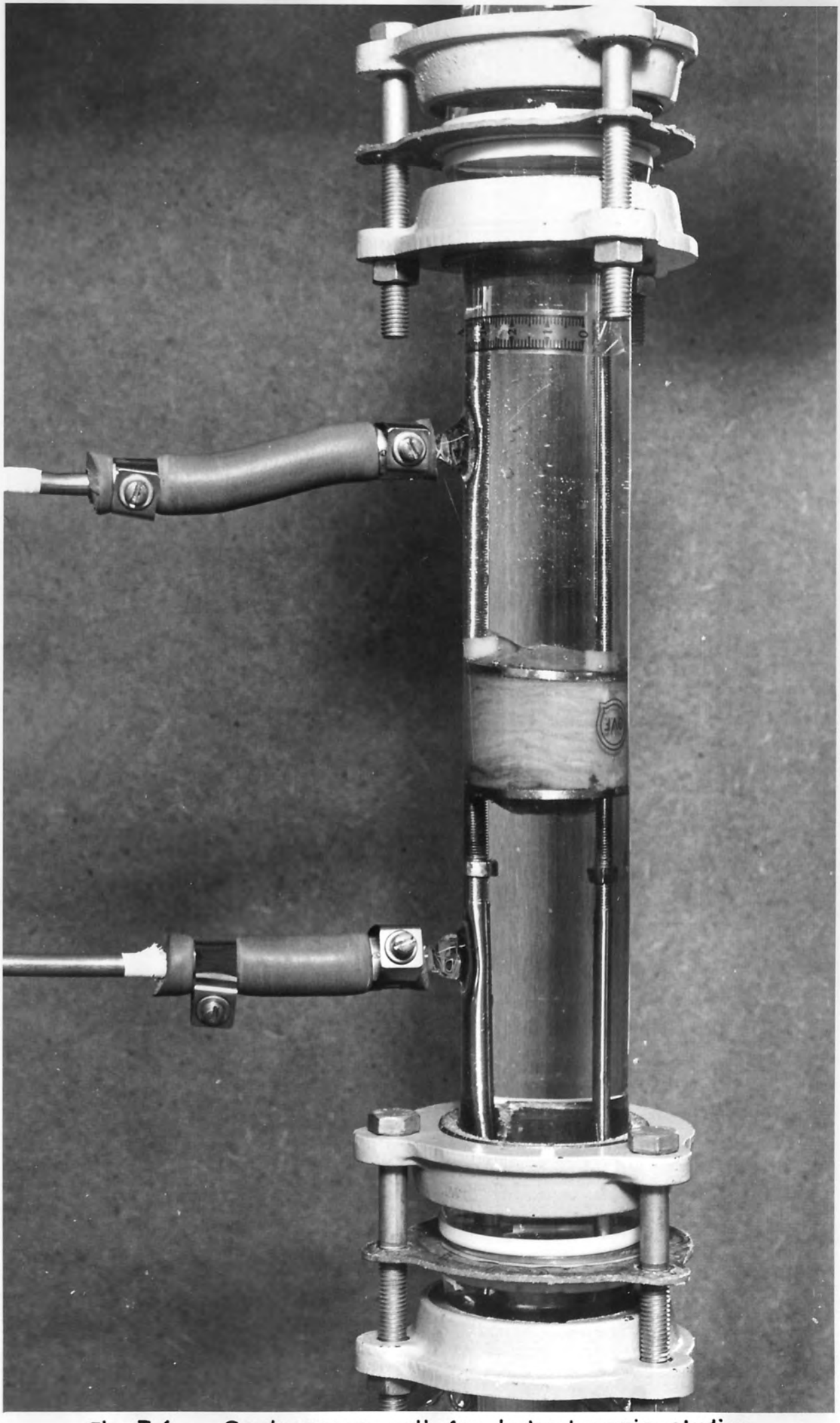

Fig. 7.6. Coalescence cell for hydrodynamic studies

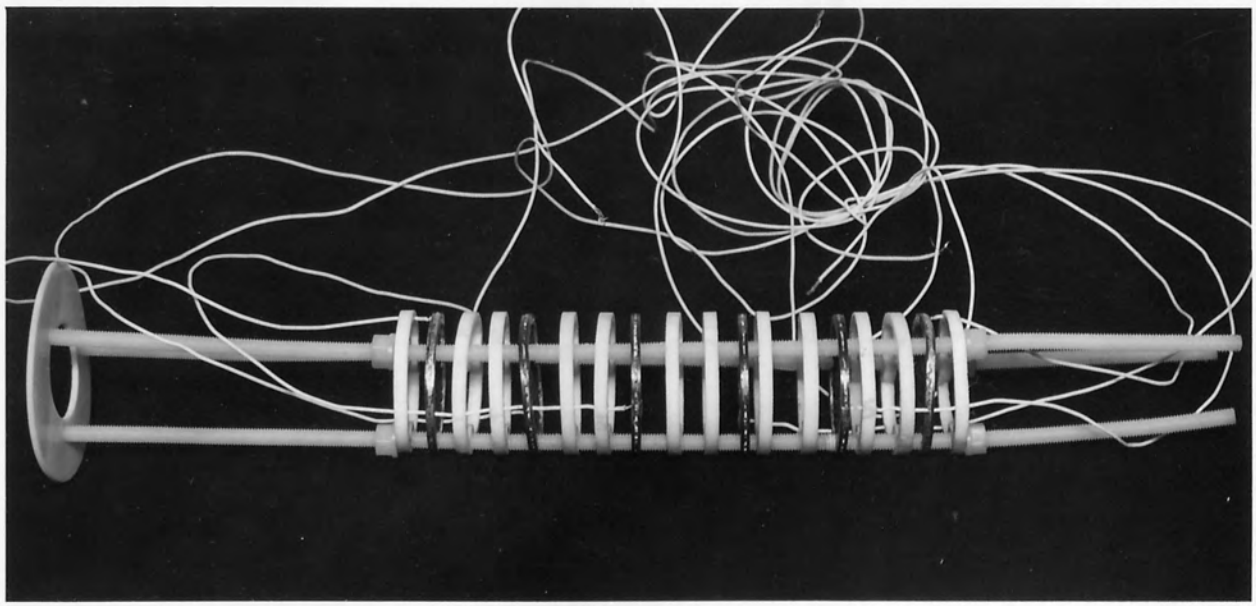

Fig. 7.7. Packing holder for conductivity measurements

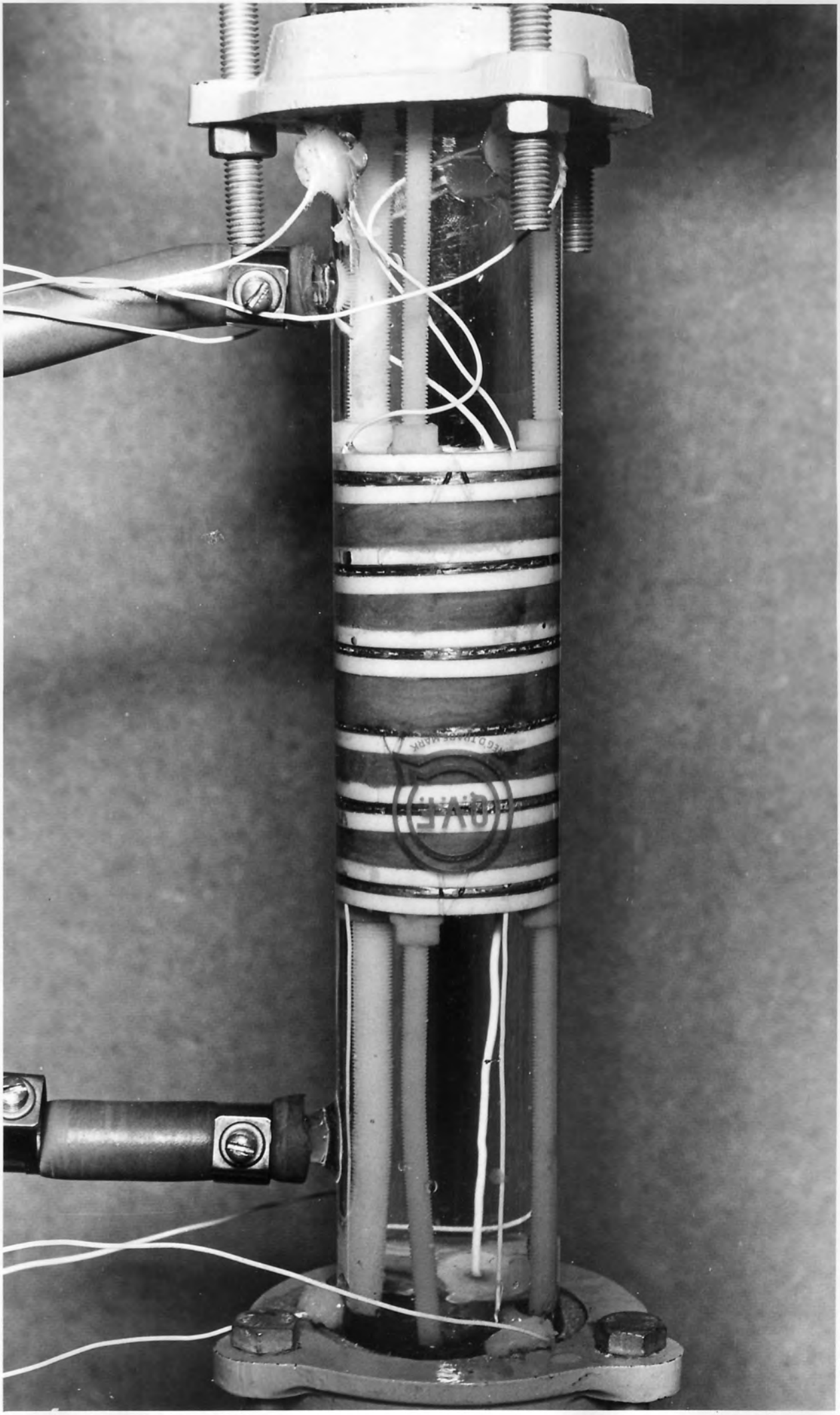

Fig. 7. 8. Coalescence cell for conductivity measurements

The six sensing plates were made from copper mesh with two millimetre holes. A p.t.f.e. insulated silver wire was soldered onto each mesh which was sandwiched between two p.t.f.e. rings to obtain a good seal. A packing section of known thickness and porosity was placed between each consecutive pair of meshes, with the wires passing through drilled holes in the sides of the meshes and p.t.f.e. rings, and out through holes in the glass column as shown in Figure 7.8. The drilled holes were sealed by a Silicon Rubber type compound which was easily removable. The wires from the copper meshes were connected to a junction box possessing a selector switch. The signal was fed into an a.c. conductivity meter with a range of 0 to 10 x 10^{-6} ohm^{-1} in order to prevent any polarization taking place. From this the conductivity at different planes along the bed could be estimated, as shown in Figure 7.4.

7.4 SELECTION AND HANDLING OF LIQUID-LIQUID SYSTEMS

Throughout the course of this investigation, the system toluene dispersed in distilled water was used. Toluene was chosen for its relatively non-toxic and non-corrosive properties as well as its availability to a fixed specification. G.P.R. grade was used to the specification given in Appendix D.

Since contamination could affect the physical properties of the system, affecting the coalescence results, special care was taken in the distillation, handling and storage of the liquids used. Toluene was distilled before each experiment to within $\pm$ 1^{o} C of its boiling point and stored in clean dark glass containers to eliminate the possibility of deterioration due to exposure to sunlight[63]. Tap water was continuously distilled in a four litre per hour capacity Vigreux column and the

resulting distilled water was stored in twenty litre capacity glass aspirators. Presaturation of the phases was achieved by contacting the continuous phase with the dispersed phase, and by agitation of the dispersed phase with distilled water in two separating vessels for four hours. The phases were then left in contact overnight at a constant temperature.

As a check on phase purity, the interfacial tension of the liquids was determined with a 'Cambridge Du Nouy Tensiometer'. In addition the interfacial tension was frequently checked throughout the experimental work to ensure that it remained constant at 34.5×10^{-3} Nm^{-1} at 25^{o} C. Toluene was found to be unaffected by the glass fibre coalescing media used. Pads of the packing were immersed in toluene for up to one month and the density, viscosity and interfacial tension were found to remain constant throughout this period. Chromotographic analysis gave a trace characteristic of the original G.P.R. toluene.

7.5 SELECTION OF FIBROUS MATERIAL

The coalescence beds were composed of phenol-formaldehyde bonded glass fibre manufactured by 'Pilkington Glass Fibre, Ltd.' with a fibre diameter of seven micrometres[169]. This material was selected because of its widespread use in commercial coalescers. The pads were cut into one and a half inch diameter discs and placed in the packing holder. Here they were compressed using the two rings, shown in Figure 7.5, to achieve the required packing thickness. A Stereoscan of the fibres used is shown in Figure 7.9.

Compression was applied to each set of three discs until a constant reduction in thickness was obtained. This ensured that a constant average porosity was attained within the desired range.

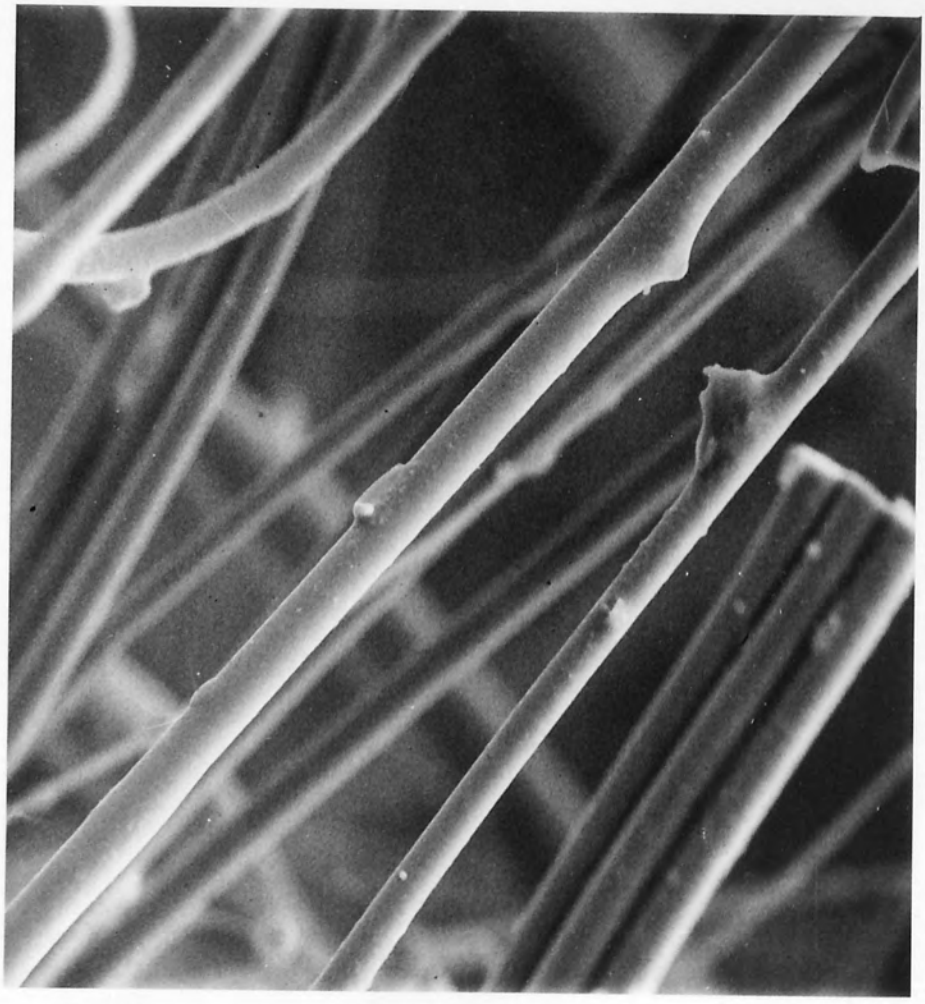

Fig. 7.9. Stereoscan of glass fibres showing surface of bed

Clean glass fibres were found to be preferentially wetted by the aqueous phase and completely unaffected by the toluene. In view of the consensus that dispersed phase wettability of the fibres is not a factor affecting secondary dispersion coalescence, and the results of a parallel study initiated on single fibres described in Section 8.13, no dispersed phase wetted packings were used in this study.

7.6 BED VOIDAGE DETERMINATION

The initial bed voidage was determined using a displacement method. Distilled water was pumped through the bed at high flow rates, 6×10^{-2} ms^{-1}, for fifteen to twenty minutes to displace all air bubbles. Some of the water was then drained down the bed to a predetermined level fifteen centimetres above the packing. This level was ascertained using a travelling microscope and was taken as the datum. A measured volume, twenty millilitres, of water was removed from the column and the distance the water level dropped was measured. This procedure was repeated until the water level was about one centimetre above the packing. These initial measurements were used to obtain an average value for the water level drop per twenty millilitres since the column diameter could not be assumed uniform. Following this, twenty millilitres were collected and the water level receded to beneath the packing. This reduction in the water level was measured, from this value together with the packing thickness, packing bulk volume and the initial average value recorded, the bed voidage was calculated, as shown in Appendix C.

Voidages in the range 0.90 to 0.94 were utilized in this study. This was chosen on the basis of the previous work reported by Sherony[151] and Spielman[139] who used voidages in the range 0.70 to 0.95. This was an average voidage determined over the whole bed and no attempt was made

to measure the pore size distribution. An average fibre pitch of seventy micrometres was determined using the Stereoscan shown in Figure 7.9.

7.7 CLEANING PROCEDURE

Since it has been shown with primary dispersions that coalescence results are affected by impurities, great care was taken in cleaning the apparatus. The following procedure was adopted:

After each set of experiments the equipment was flushed through with hot distilled water. It was then filled with a solution of 2% Decon in distilled water and was allowed to stand for two days, after which the apparatus was drained. Care was taken to prevent any of the detergent solution remaining in the equipment since it would act as a stabilizer and affect the coalescence results drastically. This is discussed in Chapter 5. The equipment was finally washed thoroughly with distilled water and then allowed to stand full of distilled water for one day. Upon completion of cleaning, the coalescence packing cell was placed in position, the continuous and dispersed phase reservoirs filled and the equipment operated as follows.

7.8 OPERATING PROCEDURE

Water was pumped through the coalescence cell at a flow rate of 6×10^{-2} m s^{-1} until the settler was full; the water was then recycled and this was continued for fifteen to twenty minutes to ensure that all the air trapped in the bed had been displaced. The water flow rate was then reduced to 0.6×10^{-2} m s^{-1} and the single phase pressure drops across the bed were determined and recorded with incremental increases in water flow rate.

The water flow rate was then reduced to 1×10^{-2} m s^{-1} and dispersed phase was introduced at a controlled flow rate to yield the required dispersion phase ratio e.g. initially 3% by volume dispersed phase. The mixture passed through the emulsification device with the recirculating pump running at a speed preset to achieve the required inlet drop size distribution. The dispersion so formed was pumped through the coalescence device for fifteen to twenty minutes until steady state had been attained. This condition was judged to have been achieved when the pressure drop remained constant for five minutes and there was no change in exit drop size. A sample of the dispersion was taken, for inlet drop size analysis, as described in Section 7.9; three photographs were taken at the exit side of the bed for exit drop size analysis as discussed in Section 7.10. The two phase flow pressure drop across the bed was recorded. The flow rates of both phases were then increased incrementally at a constant phase ratio and results recorded as before.

The same packing was used for a set of three experiments to examine the effect of inlet drop size and phase ratio on exit drop size and pressure drop across the bed. Before starting each experiment, it was noticed that the single phase flow pressure drop increased, possibly due to the presence of entrapped liquid drops within the bed but after washing the bed at high water flow rates, of the order of 6×10^{-2} m s^{-1}, and then draining, the original pressure drop value was achieved. This was taken as a criteria that the bed's condition had not changed, and that each experiment with a particular bed had been carried out at exactly the same packing conditions.

The same operating procedure was used with the second coalescence device and conductivity values at different planes in the bed were recorded for both one phase and two phase flow.

7.9 INLET DROP SIZE ANALYSIS

Possible methods for particle size analysis are discussed in Chapter 6. In this work a Coulter Counter-Industrial Model ZB was used; this facilitated particle size analysis over the range 0.6×10^{-6} to 300×10^{-6} m. It had an access for a Model M2 Volume Converter which eliminated up to 90% of operator responsibility for computation. These are shown in Figure 7.10.

The Coulter Counter determined the number and size of particles suspended in an electrically conductive liquid e.g. 0.9% Sodium Chloride solution. For this purpose the suspension was forced to flow through a small aperture having an immersed electrode on either side. As a drop passed through the aperture, it altered the resistance between the electrodes. This produced a voltage pulse of short duration whose amplitude was proportional to the drop size. The series of pulses were then amplified and transferred to the pulse-height analyzer, which sorted and counted the signals according to amplitude. The spectrum of amplitudes accumulated could be converted directly to a spectrum of particle sizes through calibration with monodisperse particles of known size. This is discussed in Appendix A.

The Model M2 Volume Converter, through the use of a Timer Circuit and a Divider Circuit, provided relative cumulative or differential volume of the sample, thereby reducing data handling. Assuming constant density of the sample, which was justified within the range 3% to 7% phase ratios involved, volume and weight percentages were interchangeable.

The Coulter Counter had a facility for analysing samples of 0.05×10^{-6}, 0.5×10^{-6} and 2×10^{-6} m^3 volume and was fitted with a one hundred and forty micrometre diameter aperture tube. The calibration particles

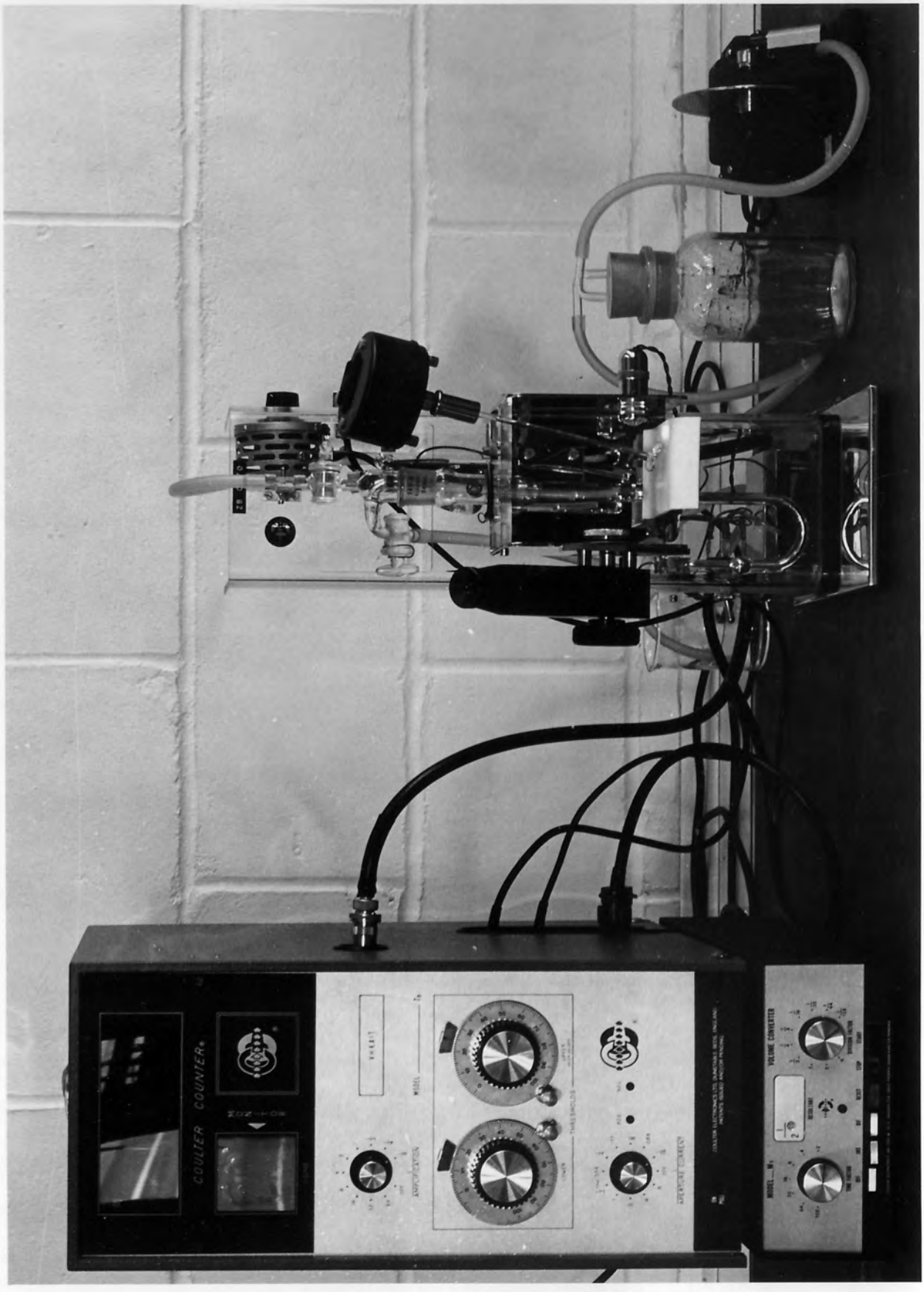

Fig. 7. 10. Coulter counter model ZB with M2 volume converter

were Lycopodium powder of twenty eight micrometres diameter.

Samples for inlet drop size analysis were taken via the sampling valve. The sampling rate was kept sufficiently small, two millilitres per second, so that no significant disturbance occurred in flow conditions. A ten millilitre sample was removed and diluted into twenty five millilitres of millipore filtered distilled water with dissolved Hyamine 2389 to stabilize the drops, and so prevent self-coagulation in the sample beaker. Five millilitres was then withdrawn and diluted into two hundred and fifty millilitres of 0.9% sodium chloride solution, the electrolyte used for analysis, and dissolved Hyamine 2389. The dilution served to decrease the number counts to values suitable for Coulter Counter analysis. If the count was high, errors in counting could arise due to the occurrence of coincidence particles in the aperture as well as counting losses resulting from the incapability of the pulse-height analyzer to process electronic pulses occurring in too rapid succession. The quantitatively diluted sample was then analysed using the Coulter Counter apparatus as discussed in Appendix A.

7.10 EXIT DROP SIZE ANALYSIS

Of the methods available for primary drop size analysis it was concluded that photography was the best[170]. Recently Wilkinson[127] analysed photographs of a polydispersion automatically using a Quantimet. However, no means of allowing for spurious results, due to overlapping drops, has yet been developed. In this work, semi-automatic counting of drops was performed using the Zeiss TG3 Particle Counter shown in Figure 7.11. Photographs of the exit drops at the wall of the coalescence device were taken using a Nikkormat still camera fitted with an f 3.5, 55 m.m. Nikkor Lens on Kodak TriX-Pan

Fig. 7.11. Zeiss TG 3 particle counter

35 m.m., 400 A.S.A. film. Shutter speed of 1×10^{-3} s was used to 'freeze' the movement of the drops with illumination provided by a Bowen Monolite Flash Unit.

The negatives were enlarged to give an overall magnification of the true drop size and were printed on grade 4 'Bromesko' paper. This gave sufficient magnification and contrast for counting. A Honeywell 316 digital computer was used to analyse the measurements as described in Appendix B. At least 300 drops were counted for each measurement taken from three negatives. Calibration of the counting technique was performed by photographing a graduated millimetre scale on the outside wall of the device. The enlarged photograph of the scale was then compared with readings on the counter. Distortion and magnification caused by the circular wall of the column were found to be negligible. This was shown by photographing and enlarging a similar scale inside the column under exactly the same conditions.

CHAPTER 8

DISCUSSION OF RESULTS

In the present investigation, the mechanisms involved in the coalescence of a secondary dispersion of a selected pure organic liquid in distilled water have been studied using the equipment and techniques described in Chapter 7. These mechanisms were not previously well understood, partly because of interactions between the operating parameters listed in Table 5.3.2 but also because of the difficulty of observing conditions inside the bed. Even in this work an indirect method had to be used to identify conditions within the bed.

The absence of previous experimentation covering the full range of operating parameters was discussed in Chapter 5. Clearly however for the systematic design of coalescers, it would be advantageous to understand the dependence of steady-state operation and pressure drop upon operating parameters. Therefore this study was divided into four main areas:

(a) Correlation of single phase flow pressure drops.

(b) Measurement of two phase flow pressure drops and the effect of operating parameters, i.e. inlet drop size distribution, phase ratio, superficial velocity, packing thickness and voidage.

(c) Determination of the effect of the operating variables listed in (b) upon the coalescence performance using mean exit drop size as a measure of efficiency.

(d) Hold up measurements by a conductivity technique at different planes in the bed, and determination of the effect of operating parameters.

The results are presented and discussed in this chapter but the insight obtained into the mechanisms within the bed, and a model for droplet behaviour, are presented in Chapter 9.

8.1 SINGLE PHASE FLOW PRESSURE DROP

This work was undertaken:

(a) To enable two phase flow pressure drop through fibrous beds to be compared with that for one phase flow, and

(b) To determine the voidage and so allow the hold up of the dispersed phase within the bed to be calculated.

Flow in packed beds is described by the Blake-Kozeny equation in the laminar region, i.e. Re < 10, and by the Burke-Plummer equation in the turbulent region, Re > 1000. In the transition region the Ergun equation, representing the sum of these two, applies[171]. The Ergun equation is:

$$\frac{\Delta p_x g}{L} = \frac{150\mu_c V}{d_f^2} \times \frac{(1-\varepsilon)^2}{\varepsilon^3} + \frac{1.75\rho_c V^2}{d_f^2} \times \frac{1-\varepsilon}{\varepsilon} \quad \ldots\ldots\ldots \quad 8.1.1$$

Blake-Kozeny Burke-Plummer

In a fibrous bed the velocity is normally within the range, 0.01×10^{-2} ms^{-1} to 5.0×10^{-2} ms^{-1}, as shown in Table 5.3.1. The range of Reynolds Number is therefore 0.07×10^{-2} to 0.35. These low values arise because of the small fibre diameter, e.g. seven micrometres. Thus, if single phase and two phase flow in fibrous beds is analagous to single phase flow in packed beds, the Blake-Kozeny equation should be applicable in the form:

$$\Delta p = \frac{150\ \mu_c\ L}{g\ d_f^2} \times \frac{(1-\varepsilon)^2}{\varepsilon^3} \times V \quad \ldots\ldots\ldots\ldots\ldots\ldots \quad 8.1.2$$

Hence

$$\ln \Delta p = \ln \left(\frac{150\ \mu_c L}{g d_f^2} \times \frac{(1-\varepsilon)^2}{\varepsilon^3}\right) + \ln V \quad \ldots\ldots\ldots \quad 8.1.3$$

Therefore a plot of pressure drop against velocity on logarithmic co-ordinates should give a straight line with a slope of unity. A plot of pressure drop

against packing thickness on arithmetic co-ordinates should also give a straight line.

Typical plots of experimentally determined one phase flow pressure drop against superficial velocity are shown in Figures 8.1 to 8.14. These cover a range of Reynolds Number from 0.042 to 0.21 and exhibit a slope of unity. Similar slopes were obtained in work, initiated to study coalescence at low phase ratios and velocities, with Reynolds Numbers in the range 0.007 to 0.098[172]. Graphs of single phase flow pressure drop against packing thickness are shown in Figure 8.15. These also show good agreement with the Blake-Kozeny equation.

In earlier studies of the flow of gases[173], the constant in the Blake-Kozeny equation was reported to be a function of the packing voidage. In the present investigation however average bed voidages determined from the pressure drop data using equation 8.1.2 and determined experimentally using the displacement method discussed in Section 7.6 are in good agreement. Thus over the range investigated, $0.9 < \varepsilon_1 < 0.94$, the equation constant was independent of void fraction. Sherony[151] obtained a similar result for voidages in the range $0.7 < \varepsilon_1 < 0.92$. Calculated and experimentally determined voidages are shown in Table 8.1.

The data in Table 8.2 shows that the value of the calculated voidage does not vary with superficial velocity. This is to be expected since all the voids are occupied by the continuous phase. However the data confirms that no bed compaction or solids deposition occurred following prolonged operation.

An attempt was made to fit some of the data to the Rosenfeld correlation in the form:

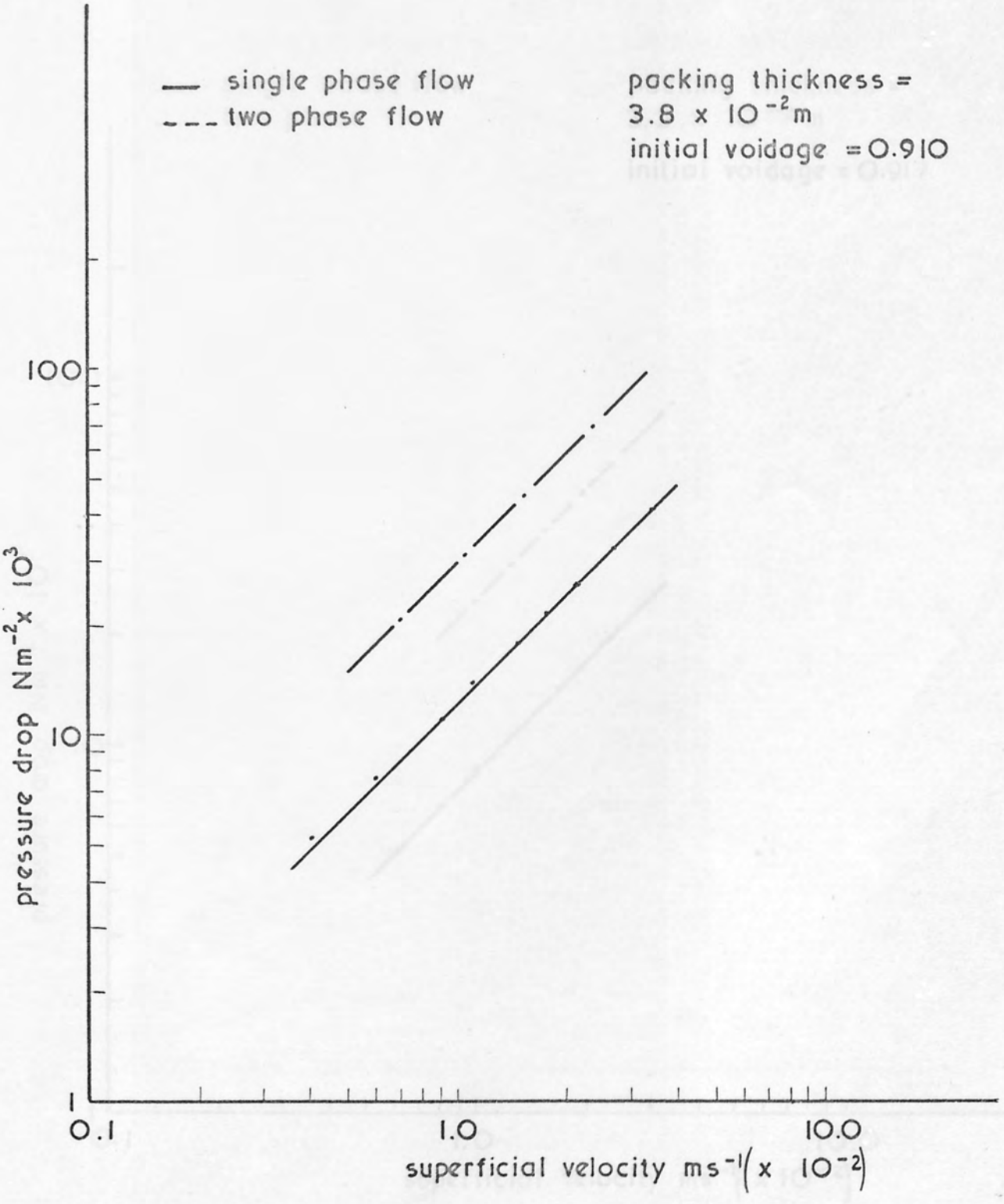
single phase flow
two phase flow
packing thickness =
3.8 x 10⁻²m
initial voidage = 0.910
100
10
1
pressure drop Nm⁻² x 10³
0.1
1.0
10.0
superficial velocity ms⁻¹ (x 10⁻²)

Fig. 8.1 .

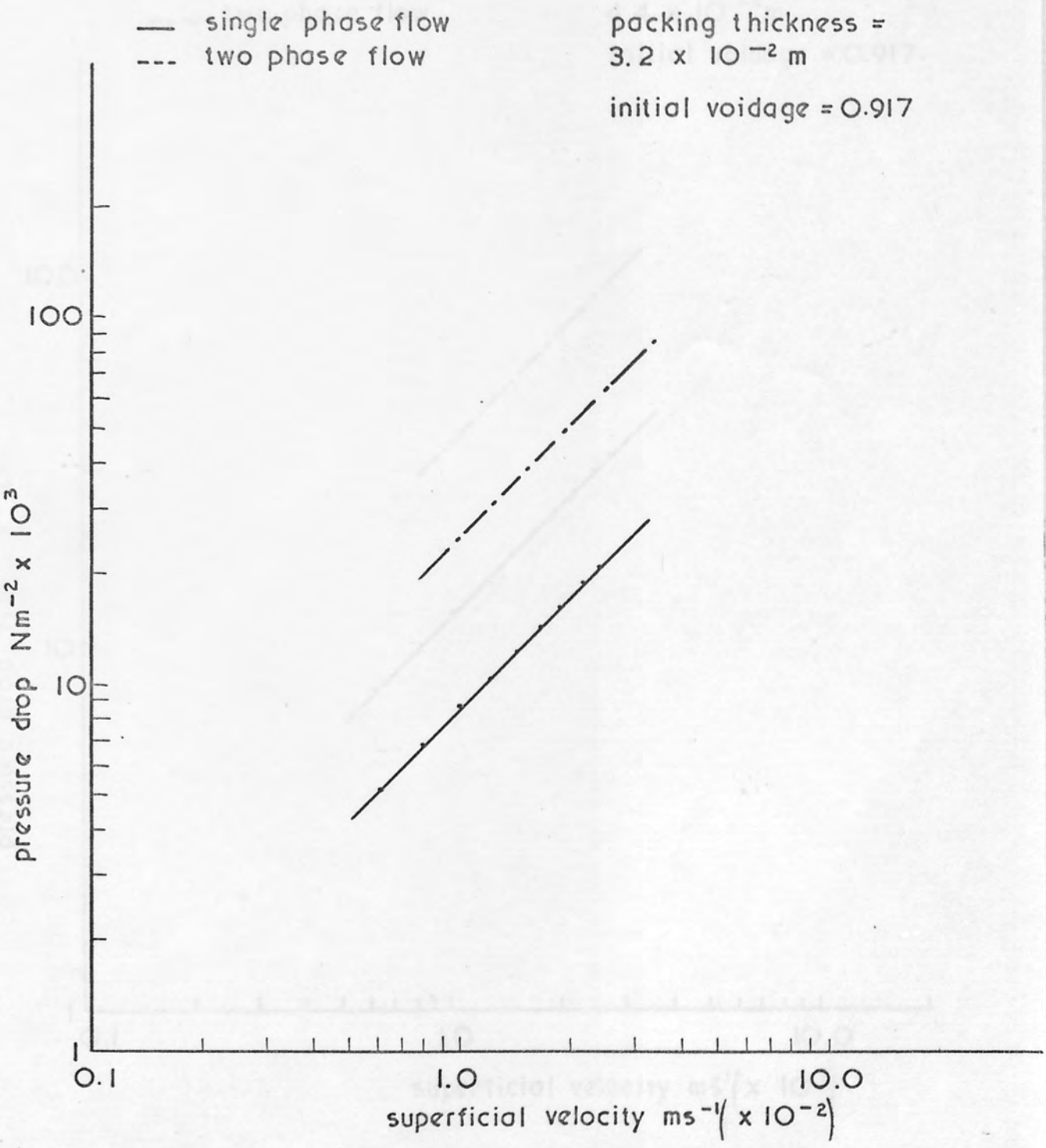
single phase flow
two phase flow
packing thickness = 3.2 x 10⁻² m
initial voidage = 0.917
100
10
1
pressure drop Nm⁻² x 10³
0.1
1.0
10.0
superficial velocity ms⁻¹ (x 10⁻²)

Fig . 8.2

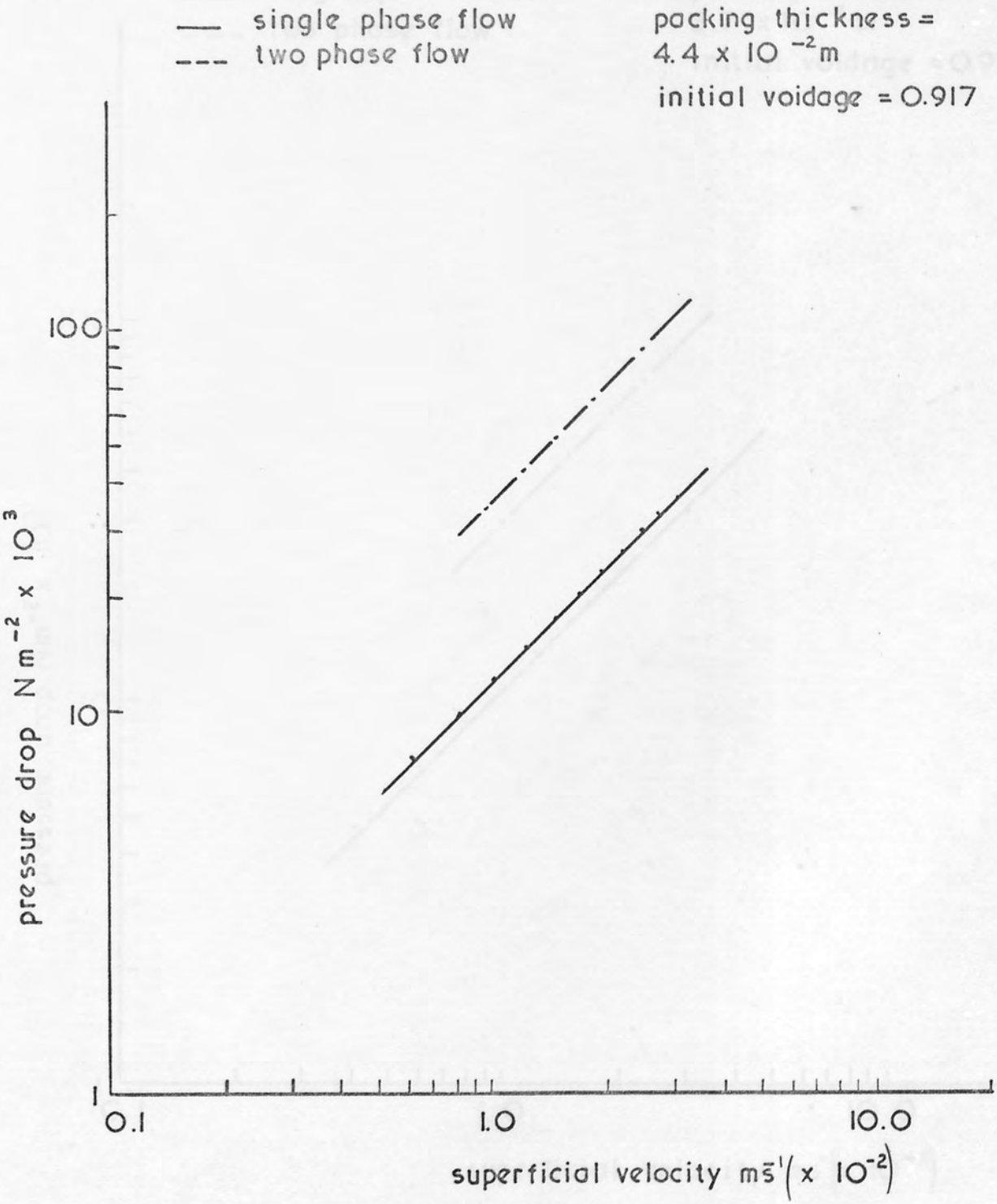
single phase flow
two phase flow
packing thickness =
4.4 x 10 -2 m
initial voidage = 0.917
100
10
1
pressure drop N m-2 x 10 3
0.1
1.0
10.0
superficial velocity ms-1 (x 10-2)

Fig. 8.3

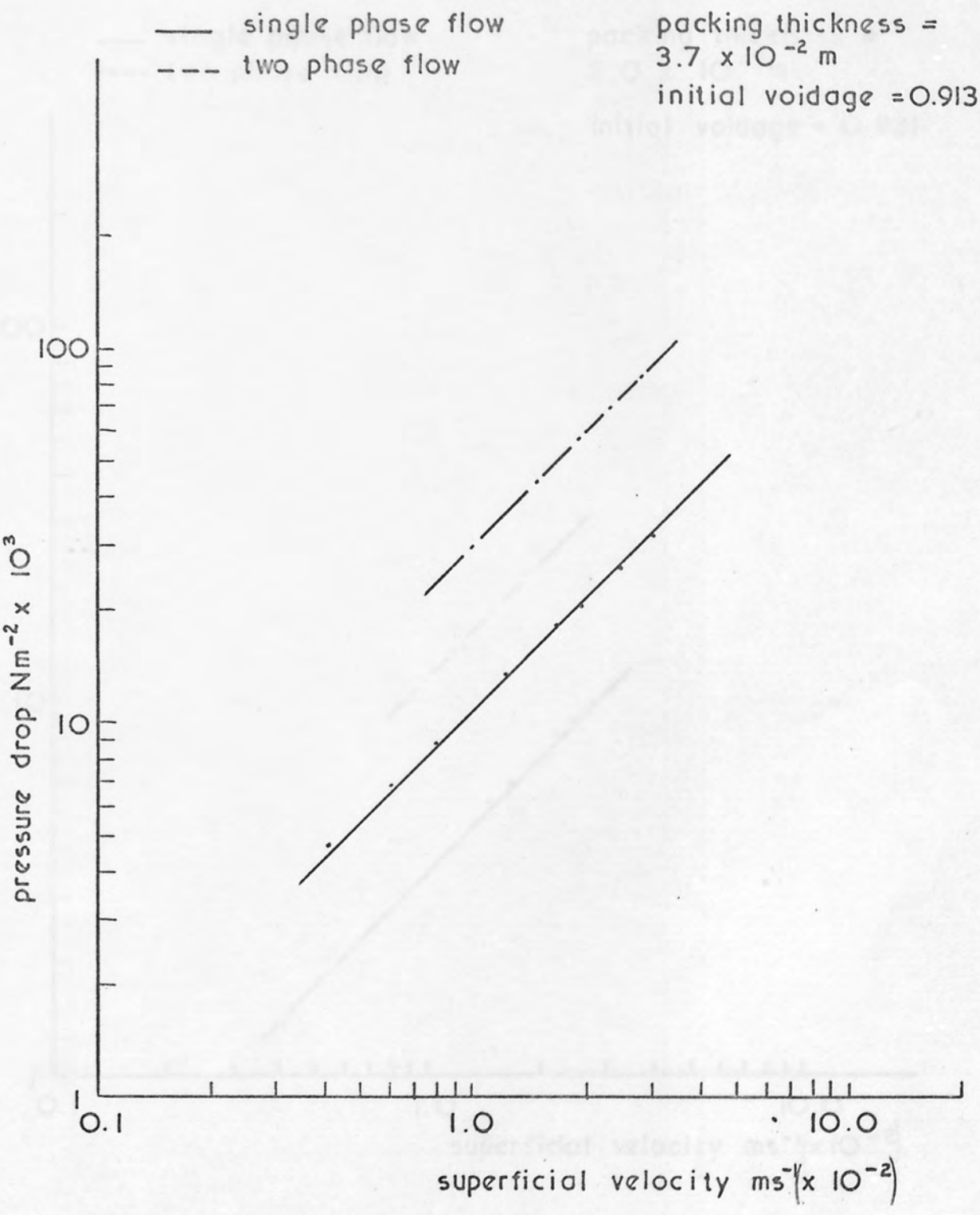
single phase flow
two phase flow
packing thickness = 3.7 x 10⁻² m
initial voidage = 0.913
100
10
1
pressure drop Nm⁻² x 10³
0.1
1.0
10.0
superficial velocity ms⁻¹ (x 10⁻²)

Fig. 8.4

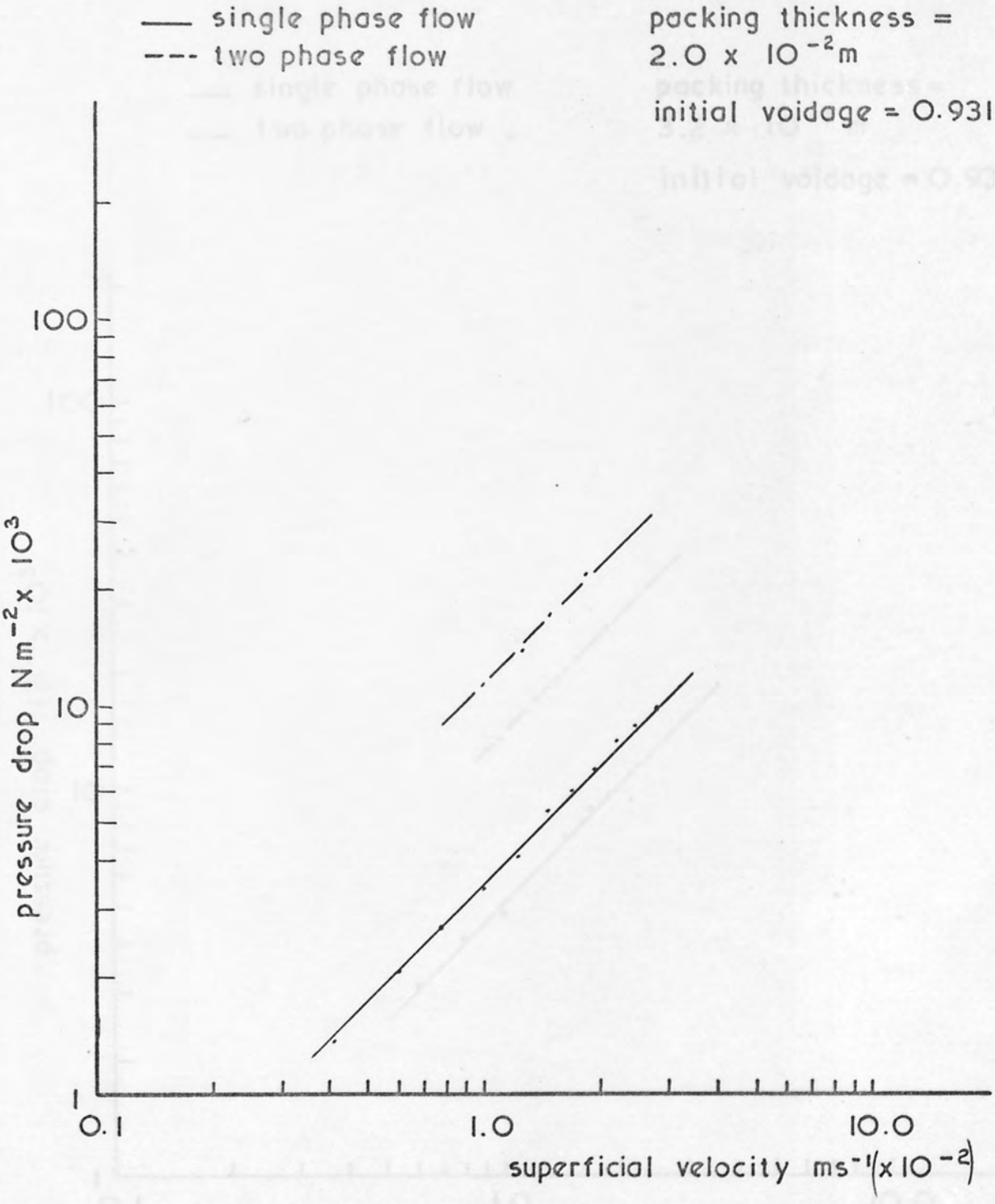
—— single phase flow
--- two phase flow
packing thickness =
2.0 x 10⁻²m
initial voidage = 0.931
100
10
1
pressure drop Nm⁻²x 10³
0.1
1.0
10.0
superficial velocity ms⁻¹(x 10⁻²)

Fig . 8. 5

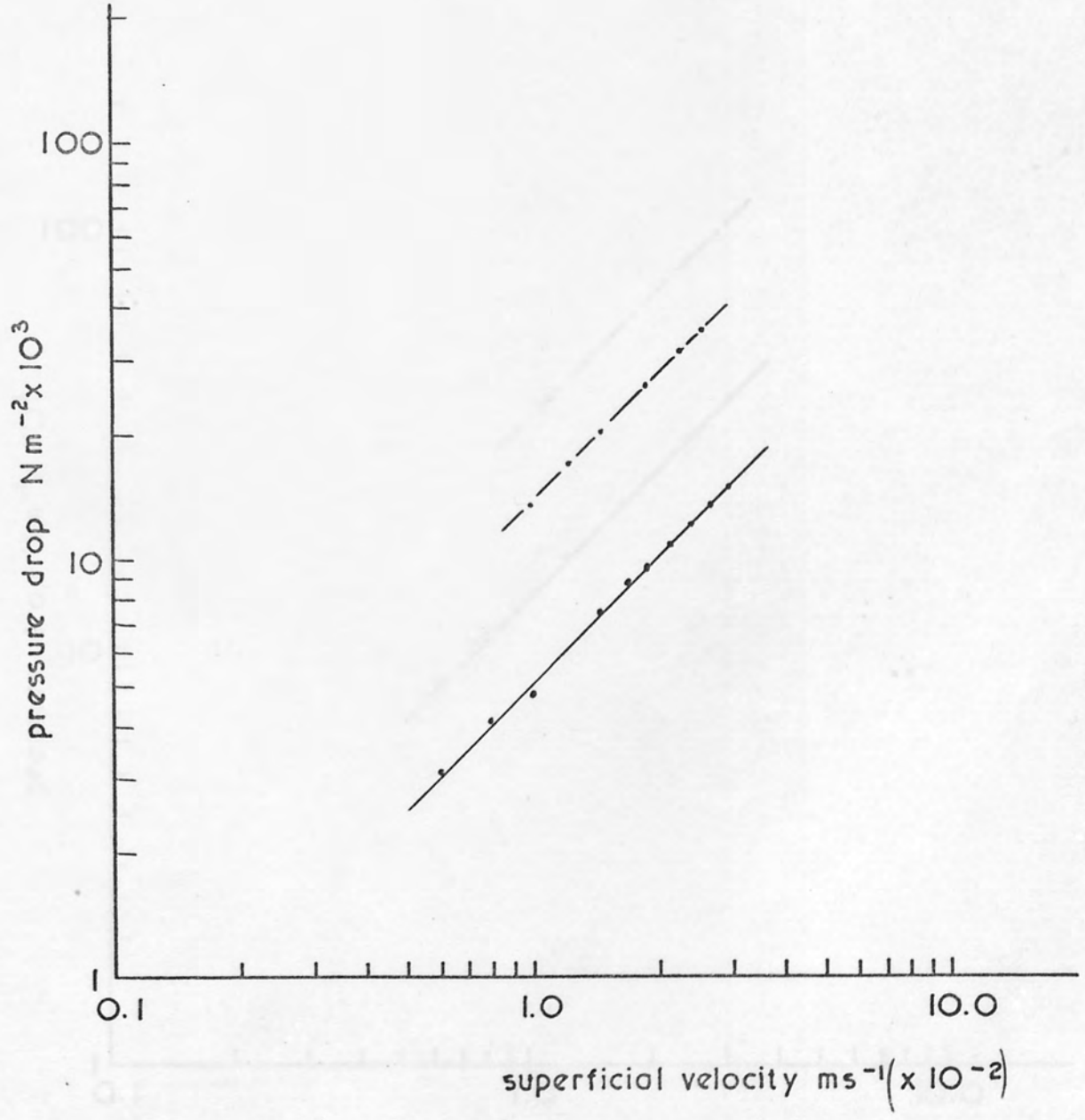
single phase flow
two phase flow
packing thickness = 3.2 x 10⁻² m
initial voidage = 0.934
100
10
1
pressure drop N m⁻² x 10³
0.1
1.0
10.0
superficial velocity ms⁻¹ (x 10⁻²)

Fig. 8.6

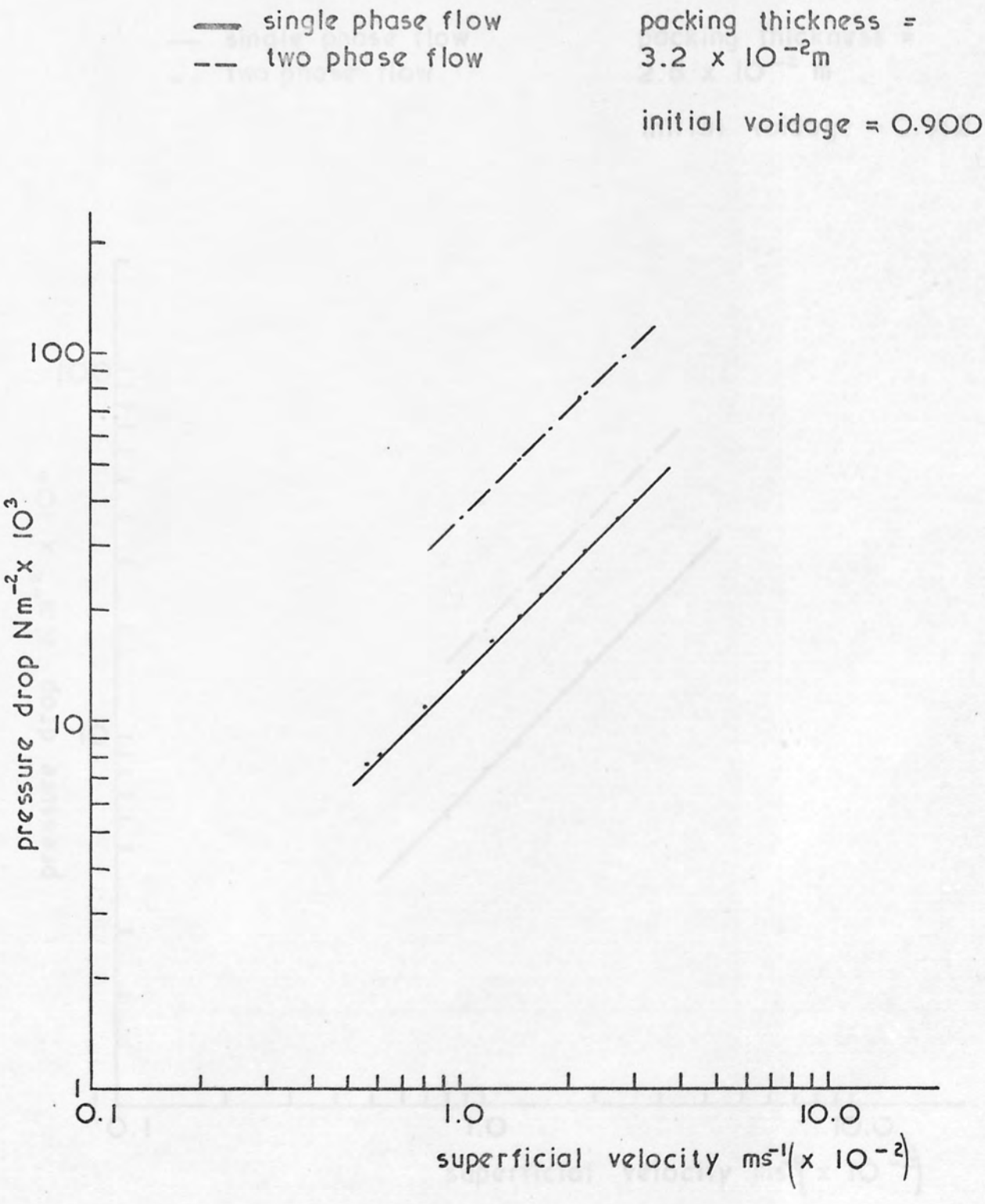
single phase flow
two phase flow
packing thickness = 3.2 x 10⁻²m
initial voidage = 0.900
100
10
1
pressure drop Nm⁻² x 10³
0.1
1.0
10.0
superficial velocity ms⁻¹ (x 10⁻²)

Fig. 8.7

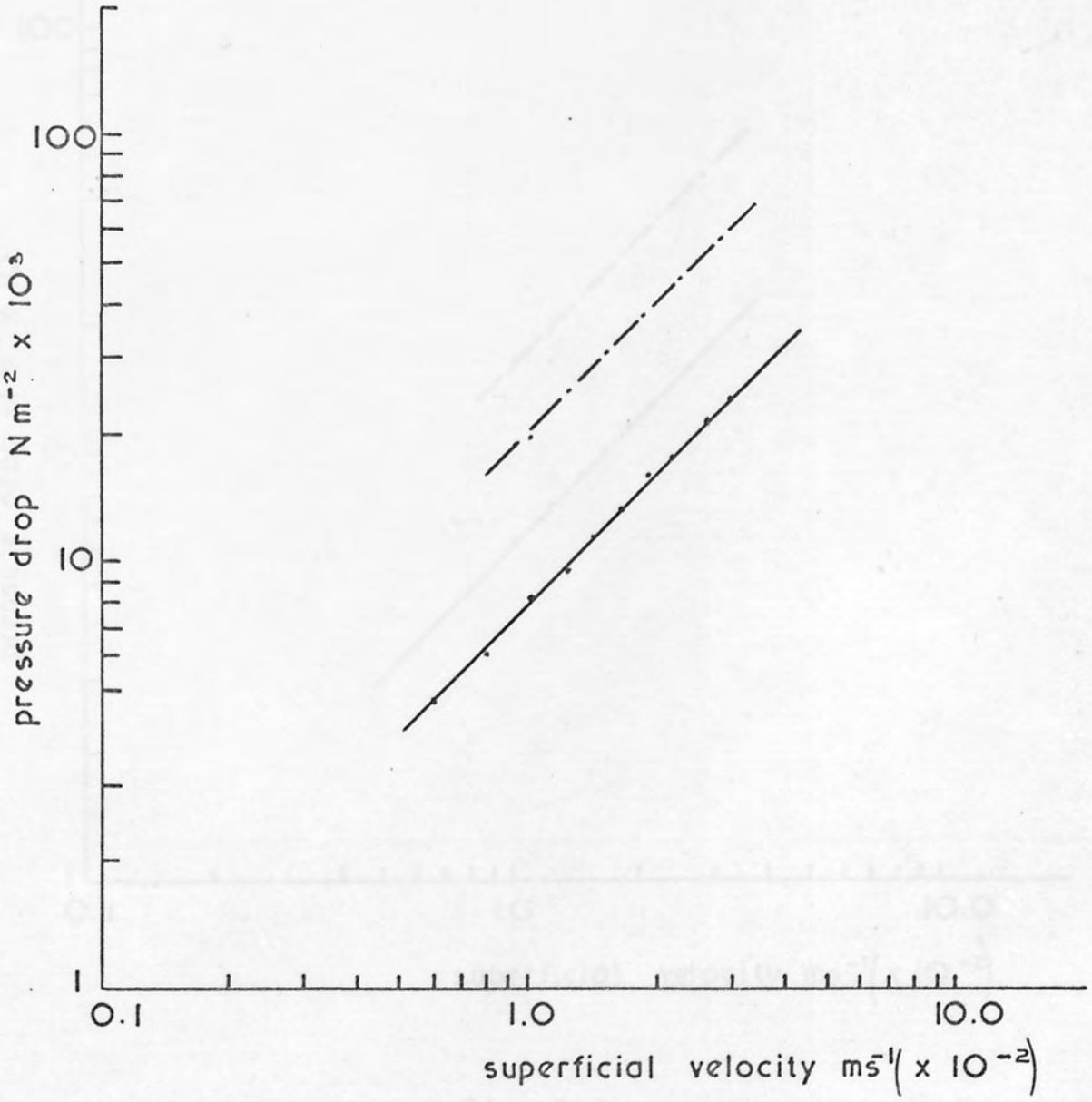
— single phase flow
-- two phase flow
packing thickness =
2.6 x 10⁻² m
initial voidage = 0.912
pressure drop N m⁻² x 10³
100
10
1
0.1
1.0
10.0
superficial velocity ms⁻¹ (x 10⁻²)

Fig. 8.8

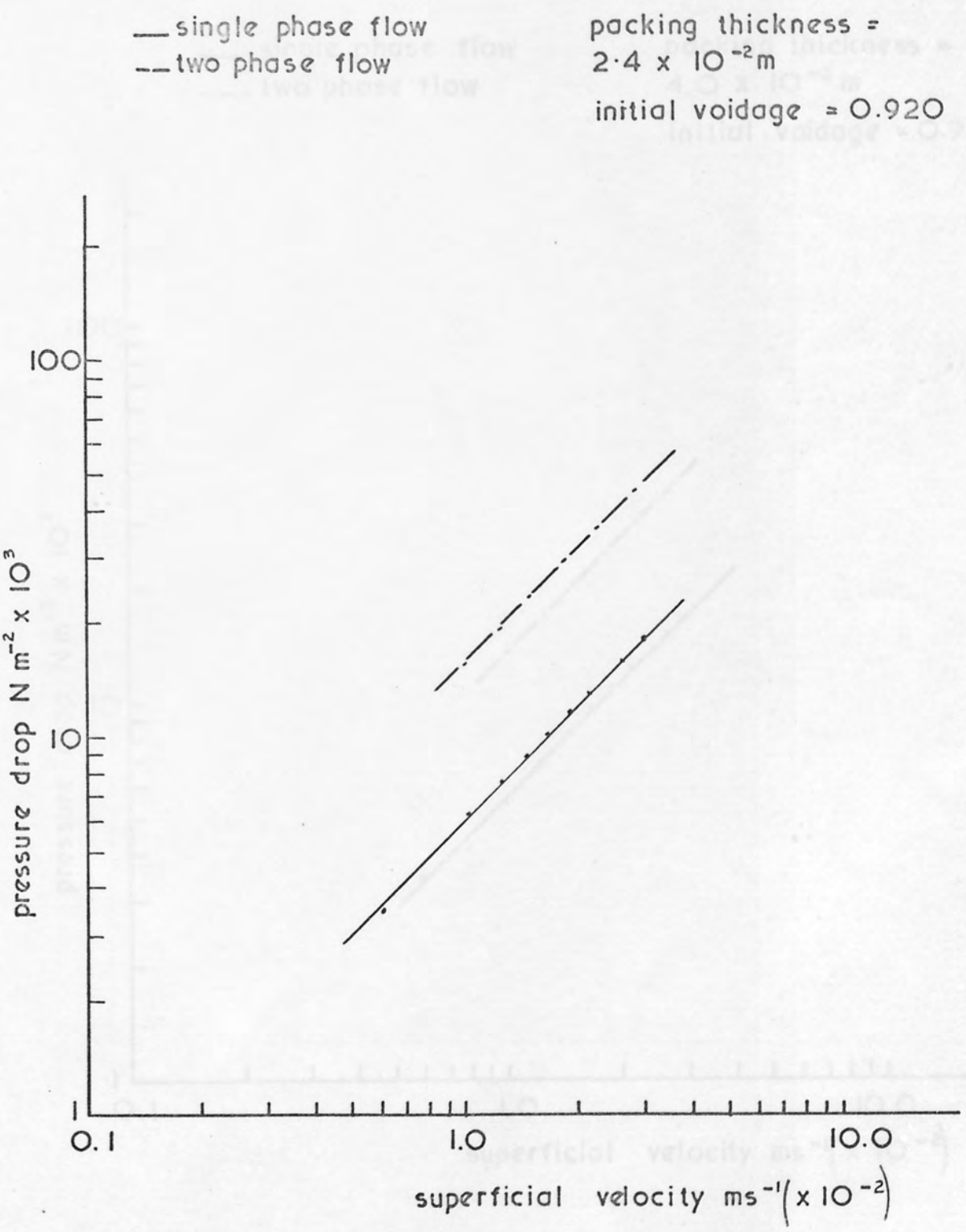
— single phase flow
-- two phase flow
packing thickness = 2·4 x 10⁻²m
initial voidage = 0.920
100
10
1
pressure drop N m⁻² x 10³
0.1
1.0
10.0
superficial velocity ms⁻¹ (x 10⁻²)

Fig. 8.9

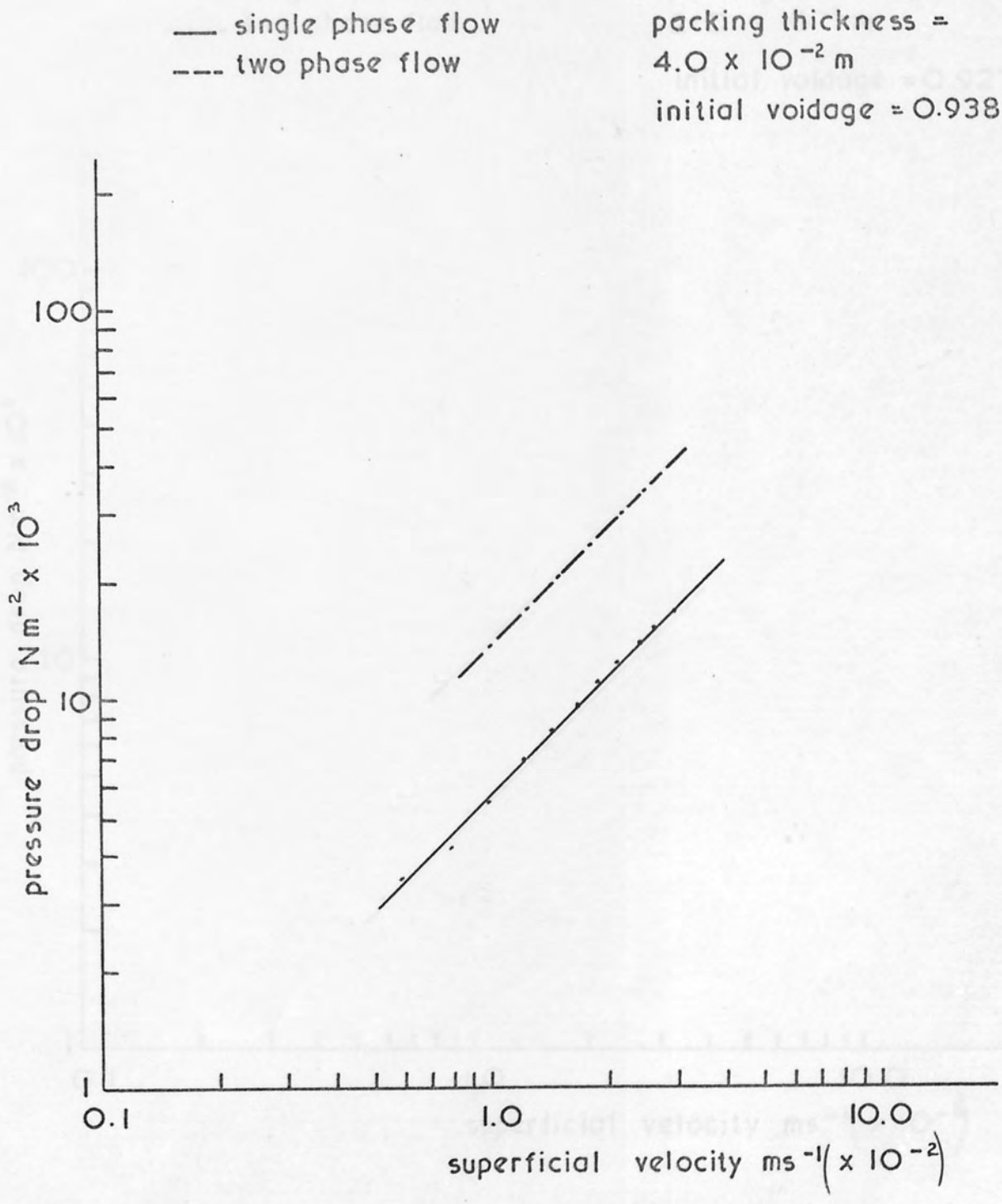
single phase flow
two phase flow
packing thickness = 4.0 x 10⁻² m
initial voidage = 0.938
pressure drop N m⁻² x 10³
100
10
1
0.1
1.0
10.0
superficial velocity ms⁻¹ (x 10⁻²)

Fig. 8.10

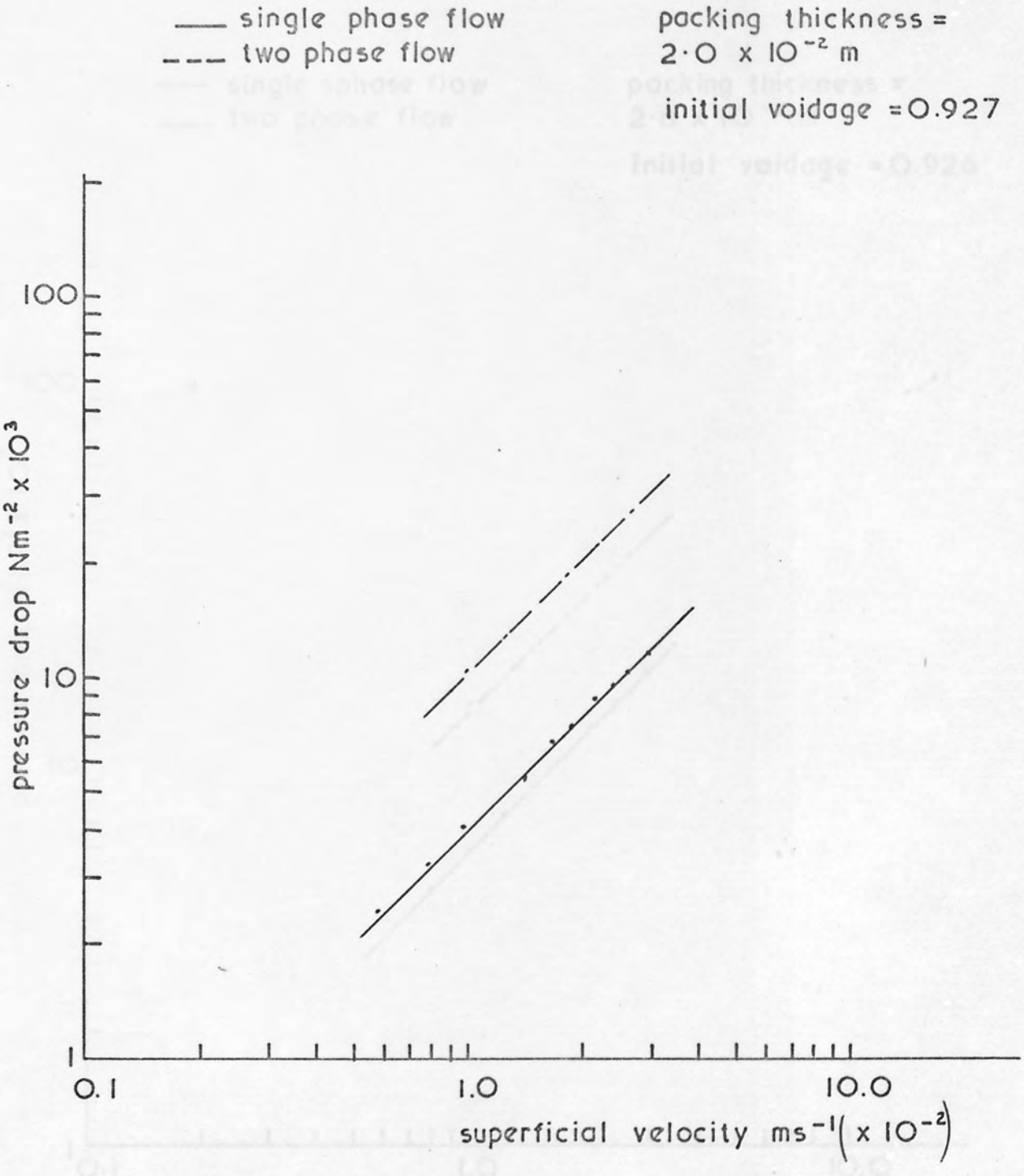
single phase flow
two phase flow
packing thickness = 2·0 x 10⁻² m
initial voidage = 0.927
pressure drop Nm⁻² x 10³
100
10
1
0.1
1.0
10.0
superficial velocity ms⁻¹ (x 10⁻²)

Fig . 8. 11

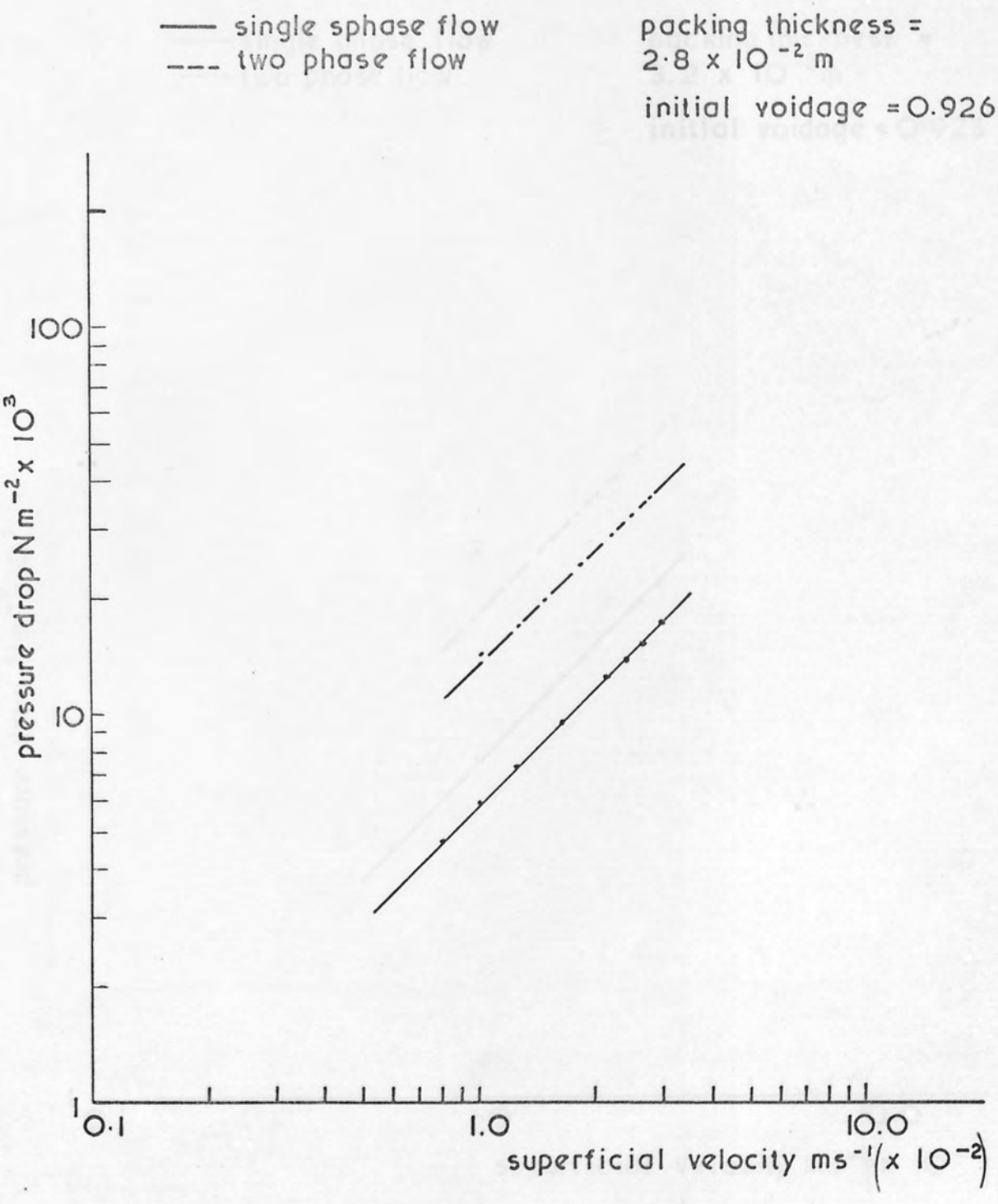
single sphase flow
two phase flow
packing thickness =
2·8 x 10⁻² m
initial voidage = 0.926
pressure drop N m⁻² x 10³
100
10
1
0·1
1.0
10.0
superficial velocity ms⁻¹ (x 10⁻²)

Fig. 8.12

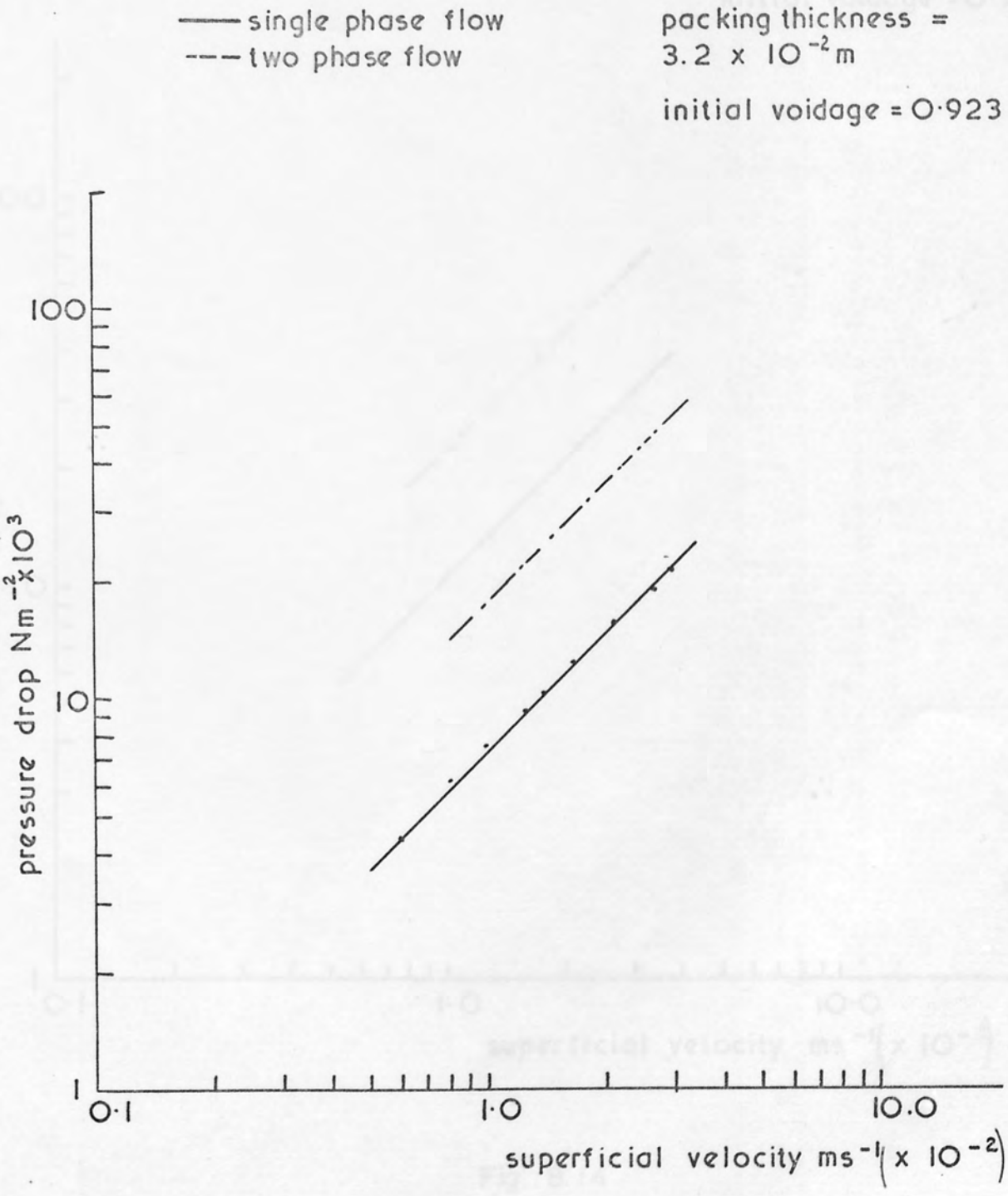
single phase flow
two phase flow
packing thickness = 3.2 x 10⁻² m
initial voidage = 0·923
pressure drop Nm⁻² x 10³
100
10
1
0·1
1·0
10.0
superficial velocity ms⁻¹ (x 10⁻²)

Fig. 8.13

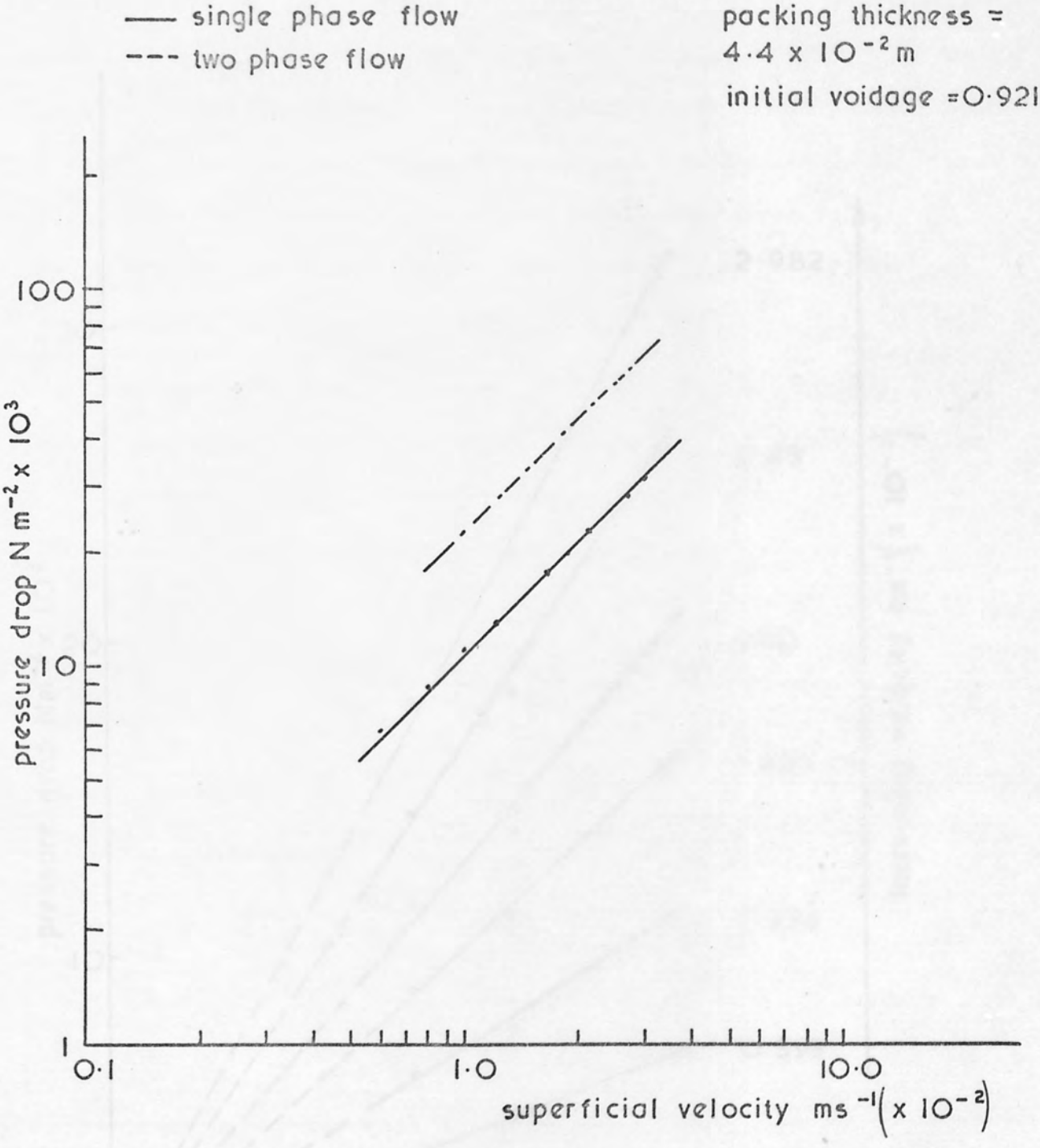
—— single phase flow
--- two phase flow
packing thickness =
4·4 x 10⁻² m
initial voidage =0·921
100
10
1
pressure drop N m⁻² x 10³
0·1
1·0
10·0
superficial velocity ms⁻¹ (x 10⁻²)

Fig. 8.14

Variation of one phase flow pressure drop with packing thickness at different superficial velocities

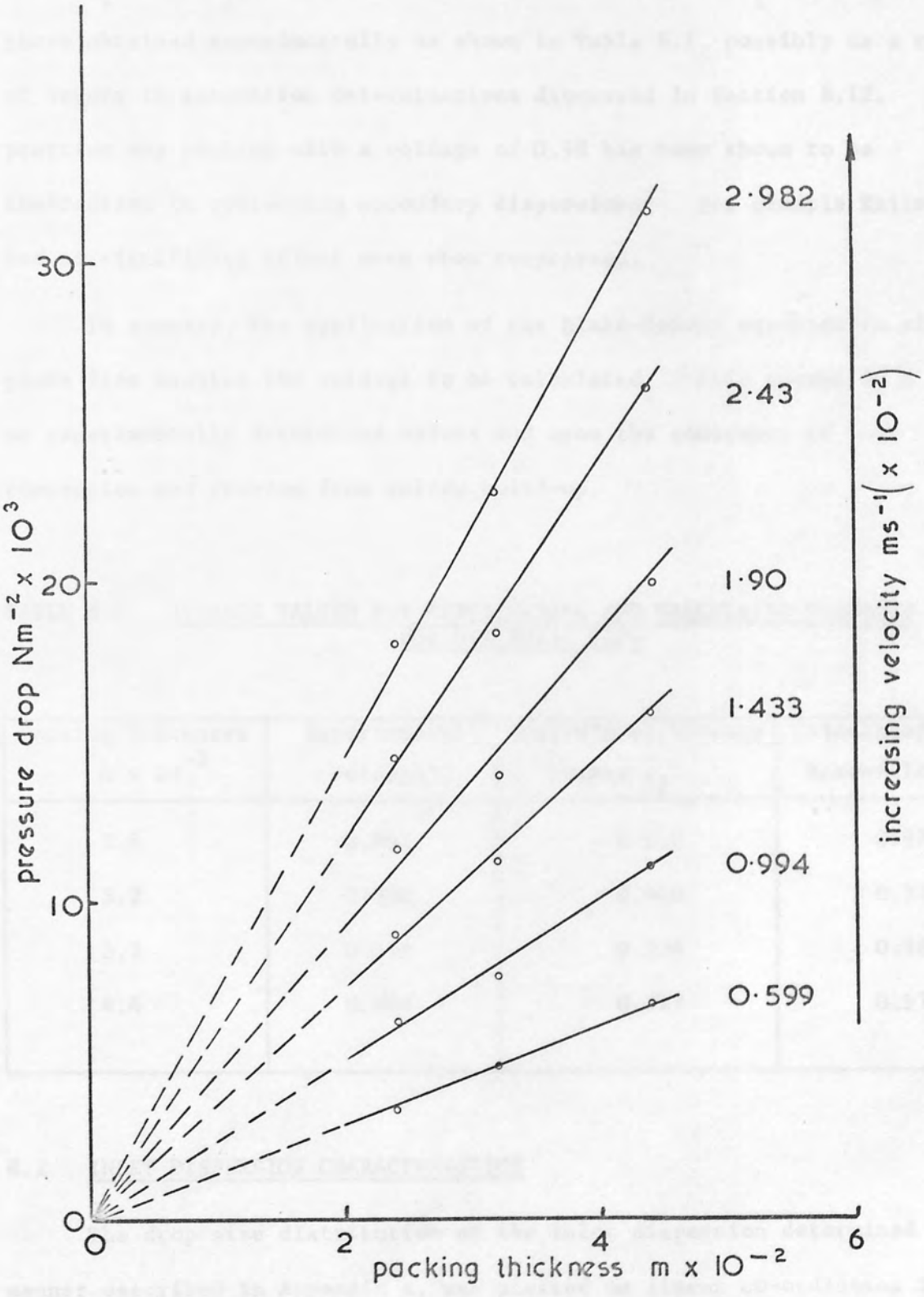

Fig. 8.15

$$\Delta p_2 = \frac{18281.25\ V'\ L\ \alpha_1^{2.3}(1 - 0.8\ V'^{-0.2})^{2.3}}{d_f^{3/2}} \quad \ldots\ldots\ldots\ldots\ldots\ldots 8.1.4$$

where $\alpha_1 = 1 - \varepsilon_1$. However the calculated values of ε_1 were higher than those obtained experimentally as shown in Table 8.1, possibly as a result of errors in saturation determinations discussed in Section 8.12. In practice any packing with a voidage of 0.98 has been shown to be ineffective in coalescing secondary dispersions; for example Knitmesh had no significant effect even when compressed.

In summary, the application of the Blake-Kozeny equation to single phase flow enables the voidage to be calculated; this serves as a check on experimentally determined values and upon the constancy of bed compaction and freedom from solids build-up.

TABLE 8.1 AVERAGE VALUES FOR EXPERIMENTAL AND CALCULATED VOIDAGES FOR ONE PHASE FLOW

Packing Thickness m x 10^{-2}	Experimental Voidage ε_1	Calculated Voidage Kozeny ε_1	Calculated Voidage Rosenfeld ε_1
2.6	0.892	0.912	0.976
3.2	0.886	0.900	0.972
3.2	0.910	0.934	0.981
4.4	0.896	0.917	0.978

8.2 INLET DISPERSION CHARACTERISTICS

The drop size distribution of the inlet dispersion determined in the manner described in Appendix A, was plotted on linear co-ordinates in the form Cumulative Weight Per Cent Oversize versus Drop Diameter in micro-

TABLE 8.2

VARIATION OF CALCULATED ONE PHASE FLOW VOIDAGE WITH SUPERFICIAL VELOCITY

Packing Thickness = 3.2×10^{-2} m

Average Calculated Voidage ε_1 = 0.900

Average Experimental Voidage ε_1 = 0.886

Superficial Velocity $ms^{-1}\left(\times 10^{-2}\right)$	Voidage ε_1 Kozeny Equation
0.599	0.899
0.789	0.898
0.994	0.899
1.213	0.899
1.433	0.900
1.667	0.901
1.900	0.900
2.164	0.900
2.43	0.900
2.69	0.900
2.982	0.900

metres. This is shown in Fig. 8.16 which was obtained at a phase ratio of 3% and a pump speed of 86.7 revs s^{-1}. The distribution was unimodal and the mean inlet drop diameter, that is the size which exceeded the diameter of 50% of the droplets, was determined. A value of twenty seven micrometres was generally obtained under these experimental conditions.

Preliminary studies proved that the distribution at a constant pump speed was reproducible to within $\pm$ two micrometres of its mean value for phase ratios up to 7%. A decrease in pump speed resulted in an increase in the number of larger drops and hence an increase in mean inlet drop size. The change of mean inlet drop size with pump speed in the range 33.3 to 86.7 revs s^{-1} at a phase ratio of 3% is shown in Figure 8.17. As a result of this three pump speeds were used in the subsequent experiments.

8.3 TWO PHASE FLOW PRESSURE DROP

Whenever a dispersion was pumped through the fibrous bed at a constant superficial velocity, the pressure drop increased to a value higher than that for the corresponding single phase flow. The rate of increase was initially slow but gradually increased until constant pressure drop, i.e. a steady state condition, was obtained. This was generally achieved after fifteen to twenty minutes operation. This increase in pressure drop was characteristic in all thecoalescence experiments and large drops of coalesced toluene were observed at the bed exit shortly before steady state was attained. At steady state drops of constant size detached from fixed points at the bed exit. This is illustrated in Figure 8.18A, for a low phase ratio operation, i.e. 3% by volume dispersed phase. In a study of coalescence of primary dispersions in packed beds, Thomas[110] referred to this as channelling and attributed it to preferential wetting of sections of packing by the dispersed phase. However, Wilkinson[127] observed no

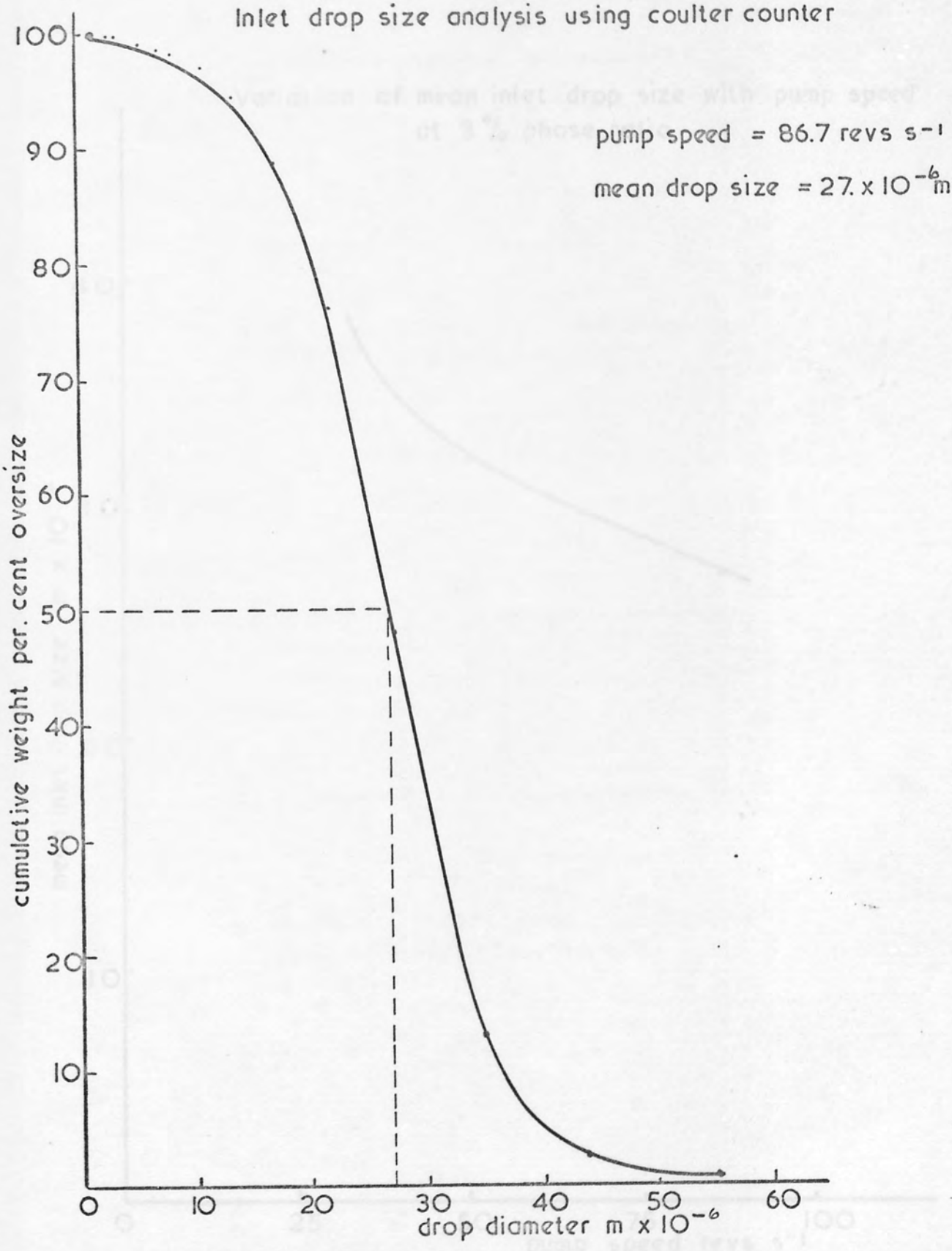
Inlet drop size analysis using coulter counter
pump speed = 86.7 revs s-1
mean drop size = 27. x 10-6m
cumulative weight per. cent oversize
100
90
80
70
60
50
40
30
20
10
0
10
20
30
40
50
60
drop diameter m x 10-6

Fig. 8.16

Variation of mean inlet drop size with pump speed at 3 % phase ratio

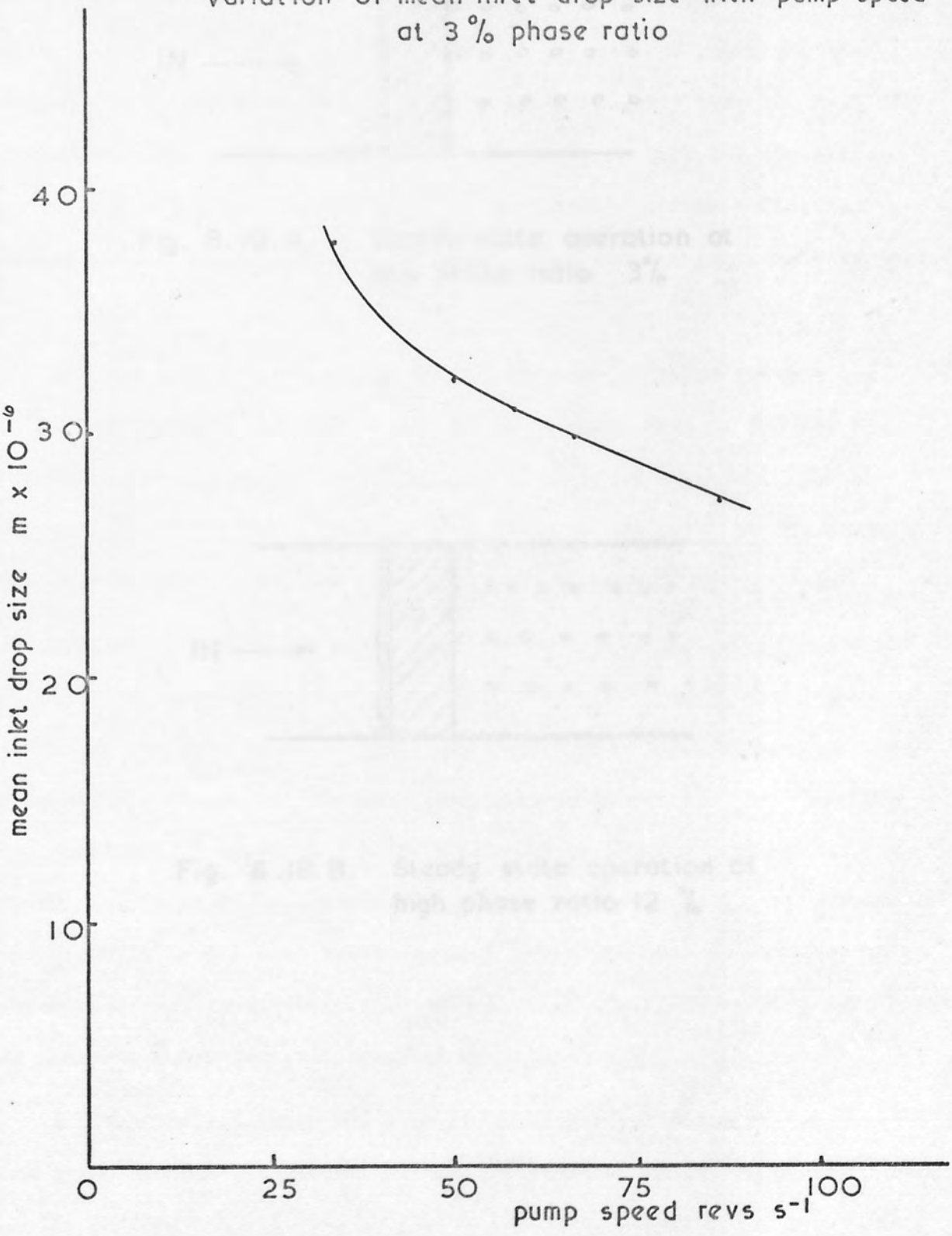

Fig . 8.17

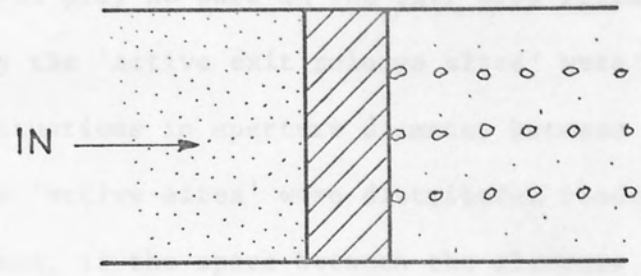

Fig. 8.18.A. Steady state operation at low phase ratio 3%

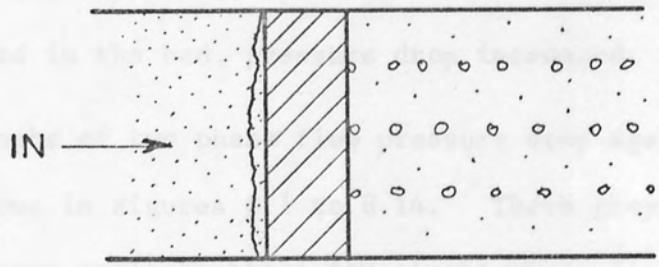

Fig. 8.18.B. Steady state operation at high phase ratio 12 %

significant difference in performance between wetted and non-wetted packings placed at the exit of the bed suggesting that preferentially wetted channels play no part in the exit drop release mechanism. Alternatively the 'active exit release sites' were thought to be related to local fluctuations in aperture diameter between the packing elements. However these 'active sites' were distributed randomly over the exit of the bed whereas, if the space between the elements were the dominant factor, the majority of sites would occur near the column walls since Ridgway and Tarbuck[174] found a high voidage within two particle diameters of the wall.

In this work fifteen to twenty minutes were required for a 4.4 x 10^{-2} m bed to reach its equilibrium pressure drop, that is for the bed hold up to reach a steady state value. This is in agreement with the observations of Sherony[151] and Spielman[139] who found that as the dispersed phase accumulated in the bed, pressure drop increased.

Typical graphs of two phase flow pressure drop against superficial velocity are shown in Figures 8.1 to 8.14. These graphs, which are plotted on the same scale as those for single phase flow to aid comparison, demonstrate a linear relationship with a slope of unity. In a similar work, Spielman[139] observed a linear increase in pressure drop with superficial velocity but at small flow rates the rate of increase was significantly lower. At these low flow rates bed hold up required up to one hour before steady state was reached, thus the pressure drop determined was probably under unsteady state conditions.

A linear relationship was also obtained for variation of two phase flow pressure drop with packing thickness as shown in Figure 8.19. These results confirm the validity of the Blake-Kozeny equation for two phase flow. Therefore since the Blake-Kozeny equation constant was found to

Variation of two phase flow pressure drop with packing thickness at different superficial velocities

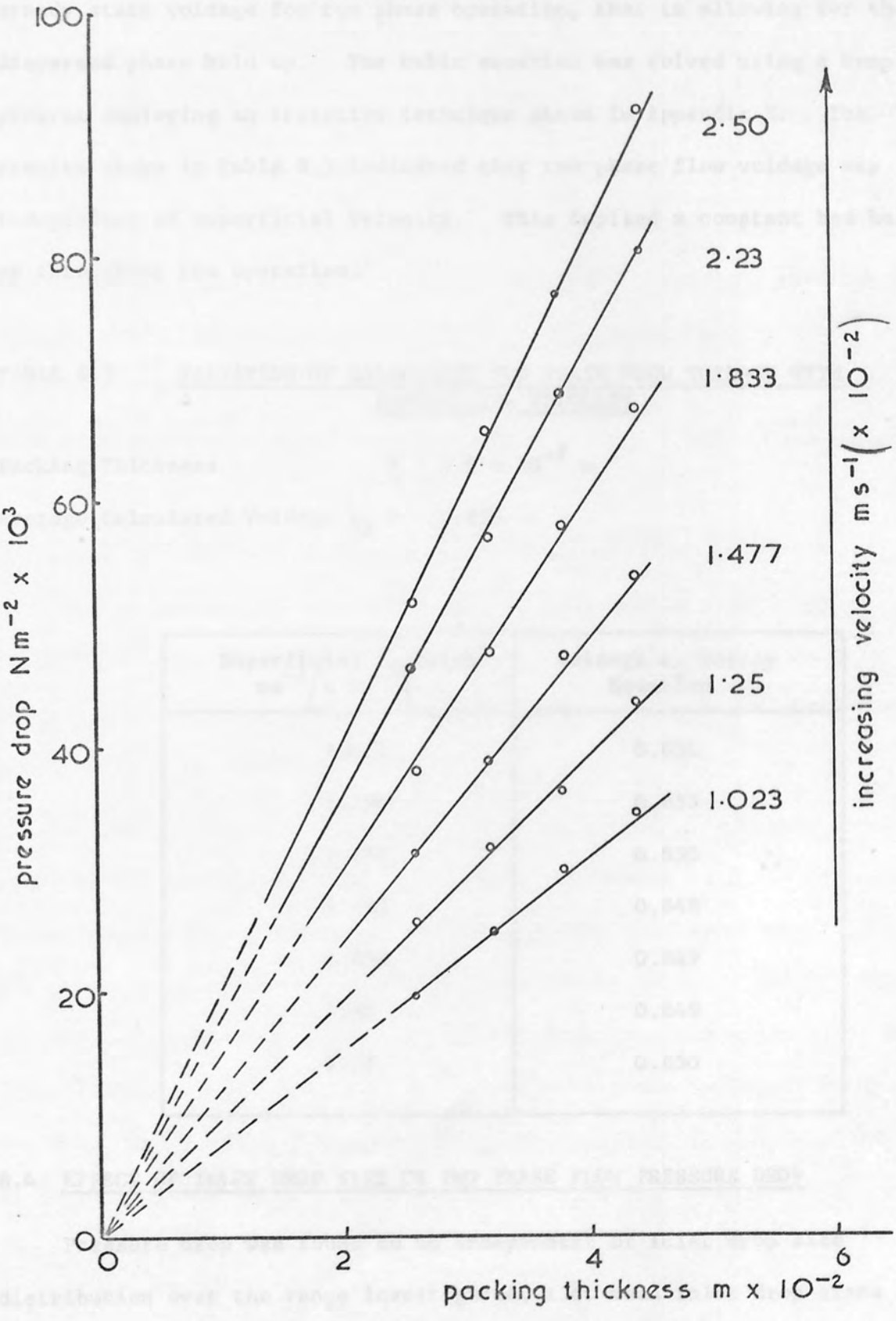

Fig . 8. 19

be independent of void fraction this equation was used to calculate the steady state voidage for two phase operation, that is allowing for the dispersed phase hold up. The cubic equation was solved using a computer program employing an iterative technique shown in Appendix E. The results shown in Table 8.3 indicated that two phase flow voidage was independent of superficial velocity. This implied a constant bed hold up throughout the operation.

TABLE 8.3 VARIATION OF CALCULATED TWO PHASE FLOW VOIDAGE WITH SUPERFICIAL VELOCITY

Packing Thickness = 3.2×10^{-2} m

Average Calculated Voidage ε_2 = 0.850

Superficial Velocity ms^{-1} $(\times 10^{-2})$	Voidage ε_2 Kozeny Equation
1.023	0.851
1.250	0.853
1.477	0.850
1.833	0.848
2.230	0.849
2.50	0.849
2.77	0.850

8.4 EFFECT OF INLET DROP SIZE ON TWO PHASE FLOW PRESSURE DROP

Pressure drop was found to be independent of inlet drop size distribution over the range investigated, i.e. mean inlet drop sizes between twenty six and thirty eight micrometres. Plots of steady state flow pressure drop against superficial velocity are therefore reproduced

in Figures 8.1 to 8.14 using the average pressure drop values for these two mean inlet drop sizes. Typical data are presented in Appendix E. This indicates that at the relatively low phase ratios involved, the presence of the dispersed phase did not affect the dispersion physical properties, in particular its viscosity.

This has been observed before provided the droplets were small and the dispersed phase dilute[175]. Later Spielman[139] observed that for his system, which also met these requirements, the pressure drop was independent of the inlet drop size. Therefore it is considered that both requirements were met in this study.

8.5 EFFECT OF PHASE RATIO ON TWO PHASE FLOW PRESSURE DROP

The pressure drop was independent of phase ratio within the range 3% to 7%. Thus the pressure drop data shown in Figures 8.1 to 8.14 represent the average value for these two phase ratios. Typical data are presented in Appendix E.

A limited number of experiments were performed at a higher phase ratio of 12% and again pressure drop was independent of phase ratio. However operation at the same flow rates as for the lowest phase ratio, 3%, produced a layer of coalesced toluene at the inlet. Despite this large drops left the exit side of the bed from the same sites as at the lower phase ratio. This mode of operation is shown in Figure 8.18B and could be defined as a 'Pseudo flooding' condition. It follows that even up to a 12% phase ratio the dispersed phase was sufficiently dilute and the inlet drop size small so as not to affect the bulk properties of the mixture.

In a parallel study, pressure drop was independent of phase ratio in the range 0.1% to 0.6%, but the time to achieve the equilibrium

pressure drop increased up to one hour[172]. This was probably due to the very small dilution of the dispersed phase necessitating a longer time for a sufficient number of drops to be captured for the hold-up to reach its equilibrium value.

In conclusion, the results discussed so far imply the presence of a constant bed hold-up independent of superficial velocity, inlet drop size and phase ratio. These support the contentions that 'priming' of coalescing beds is in fact no more than a convenient way of establishing steady state hold-up.

8.6 CHARACTERISTIC EXIT DROP SIZE

At the beginning of this work attempts were made to analyse the effluent drops using the Coulter Counter. The particle count was found to be so small that background electronic noise, or inadequate statistics, precluded accurate determination especially at the lowest size detected with a given aperture. This was taken as further proof that the packing was an efficient coalescer.

Larger coalesced drops were therefore analysed photographically as discussed in Section 7.10. A number of mean drop diameters were calculated statistically using the Honeywell 316 computer. The computer program and a typical output are shown in Appendix B. Two mean diameters were of importance:

$$\text{Mean Linear Diameter, MLD} = \frac{\sum n_i d_i}{\sum n_i}$$

$$\text{Mean Volume Diameter, MVD} = \sqrt[3]{\frac{\sum n_i d_i^3}{\sum n_i}}$$

8.7 EFFECT OF SUPERFICIAL VELOCITY ON EXIT DROP SIZE

The mean linear drop diameter in the exit dispersion decreased with

increase in superficial velocity as shown in Figures 8.20 and 8.21. This is in agreement with other workers[20, 107, 139, 151] who found that the degree of coalescence decreased with increase in superficial velocity.

Figure 8.22 shows that the mean volume drop diameter also decreased with increase in superficial velocity until a plateau was reached followed by a further decrease. The velocity corresponding to the start of the plateau of constant drop size was defined as a 'critical separating velocity' after which bed breakthrough occurred. In this work it was of the order of 2.0×10^{-2} ms^{-1}; critical velocities obtained by other workers are shown in Table 5.3.1. Figure 8.23 shows typical exit drop sizes obtained in this study at different superficial velocities.

Davies and Jeffreys[121] reported that there was an optimum velocity, for a given packing, above which the degree of coalescence decreased due to the local viscous shear forces within the bed being greater than the force of adhesion of the drops on the packing. Rosenfeld[146] derived an equation for calculating the critical separating velocity based on this hypothesis, i.e. the velocity at which the drag force equals the sum of the Van der Waals force and the adhesion force. However this neglected the effect of neighbouring fibres. Using the data of Spielman[139] a critical velocity of 3.27×10^{-2} ms^{-1} was calculated but his analysis of results gave a value of the order of 0.15×10^{-2} ms^{-1}. Thus the effect of fibre interactions, that is fibre orientation, cannot be ignored. Therefore further experimentation is clearly needed before this concept of critical velocity can be defined qualitatively.

8.8 EFFECT OF PACKING THICKNESS ON EXIT DROP SIZE

An increase in packing thickness from 2×10^{-2} m to 4.4×10^{-2} m led to an increase in exit drop size as well as critical separating

Variation of mean linear diameter of exit drops with packing thickness for two mean inlet drop diameters

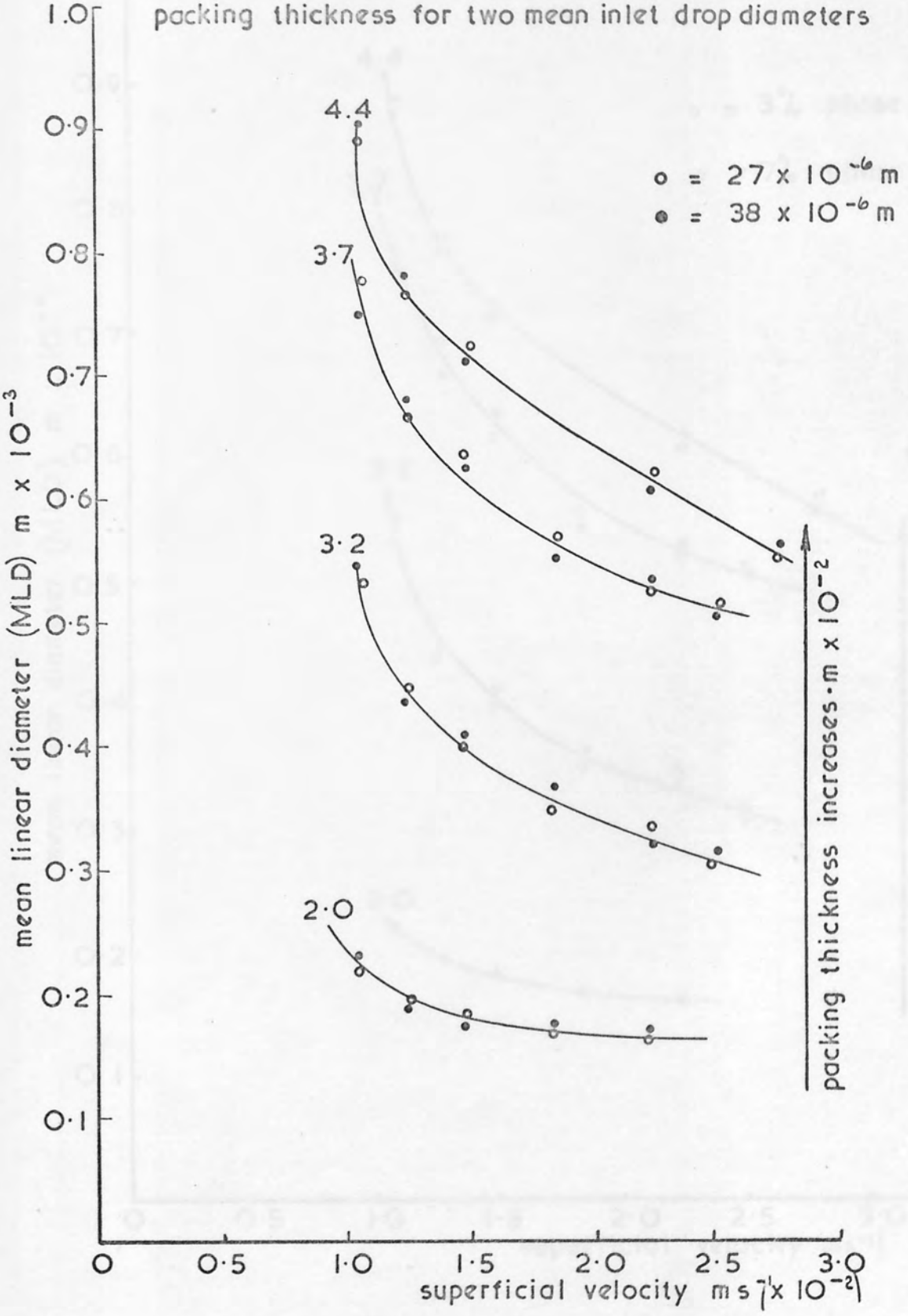

Fig. 8.20

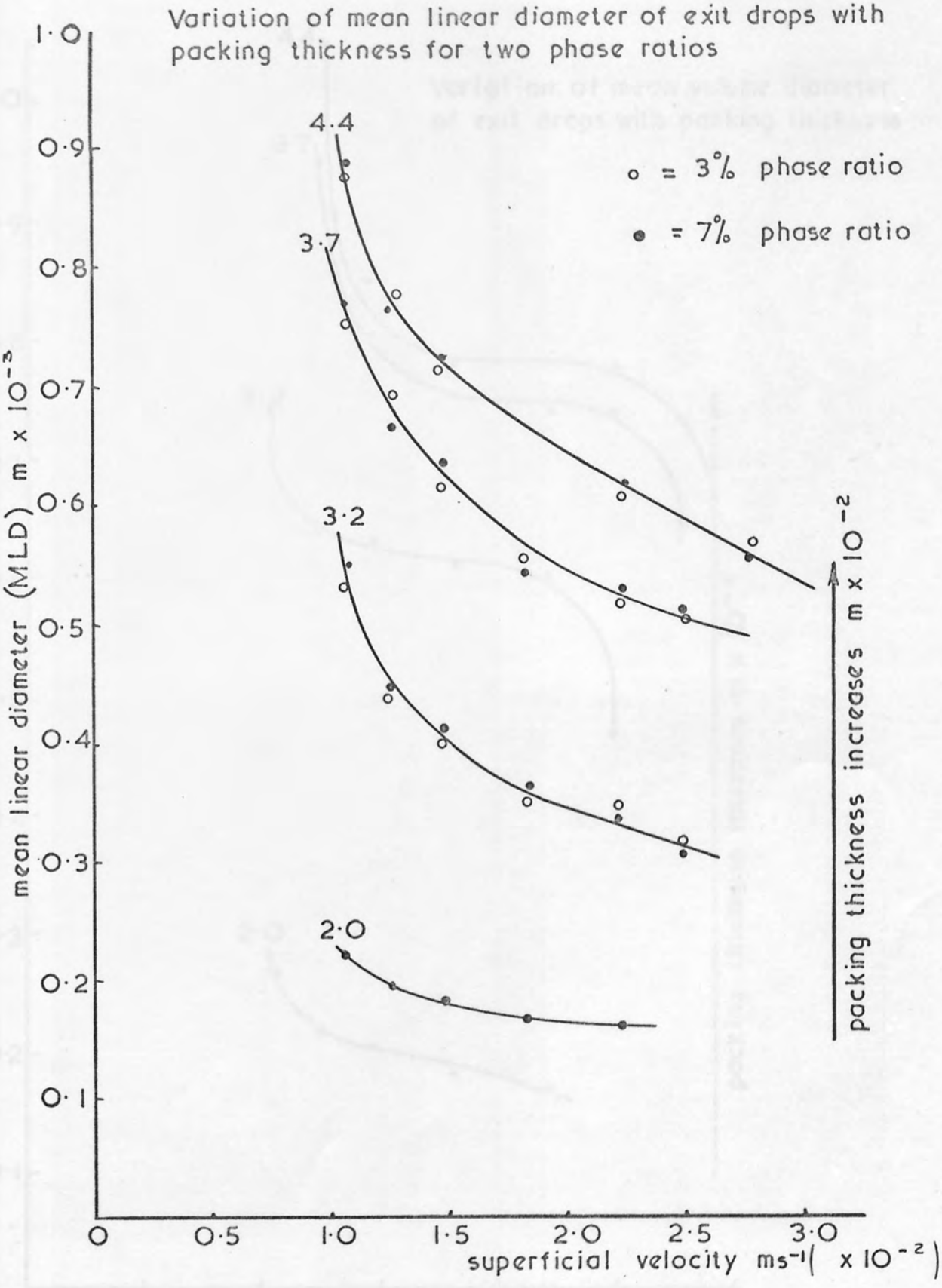
Variation of mean linear diameter of exit drops with packing thickness for two phase ratios
o = 3% phase ratio
● = 7% phase ratio
4.4
3.7
3.2
2.0
packing thickness increases m x 10⁻²
mean linear diameter (MLD) m x 10⁻³
1·0
0·9
0·8
0·7
0·6
0·5
0·4
0·3
0·2
0·1
0
0·5
1·0
1·5
2·0
2·5
3·0
superficial velocity ms⁻¹(x 10⁻²)

Fig. 8.21

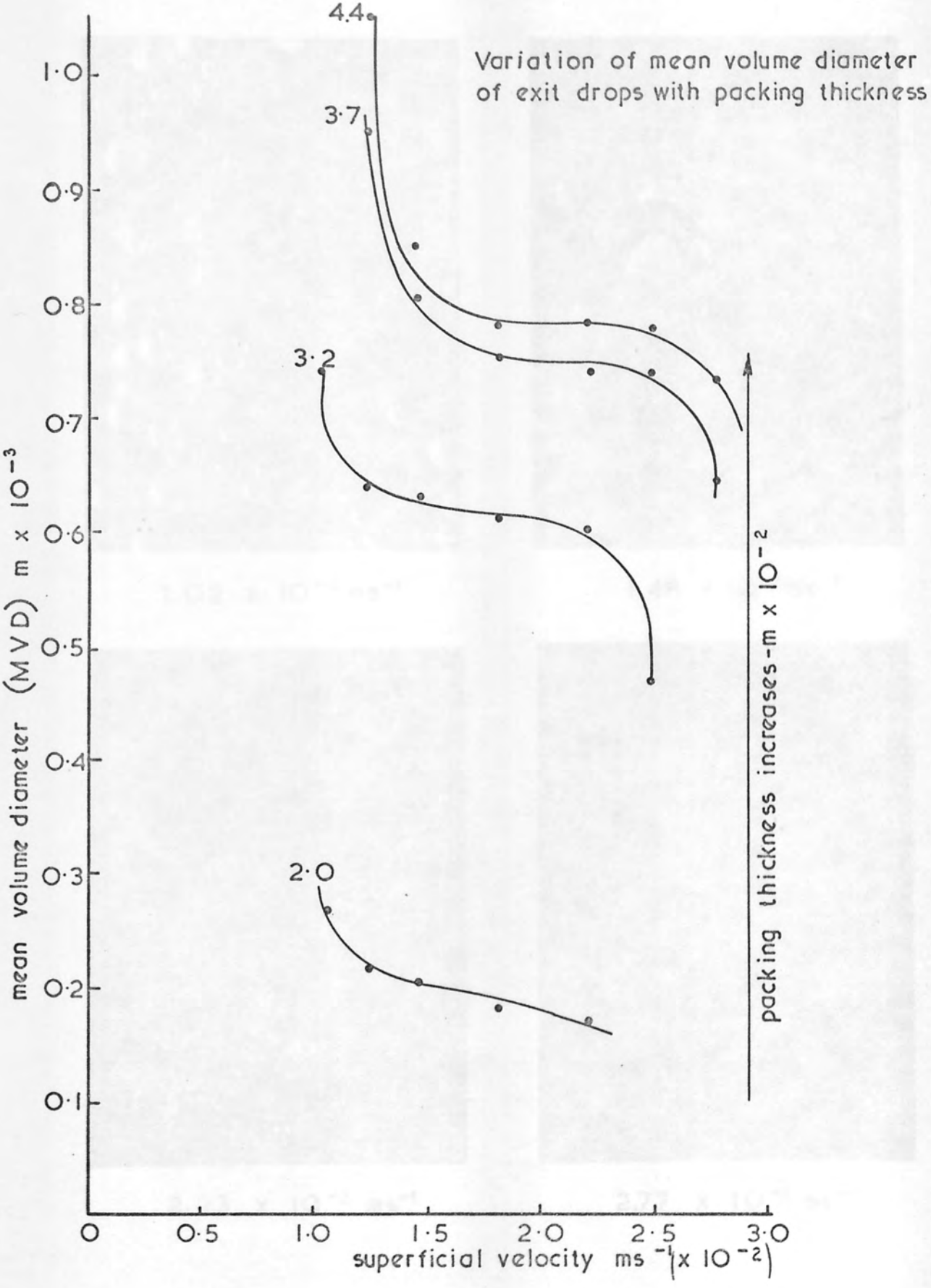
Variation of mean volume diameter of exit drops with packing thickness
4.4
3·7
3·2
2·0
packing thickness increases-m x 10⁻²
mean volume diameter (MVD) m x 10⁻³
superficial velocity ms⁻¹ (x 10⁻²)
1·0
0·9
0·8
0·7
0·6
0·5
0·4
0·3
0·2
0·1
0
0·5
1·0
1·5
2·0
2·5
3·0

Fig. 8.22

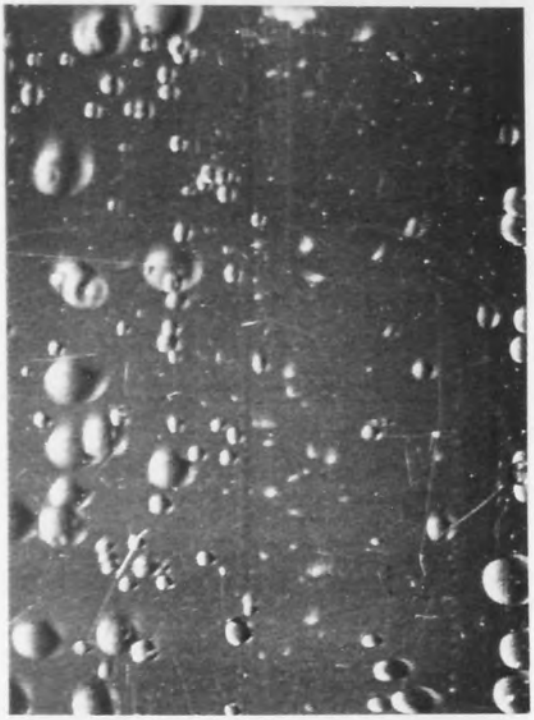

$1.02 \times 10^{-2}\ ms^{-1}$

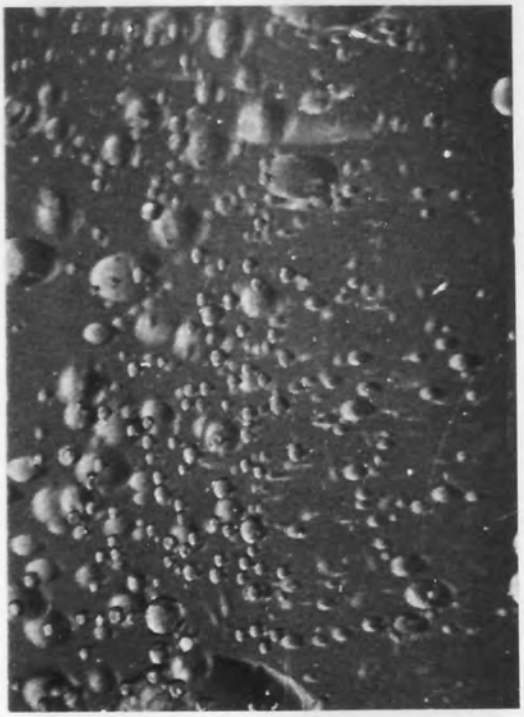

$1.48 \times 10^{-2} ms^{-1}$

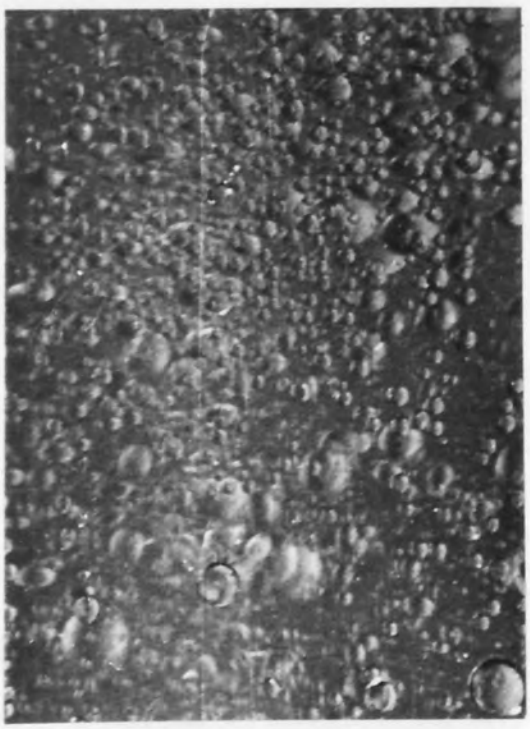

$2.23 \times 10^{-2}\ ms^{-1}$

$2.77 \times 10^{-2}\ ms^{-1}$

Fig. 8.23 Variation of exit drop size with superficial velocity

velocity. There appeared to be an optimum bed thickness after which any increase in thickness did not result in a corresponding increase in critical separating velocity as shown in Figures 8.20 to 8.22. The difference in exit drop size between a 2×10^{-2} m and 3.2×10^{-2} m packing thickness was much greater than that between 3.7×10^{-2}m and 4.4×10^{-2} m. This was in agreement with the observations of Sareen et al[20] who suggested that the degree of coalescence increased with bed depth but with a practical limit to the maximum bed thickness. Hence an optimum thickness existed for each application.

8.9 EFFECT OF INLET DROP SIZE ON EXIT DROP SIZE

Exit drop size was independent of inlet drop size as shown in Figure 8.20. This indicated that over the range of mean drop size investigated, i.e. twenty six micrometres to thirty eight micrometres, the degree of coalescence was essentially independent of inlet drop size distribution. This is not surprising since each attached droplet must first grow to a critical drop size, which for a given system is only a function of superficial velocity, before being released. Thus it could be suggested that the degree of coalescence for a given droplet size is independent of other droplet sizes present in the distribution.

8.10 EFFECT OF PHASE RATIO ON EXIT DROP SIZE

Under steady state conditions exit drop size was independent of phase ratio within the range 3% to 7%, as shown in Figure 8.21. This indicated that the degree of coalescence was independent of the ratio of dispersed phase entering the bed.

At the low phase ratios between 0.1% and 0.6% no change in exit drop size was observed with phase ratio, but there was an increase in the

number of drops leaving the packing from fixed sites[172]. This indicated the presence of a fixed number of release points.

8.11 HOLD-UP DETERMINATION

Under two phase flow conditions a finite amount of the dispersed phase was retained in the bed thus decreasing its initial voidage. Initial experimentation suggested that this coalesced toluene hold-up was an important feature, as both pressure drop and exit drop size tended to increase as droplets accumulated in the packing between start-up and the attainment of steady state.

Assuming that the change in bed voidage was due to dispersed phase held-up only, the hold-up expressed as volume of liquid retained by the bed per volume of solid can be calculated from:

$$\phi_H = \frac{\varepsilon_1 - \varepsilon_2}{1 - \varepsilon_1} \quad \ldots\ldots\ldots\ldots\ldots\ldots\ldots\ldots \quad 8.11.1$$

Calculated values are presented in Appendix E. They indicated that over the range, 1.0×10^{-2} ms^{-1} to 2.8×10^{-2} ms^{-1}, bed hold-up was independent of superficial velocity. This could in fact be deduced from the two phase flow pressure drop against superficial velocity graphs shown in Figures 8.1 to 8.14, i.e. straight lines of unit slope. This is contrary to the results of Sherony[21] in which hold-up was concluded to decrease with increase in superficial velocity, but reference to the original data[151] shows that this was based on data with a wide scatter.

Since two phase flow pressure drop was independent of inlet drop size distribution and phase ratio hold-up was independent of both. Thus an average hold-up value was determined as shown in Appendix E.

8.12 SATURATION DETERMINATION

The degree of saturation, defined as the fraction of pore space of the bed occupied by the dispersed phase, influences both pressure drop and coalescence performance. It cannot be predicted theoretically due to the difficulty of allowing for the effect of surface roughness[20,121] and the complexity of the process by which saturation occurs. However the method employed by Sherony[151] can be applied. It is assumed that the increase in pressure drop for two phase flow is due solely to the decrease in void space because of the toluene held-up within the bed. This assumption is reasonable for small drops in a dilute system since, as shown in Sections 8.4 and 8.5, they do not affect the bulk properties. The average saturation is therefore related to the average hold-up by:

$$S = \phi_H \left(\frac{1 + \varepsilon_1}{\varepsilon_1}\right) = 1 - \frac{\varepsilon_2}{\varepsilon_1} \quad \text{.....8.12.1}$$

Spielman[139] did not measure the saturation values at various velocities, but only the final saturation after dismantling the bed. Rosenfeld[146] however used Spielman's pressure drop data to calculate the saturation at arbitrary velocities. Considerations were given only to those cases when the dispersed phase did not wet the fibres, it being assumed that when the dispersed phase wetted the fibre the drop release mechanism would be different; i.e. rather than being sheared from the fibre the drops might slide along it. It was concluded that for velocities lower than 0.1×10^{-2} ms^{-1} saturation was independent of velocity. The pressure drop data then were probably determined under unsteady state conditions as discussed in Section 8.3. As the velocity increased, the saturation reached a lower limiting value for velocities greater than 1.2×10^{-2} ms^{-1}. The saturation was correlated by:

$$S = \frac{2.92\ (1 - \varepsilon_1) \times V'^{-\ 0.2}}{\varepsilon_1} \quad \ldots\ldots\ldots\ldots\ldots\ldots\ 8.12.2$$

This is clearly of limited application however since as V' approaches zero, the saturation approaches infinity, whereas in practice a finite and reasonably constant saturation value exists for any given system.

In this study saturation was independent of superficial velocity over the range 1.0×10^{-2} ms^{-1} to 2.7×10^{-2} ms^{-1}, since hold up was constant. An average saturation was therefore calculated as shown in Appendix E. This saturation level was also independent of inlet drop size distribution and phase ratio.

8.13 COALESCENCE ON A SINGLE FIBRE

To characterize the coalescence of micro-size drops on wetted and non-wetted fibres, and eliminate the complex effects of fibre interactions, a study was initiated on the coalescence of drops on an individual fibre. A limited number of experiments were performed using a high free energy surface, tinned copper, and a low energy surface, nylon, both of three hundred micrometres in diameter. They were positioned perpendicular to the flow of a 0.1% toluene in water and still photographs were taken of the coalescence process[177]. A typical result is shown in Figure 8.24. Major observations were:

(a) Droplets retained on a fibre coalesced with others from the main stream rather than with those on the fibre surface. There was a greater tendency for chain formation to occur on the high energy surface than on the low energy one. No coalescence occurred in the free stream. This was also observed by other workers[20,140].

(b) Coalescence of adjacent drops on a fibre was very slow especially

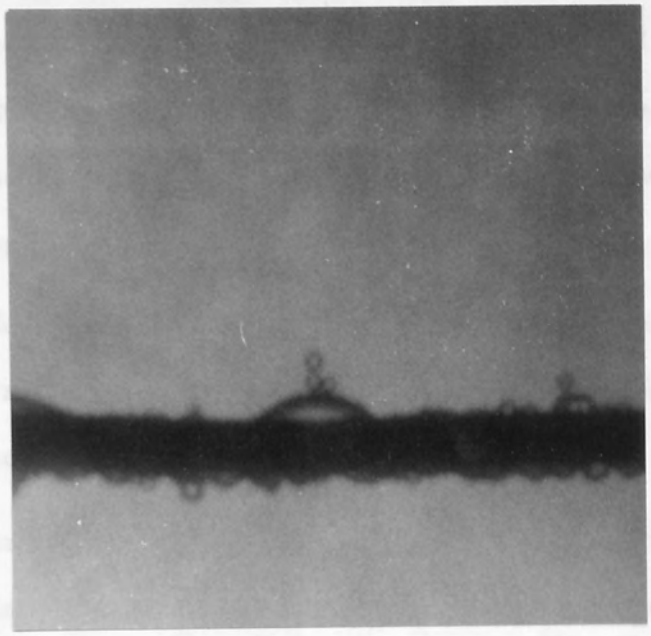

(a) Copper wire

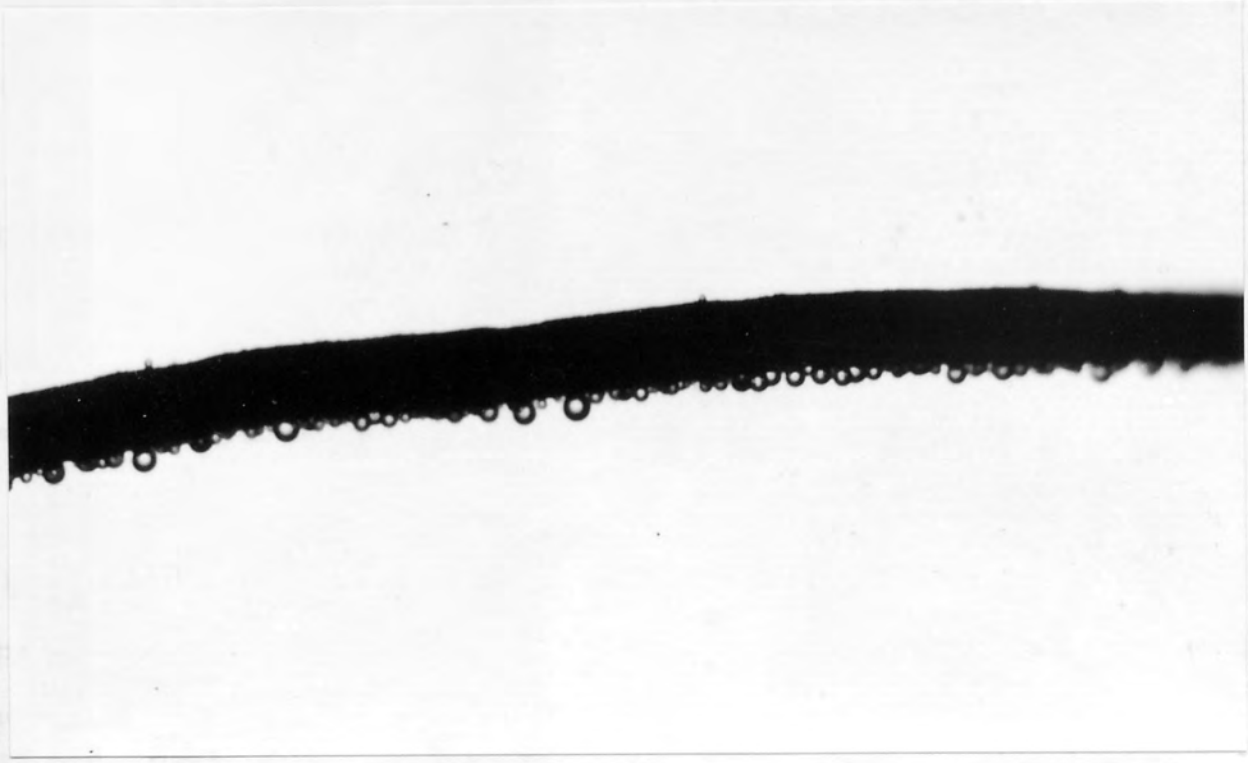

(b) Nylon thread

Fig. 8.24. Coalescence on a single fibre (toluene dispersed in water)

for nylon fibres. Thirty minutes was reported by Bitten[140].

(c) Collection and coalescence occurred on both high and low energy surfaces suggesting that preferential wetting of the fibre by the dispersed phase was not critical. This independence of surface energy is supported by other investigators[20,121].

(d) Droplets tended to collect on bends on the fibre possibly due to the presence of 'active sites' generated from a reduction in, or breakage of, intermolecular bonds.

Differences arising between coalescence on a single fibre and in a packed bed were discussed in Section 5.3.2. Although there were practical difficulties and a very wide range of variables, it would be an advantage if data were available on coalescence of a secondary dispersion on a single fibre to verify the coalescence mechanisms and correlate it to a packed bed.

8.14 CONDUCTIVITY MEASUREMENTS TECHNIQUE

The degree of saturation attained in this work was of the order of only 3% to 6% due to the small concentration of toluene in the water. At such concentrations a dispersed phase continuum cannot exist in the bed. Thus whilst photomicrographic studies[136] showed dispersed phase rivulets flowing in the bed, these do not constitute a continuum.

For a bed saturated with oil-in-water Martin et al[176] showed that as the quantity of oil held up in the bed increased the conductivity decreased linearly over the range 0% to 60%. In this study the conductivity difference between the constant value for the single phase, and the two phase system at different planes in the bed are shown in Figures 8.25 to 8.30. A histogram was plotted to represent the plane

at which the conductivity drop was determined, assuming that the hold up was in the middle of each plane, a graph representing the hold up distribution across the bed was plotted. The data shown in Appendix E, indicated that the bed inlet possessed the highest value of hold up followed by a sharp drop at approximately 1.2×10^{-2} m bed depth. The hold up retained throughout the rest of the bed did not vary until the exit side where it increased. These results are in agreement with those of Bitten[135], but contrary to those of Sherony[151], indicating that hold up is not uniformly distributed throughout the bed thickness.

8.15 EFFECT OF SUPERFICIAL VELOCITY ON MEASURED CONDUCTIVITY

As expected single phase flow conductivity was independent of superficial velocity as shown in Appendix E, since all the voids would be occupied by the continuous phase. Two phase flow conductivity increased with increase in superficial velocity. This could be explained by a decrease in bed hold up with increase in superficial velocity as postulated by Sherony[151], but this would be contrary to hold up determinations from pressure drop data presented in Section 8.11. Therefore the pressure drop technique is not accurate enough for determining small variations in hold up with superficial velocity and a more accurate indirect technique should be used.

8.16 EFFECT OF INLET DROP SIZE ON MEASURED CONDUCTIVITY

The drop in conductivity between any given single phase and two phase flow was independent of inlet drop size distribution as shown in Figures 8.25 to 8.30 for two mean inlet drop sizes of twenty six and thirty eight micrometres respectively. Thus the average hold up and

the hold up distribution across the bed can be considered independent of inlet drop size distribution in agreement with the data discussed in Section 8.11.

8.17 EFFECT OF PHASE RATIO ON MEASURED CONDUCTIVITY

Between the phase ratios 3% to 7% conductivity drop between any given single phase and two phase flow was independent of phase ratio as shown in Figures 8.25 to 8.30. Therefore average hold up and hold up distribution across the bed can be considered independent of phase ratio in agreement with the data discussed in Section 8.11.

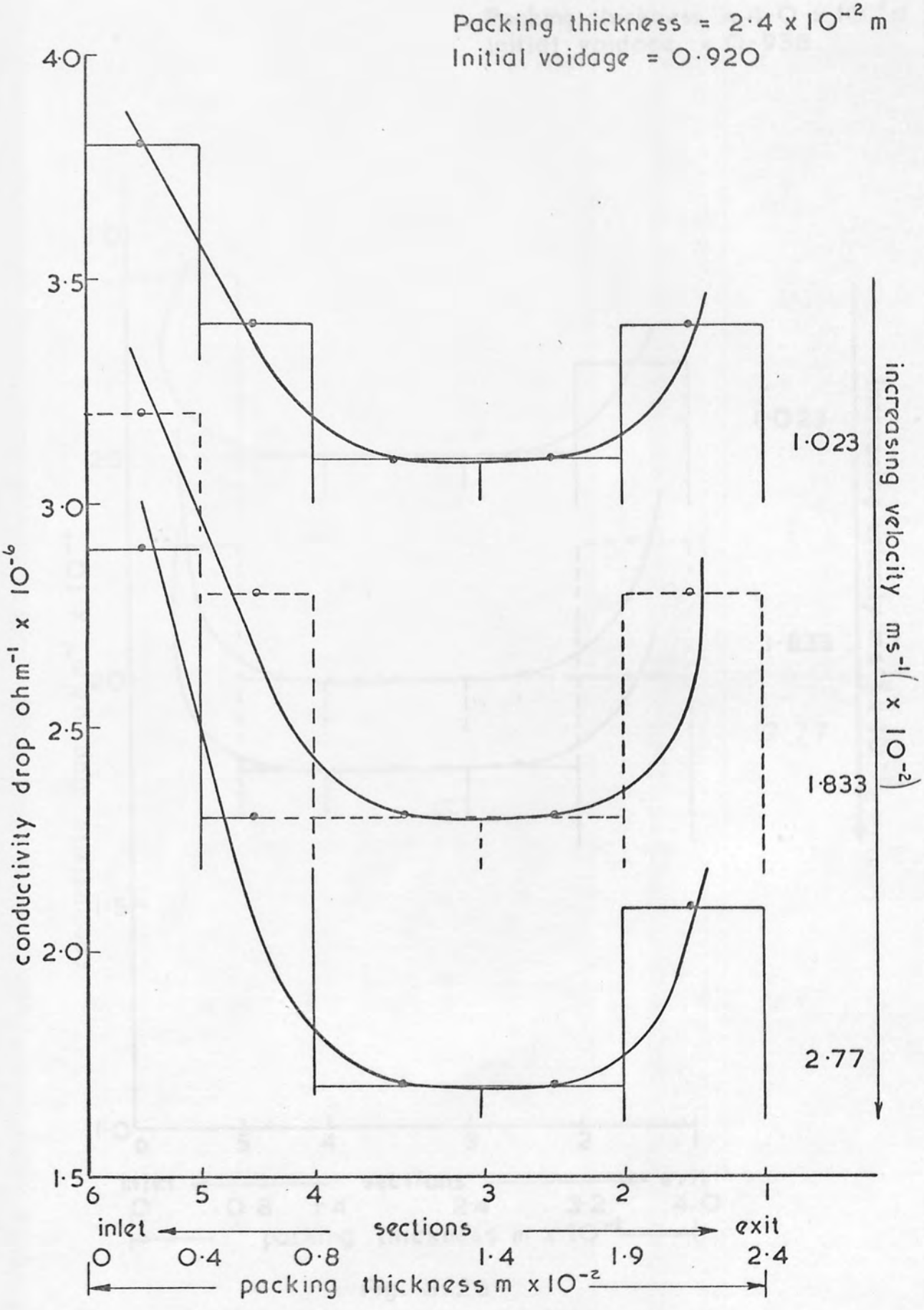
Packing thickness = 2·4 x 10⁻² m
Initial voidage = 0·920
4·0
3·5
3·0
2·5
2·0
1·5
conductivity drop ohm⁻¹ x 10⁻⁶
1·023
1·833
2·77
increasing velocity ms⁻¹ x 10⁻²
6
5
4
3
2
1
inlet
sections
exit
0
0·4
0·8
1·4
1·9
2·4
packing thickness m x 10⁻²

Fig. 8.25

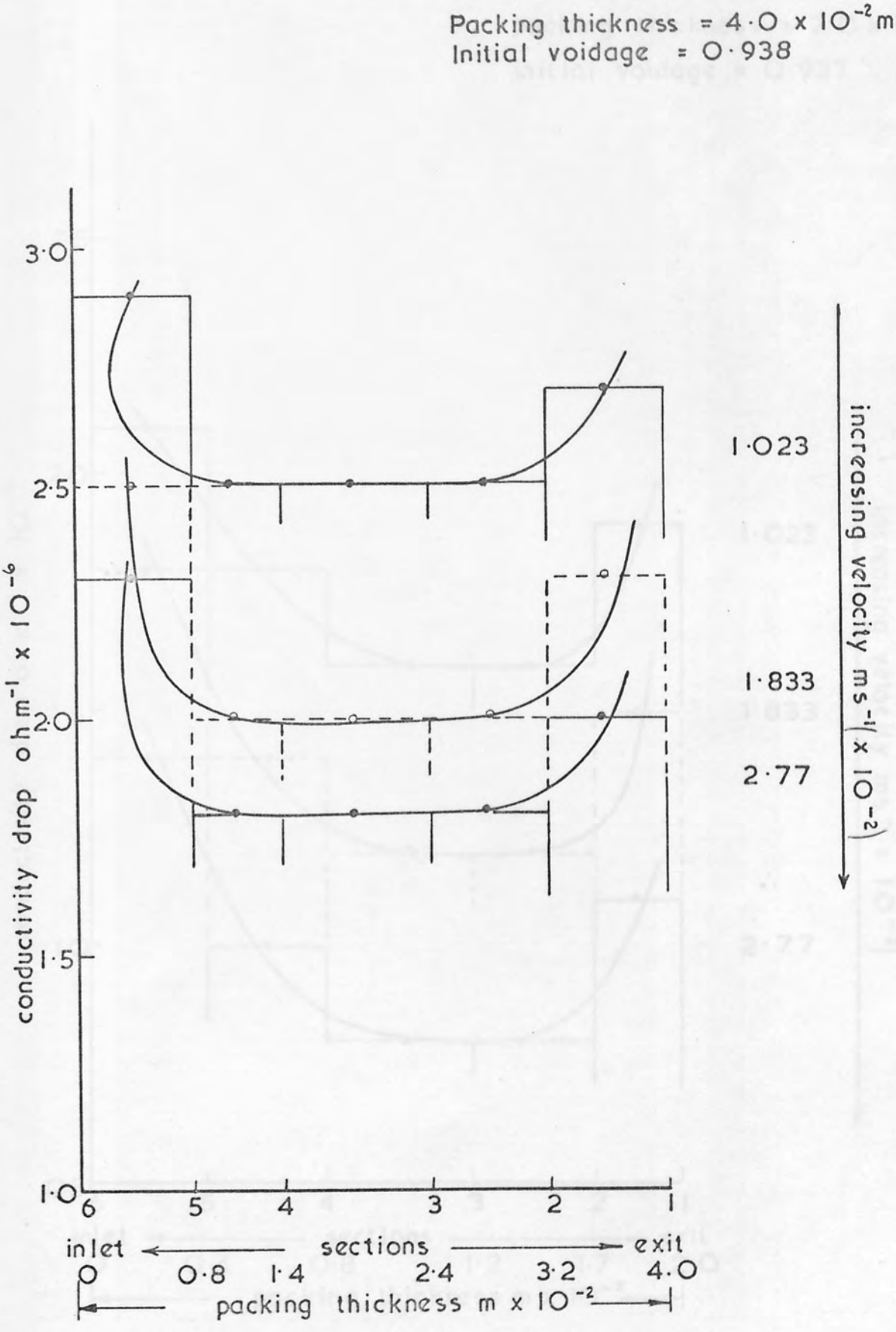
Packing thickness = 4·0 x 10⁻² m
Initial voidage = 0·938
3·0
2·5
2·0
1·5
1·0
conductivity drop ohm⁻¹ x 10⁻⁶
1·023
1·833
2·77
increasing velocity ms⁻¹ x 10⁻²
6
5
4
3
2
1
inlet
sections
exit
0
0·8
1·4
2·4
3·2
4·0
packing thickness m x 10⁻²

Fig. 8.26

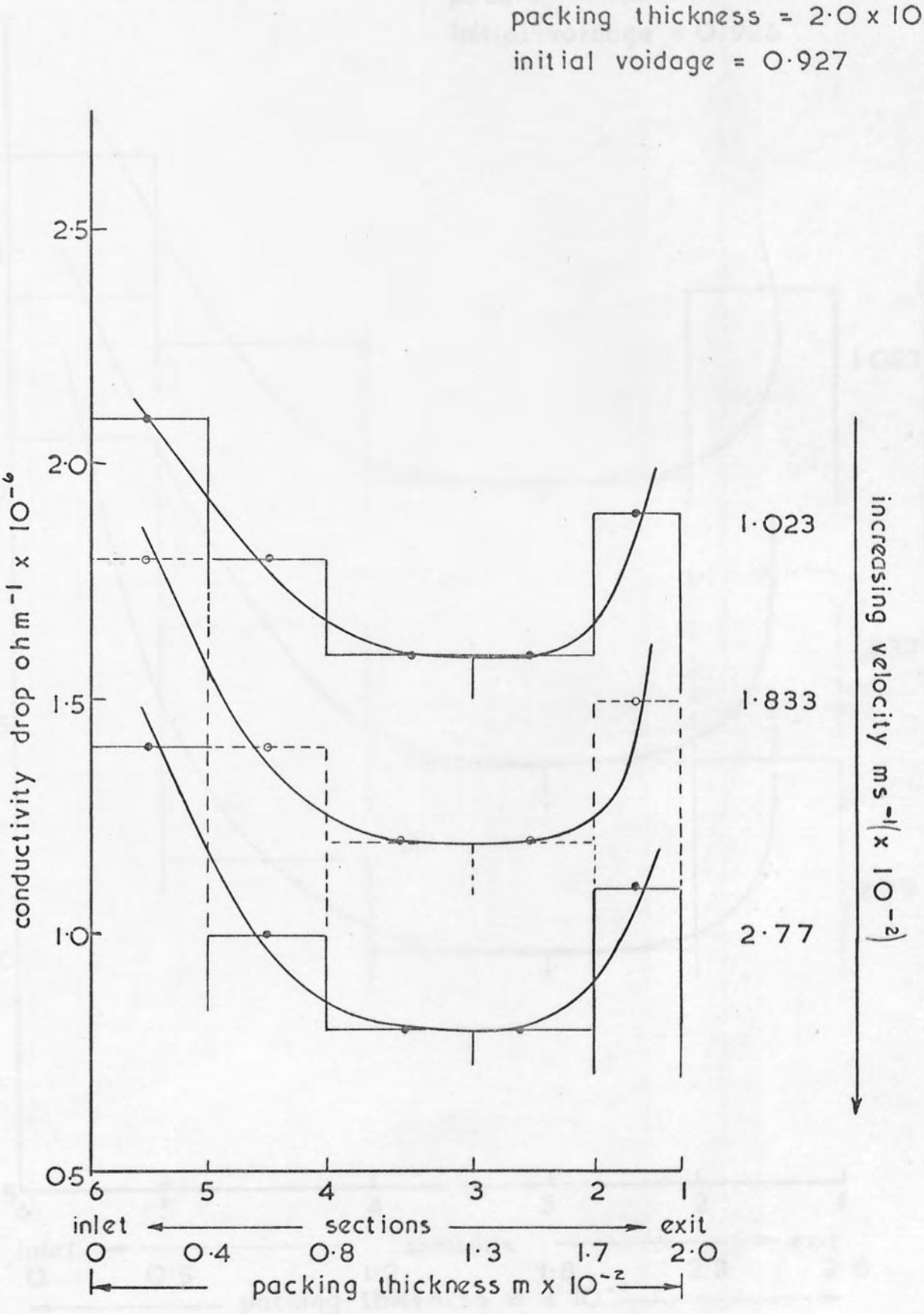
packing thickness = 2·0 x 10⁻²m
initial voidage = 0·927
conductivity drop ohm⁻¹ x 10⁻⁶
2·5
2·0
1·5
1·0
0·5
1·023
1·833
2·77
increasing velocity ms⁻¹ (x 10⁻²)
6
5
4
3
2
1
inlet
sections
exit
0
0·4
0·8
1·3
1·7
2·0
packing thickness m x 10⁻²

Fig. 8.27

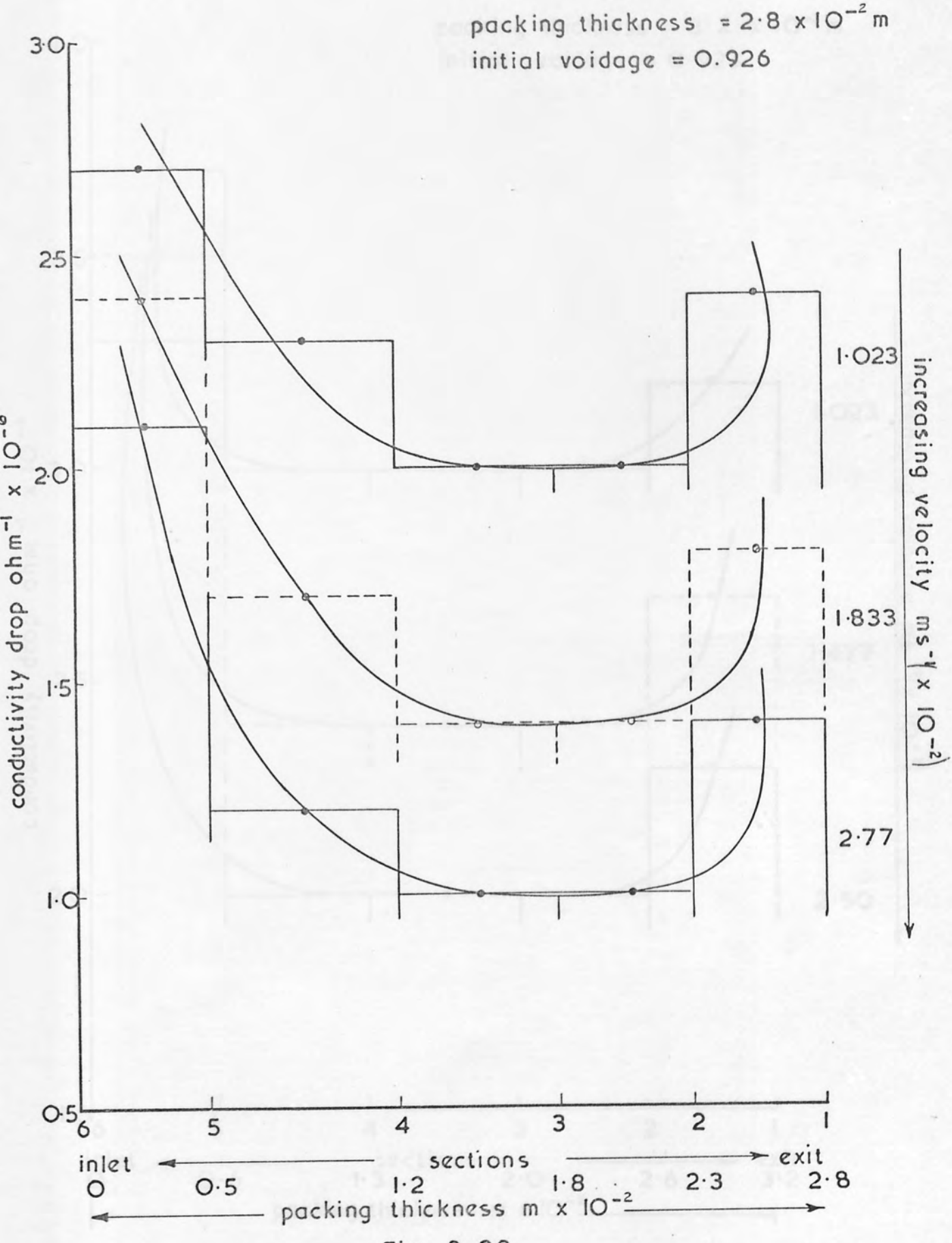
packing thickness = 2·8 x 10⁻² m
initial voidage = 0.926
3·0
2·5
2·0
1·5
1·0
0·5
conductivity drop ohm⁻¹ x 10⁻⁶
1·023
1·833
2·77
increasing velocity ms⁻¹ (x 10⁻²)
6
5
4
3
2
1
inlet
sections
exit
0
0·5
1·2
1·8
2·3
2·8
packing thickness m x 10⁻²

Fig. 8.28

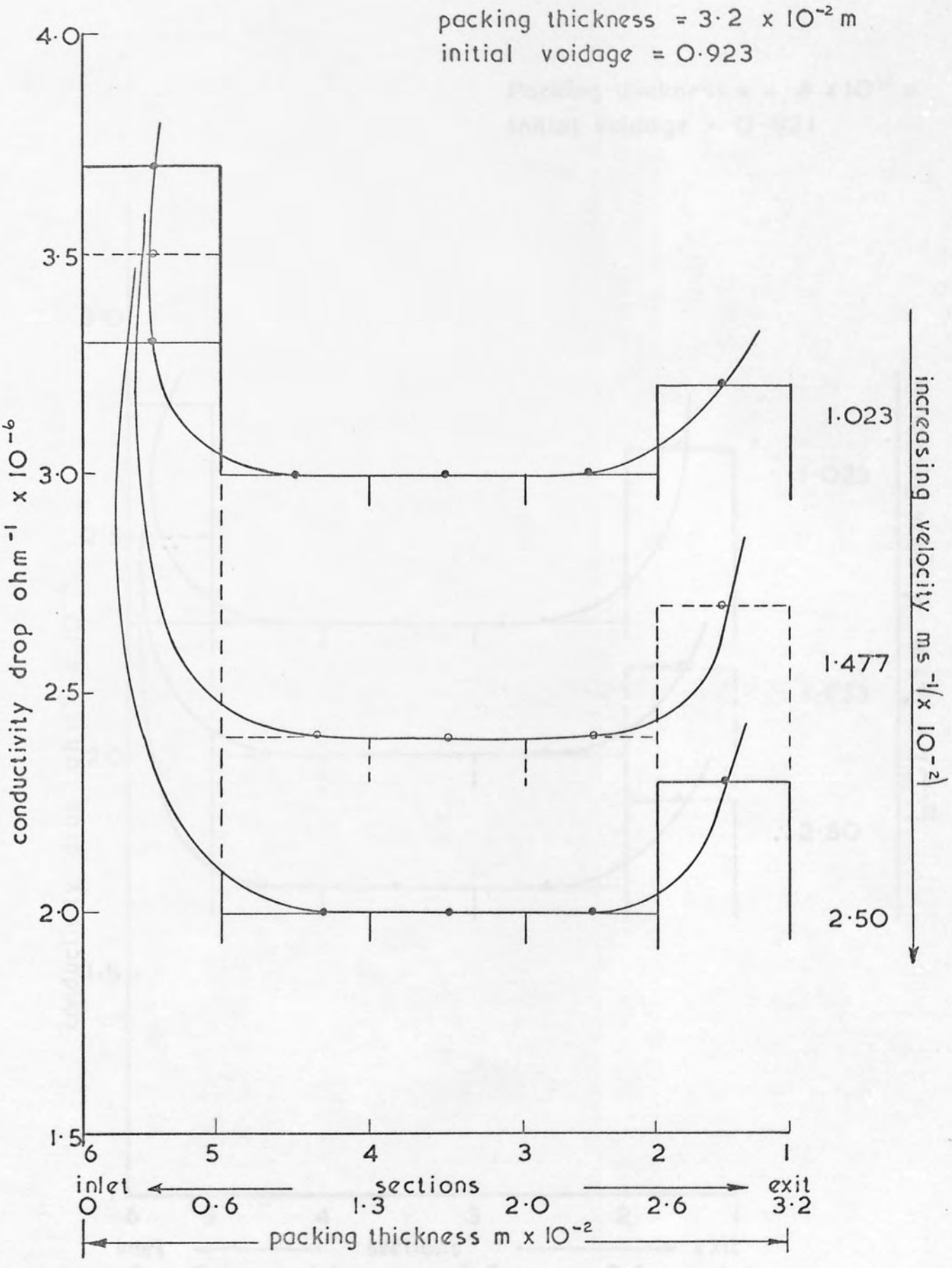
packing thickness = 3·2 x 10⁻² m
initial voidage = 0·923
4·0
3·5
3·0
2·5
2·0
1·5
conductivity drop ohm⁻¹ x 10⁻⁶
1·023
1·477
2·50
increasing velocity ms⁻¹/x 10⁻²)
6
5
4
3
2
1
inlet
sections
exit
0
0·6
1·3
2·0
2·6
3·2
packing thickness m x 10⁻²

Fig. 8.29

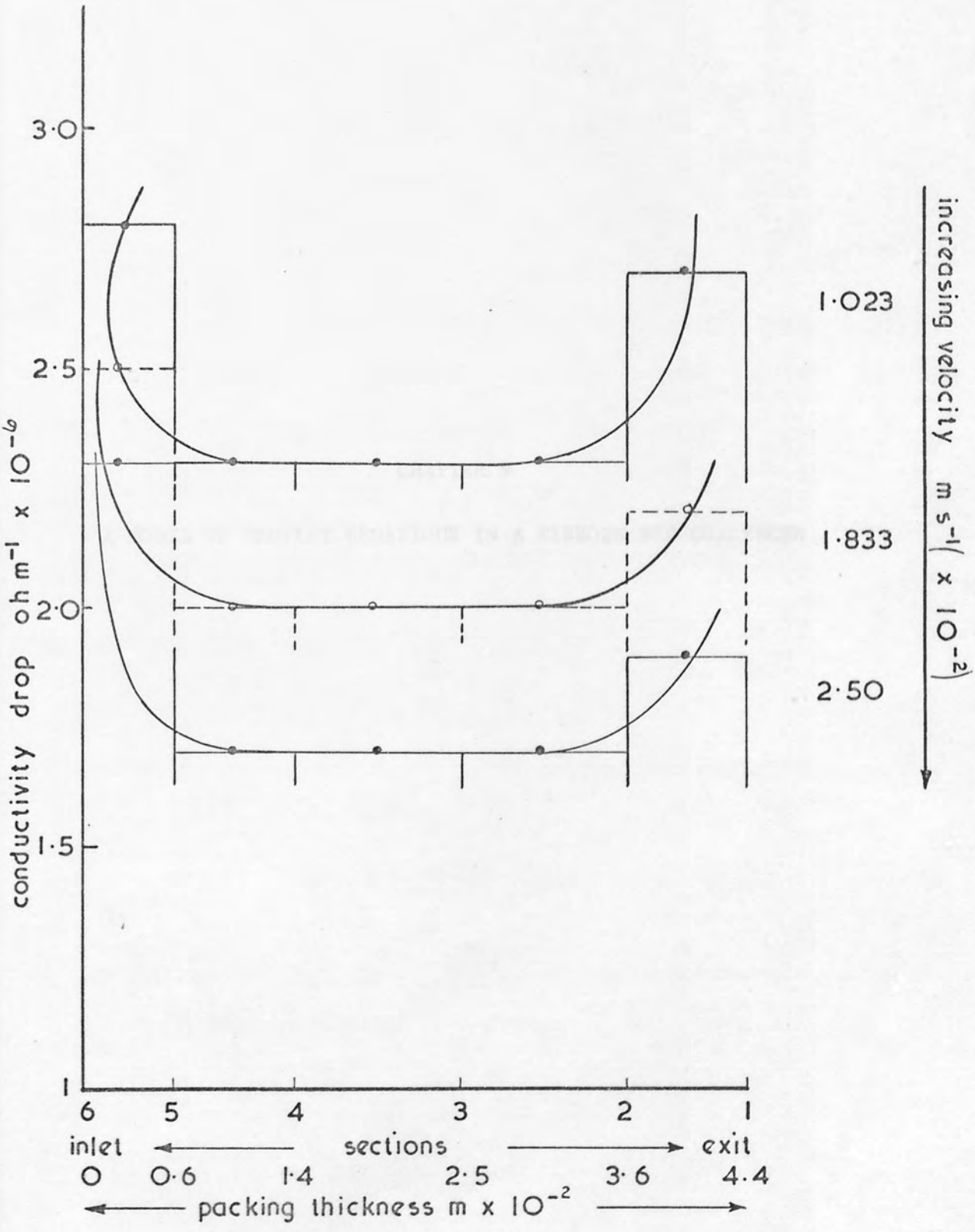
Packing thickness = 4·4 x 10⁻² m
Initial voidage = 0·921
conductivity drop ohm⁻¹ x 10⁻⁶
3·0
2·5
2·0
1·5
1
1·023
1·833
2·50
increasing velocity m s⁻¹ (x 10⁻²)
6 5 4 3 2 1
inlet ← sections → exit
0 0·6 1·4 2·5 3·6 4·4
packing thickness m x 10⁻² →

Fig. 8. 30

CHAPTER 9

A MODEL OF DROPLET BEHAVIOUR IN A FIBROUS BED COALESCER

From the results discussed in Chapter 8 it is possible to postulate certain mechanisms for the coalescence of 27 x 10^{-6} m to 1 x 10^{-3} m drops in fibrous beds. This chapter represents an attempt to elucidate the main modes of operation in three distinct processes shown in Figure 9.1, viz:

(a) Collection.

(b) Flow through the bed.

(c) Release.

9.1 COLLECTION

The mechanisms of drop collection were not studied experimentally, but various mechanisms of coalescence in a fibrous bed have been observed. These include Brownian movement, coagulation in a turbulent field and direct interception. Order of magnitude estimates can be made for each of these mechanisms within the range of operating conditions of fibrous beds using the following equations:

(a) Brownian Diffusion coefficient given by[151] :

$$k_B = \frac{2\,K\,T}{3\mu_c} \qquad \text{.....9.1.1}$$

(b) Turbulent Coagulation Coefficient: Using the equation derived by Levich[180] for colloid particles

$$k_T = \frac{d_{10}^3\, V'^{3/2}}{8\sqrt{\nu\lambda_d}} \qquad \text{.....9.1.2}$$

(c) Interception: Sherony[151] developed an equation for estimating the collision coefficient as follows:

$$k_I \phi_o = \frac{V'}{\varepsilon}\ \frac{3}{4}\left(\frac{S}{1-S}\right)\frac{(1-\varepsilon)(1+d_{10}/d_f)}{d_f}\ \eta_c \qquad \text{.....9.1.3}$$

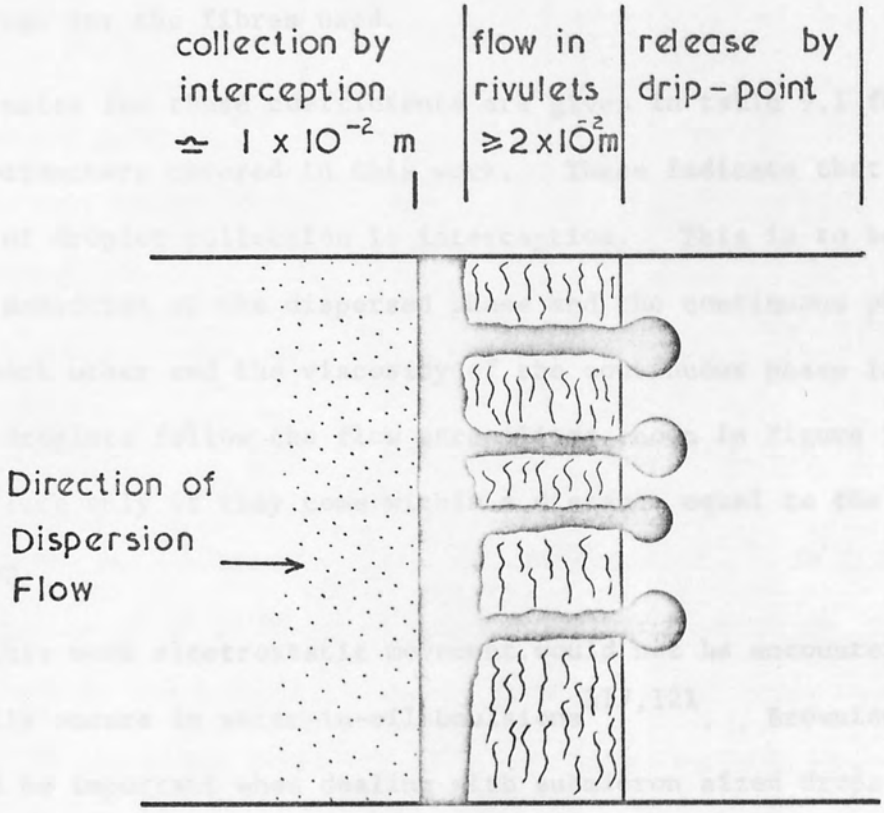

Fig 9.1. Proposed mechanisms of operation

where $\phi_o = \frac{\varepsilon S}{\frac{\pi}{6} d_{30}^3}$ 9.1.4

In estimating k_I it can be assumed that the degree of saturation S was 4%, since values obtained ranged from 3% to 6% and ε was 90% which is about average for the fibres used.

Estimates for these coefficients are given in table 9.1 for the range of parameters covered in this work. These indicate that the main mechanism of droplet collection is interception. This is to be expected since the densities of the dispersed phase and the continuous phase are close to each other and the viscosity of the continuous phase is higher. Hence the droplets follow the flow streamlines shown in Figure 5.3, and strike a fibre only if they come within a distance equal to the radius of the drop.

In this work electrostatic movement would not be encountered since it generally occurs in water-in-oil emulsions[117,121]. Brownian movement could be important when dealing with submicron sized drops. Similar conclusions were reached by other investigators[144,147], working with similar systems.

For collection to occur wetting of the fibre by the dispersed phase is not critical but surface roughness is important. Therefore any depressions or discontinuities on the fibre surface may increase their ability to capture and hold the dispersed phase drops. Any whiskers present on the fibres may also assist in the capture of drops.

Collection occurs at 'active sites' the nature of which is indeterminate, but the fibres appear to act like a catalytic surface at which adsorption takes place. An order of magnitude estimate of the number of sites is given at the end of Section 9.3.

TABLE 9.1 ORDER OF MAGNITUDE OF THE COLLISION COEFFICIENTS

$d_f = 7 \times 10^{-6}$ m, $d_{10} = 28 \times 10^{-6}$ m, $\eta_c = 0.1$		
Mechanism	k $m^3 s^{-1} \times 10^{-6}$	$V' = 1.0 \times 10^{-2}$ ms^{-1}
Brownian Movement	k_B	3×10^{-12}
Turbulent Coagulation	k_T	5×10^{-7}
Interception	k_I	5×10^{-4}

9.2 FLOW THROUGH THE BED

Average bed hold up is small, of the order of 38% to 64%, giving a bed saturation of 3% to 6% which suggests that no continuum of dispersed phase exists in the bed. Hold-up is independent of inlet drop size distribution and phase ratio but decreases with increase in superficial velocity. It is not uniformly distributed throughout the bed thickness but tends to be concentrated near the inlet.

Evidently the drops collected by the bed are not immediately released but grow by interdrop coalescence, with the majority being held up at the bed inlet. Growth occurs by the acquisition of droplets from the main stream rather than from those adhering to the fibre surface since coalescence between adjacent drops on a fibre is slow and no coalescence occurs between freely moving droplets. Collection and coalescence continues until a critical drop size is reached, which is a function of superficial velocity for any given system. This mechanism is consistent with the fact that pressure drop is independent of both mean inlet drop size and phase ratio since the minimum flow area is associated with a void space containing an equilibrium drop.

An order of magnitude of the critical drop diameter can be estimated for a single fibre by equating the drag force to the sum of the London Van der Waals force and the force of adhesion for an underformed drop[146]. For a superficial velocity of one centimetre per second and on the assumption of complete non-wetting, i.e. a contact angle of 180^{o}, the estimated size is 0.1×10^{-3} m. The situation is of course much more complex, particularly in multifibre beds, than allowed for in this calculation, but this appears to be of the right order of magnitude since inlet drops are 27×10^{-6} m and exit drops are 0.8×10^{-3} m.

Once the critical value is exceeded, the dispersed phase flows through the rest of the bed; this is evidenced by the bed hold up remaining constant until the exit plane is reached. The coalesced dispersed phase does not move through the bed in discrete drops, rather it appears to flow in rivulets which follow distinct preferred paths. Sherony[151] assumed there was complete detachment at this stage, but whether a satellite drop normally remains after detachment remains to be determined.

9.3 RELEASE

Each stream of liquid through the bed feeds a drop at the exit face. This grows into a balloon-shaped drop until the hydrodynamic forces exceed the interfacial forces and rupture occurs at the neck resulting in drip-point release. This is to be expected since calculation of jetting velocity using Ryan's equation[182] produced an order of magnitude estimate of 17 ms^{-1} due to the inevitably small aperture diameter. Thus the predominant mechanism will always be drip-point, unless interference occurs from e.g. a perforated plate. This is not to be confused with

the mechanism observed by Polichronakis[154] which was jetting after breakthrough that is when little or no collection was occurring. Although dispersion is apparently by the usual mechanism for drop formation at low velocities, the exit drop volume could not be predicted from the volumetric flow rate, aperture diameter and physical properties using the Scheele and Meister correlation[183].

The droplets leave the bed from fixed sites only after an equilibrium size is reached, which is a function of superficial velocity for a given system. Hence residence time of the exit droplets is not critical. Exit drop size is independent of inlet drop size distribution and phase ratio but decreases with increase in superficial velocity until a critical separating velocity is identified after which bed breakthrough occurs. At this velocity, the droplets will be carried away before attaining the equilibrium size due to the viscous shear being greater than the force of adhesion.

Bed hold up at the exit plane increases possibly due to the exit drop diameter being much greater than the fibre pitch diameter and because drops must be retained until the equilibrium drop size is reached.

An order of magnitude estimate of the number of 'active sites' is possible by assuming that under normal operating conditions single phase flow and two phase flow voidages are 0.900 and 0.851 respectively. Thus $\Delta\varepsilon$, the difference, equals 0.049. For a phase ratio of 3%, the number of drops of twenty seven micrometres is 3.56×10^{7}. Assuming steady state conditions the corresponding number of drops of 0.1×10^{-3} m, the 'critical' drop diameter, is 0.07×10^{7}. The calculated mean volume diameter is therefore 34×10^{-6}m. The number of 'active sites'

can then be calculated from

$$\frac{\Delta\varepsilon}{\pi d_i^3/6} \qquad \text{.....9.3.1}$$

to give 2×10^6. In fact a similar estimate is obtained if the linear-mean drop size is used as being more characteristic of the operation, i.e. 5×10^6, or indeed using the mean inlet drop size. Hence it appears that $\simeq 10^6$ 'active sites' occur per cm^3 of packing. This is simply based on each drop requiring one 'active site' whether on a fibre or on the end of a droplet chain. Evidently this definition of 'active sites' is a function not only of the packing but of superficial velocity; it is likely however, to be independent of system properties. Thus the nature of sites and the manner in which more could be promoted in a fibrous bed is clearly of considerable academic and practical interest.

CONCLUSIONS

The main conclusions from this work are as follows:

(1) A centrifugal pump with a recirculating loop provided a simple method of preparing a continuous supply of secondary dispersion with a reproducible drop size distribution. The mean drop size, as determined by a Coulter Counter, increased with decrease in turbulence, i.e. lower pump speed.

(2) Pressure drops associated with single phase flow and two phase flow through fibrous beds could be correlated by a Blake-Kozeny type equation.

(3) When coalescing a secondary dispersion in fibrous beds of voidage 0.90 to 0.94 and with superficial velocities of 1.0×10^{-2} ms^{-1} to 2.77×10^{-2} ms^{-1}, exit drop size was independent of both inlet drop size distribution and phase ratio, but decreased with increase in superficial velocity. There was a critical separating velocity above which bed breakthrough occurred. This critical velocity increased with bed thickness, but there appeared to be an optimum thickness for each application. Average bed hold up, and hence average saturation, was independent of inlet drop size distribution and phase ratio, but decreased with increase in superficial velocity.

(4) Studies of coalescence on a single fibre showed that preferential wetting of the fibre by the dispersed phase was not critical. Interdrop coalescence occurred between a retained drop and others from the main stream rather than with other retained drops.

(5) Development of a novel conductivity measurement technique enabled analysis to be made of hold up distribution across the fibrous bed. Results showed that the highest amount of hold up was at the inlet

plane of the bed followed by a sharp drop at approximately 1.2×10^{-2} m bed depth. The hold up retained throughout the rest of the bed did not vary until near the exit where it increased. The hold up distribution was independent of inlet drop size distribution and phase ratio.

(6) A mechanism for secondary dispersion separation in fibrous beds has been postulated on the basis of a certain number of 'active sites' available for drop capture at the bed inlet. Once these sites were occupied interdrop coalescence occurred by the acquisition of free droplets from the main stream until an equilibrium size had been reached; this size represented a balance between the adhesive force between the drop and the fibre and the hydrodynamic force on the drop. Equilibrium size drops subsequently moved through the rest of the bed in rivulets to feed a drop at the exit face. Enlarged droplets detached from fixed points via a 'drip point' mechanism, and their size was a function of superficial velocity.

RECOMMENDATIONS FOR FURTHER WORK

Several areas of further work appear worthwhile pursuing as summarised below:

(1) There is a lack of information on the pore size distribution within fibrous beds. It would be advantageous if work were done on experimental measurement of this distribution and the formulation of a generalized equation involving the main parameters of the bed, including for example fibre diameter and standardized compaction. This could be achieved by pouring hot molten wax into the bed and slicing it up.

(2) The present investigation could be extended using the existing apparatus to cover a range of variables. These could include:

(a) Different liquid systems covering a range of viscosities. Limitations arise in that the drop size distribution of water-in-oil systems cannot be determined using the Coulter Counter and hence they cannot be studied using the technique described here. Studies initiated into the use of holography[167] should be taken further.

(b) Different materials of construction including those whose surface roughness can be varied and measured, e.g. stainless steel or glass etched with an acid.

(c) The effect of additives such as electrolyte type and concentration, surfactants and solid contaminants.

(3) Studies of coalescence on a single fibre should be extended to cover the effect of fibre diameter, fibre orientation, fibre surface properties and flow velocity.

(4) Attempts could be made to determine the hold-up distribution across

the fibrous bed. Possible techniques include X rays or γ rays from a radioactive source, which have for example been used to determine saturation in porous media[178], or matching the refractive indices of the saturating liquids to that of the coalescing media. By local injection of a tracer the displacement of one liquid by another could be observed[179]. Heller[181] suggested the use of crystalline calcium fluoride for the solid component, because it has a low refractive index and it is relatively insoluble, chemically inert and nontoxic, so that a large assortment of matching liquids may be used.

APPENDIX A

COULTER COUNTER INSTRUCTIONS

The instrument should preferably be located in a dust free room. However any bench can be used which is not subject to excessive airborne dust, strong vibrations, high intensity sound, or electrical noise, and such a bench was used in this work. The method of operation of the Coulter Counter for sizing secondary dispersions was adopted from the Manufacturer's Manual[158], and is described below. The controls are briefly explained to assist understanding.

A.1 COULTER COUNTER MODEL ZB CONTROLS

These are shown in Figures A.1 and A.2.

(a) Lower Threshold Dial t_L: Determined the size level above which the instrument counted pulses. All tips which reached this value were counted.

(b) Upper Threshold Dial t_u: Set the 'no count' level, so facilitating an 'in between' count.

(c) $\frac{1}{\text{Amplification}}$, Attenuation A: Set the amplifier sensitivity. Each clockwise step doubled the sensitivity and gain of the instrument and hence the pulse height, i.e. for any threshold setting the droplet size volume was halved for each successive switch position.

(d) $\frac{1}{\text{Aperture Current}}$ I : Controlled the amount of current flowing between the two electrodes. Each consecutive clockwise interval increased the current by a factor of two or $\sqrt{2}$. Two lamps POS. NEG. indicated the polarity of the external electrode which was automatically reversed to minimise electrochemical effects.

(e) Vacuum Regulator: Turning this control clockwise increased the vacuum available to the aperture tube.

(f) Microscope: When set correctly, the orifice appeared as a small circle in a bright disc. Any partial or complete blockage, which would cause incorrect counts, was detectable.

A.2 ELECTROLYTE FILTRATION

It was desirable for the electrolyte background count, discussed in Section A.3.1 to be as low as possible. This was achieved by careful filtration using a Sartorius Membrane filter to retain particles down to 0.45×10^{-6} m.

A.3 OPERATION

The orifice tube selected was such that the suspected largest droplet size occupied about 40% of the aperture diameter. After fitting this to the control piece, the manometer selector switch was set to the recommended position and the glassware filled with the filtered electrolyte. A clean two hundred and fifty millilitre beaker was then filled with this electrolyte and placed on the adjustable platform and the stirrer started. The controls t_L, t_u, I and A were set to 10, 110 (out), $\frac{1}{4}$ and $\frac{1}{8}$ respectively, and a blank count made.

A.3.1 Blank Count

When tap T shown in Figure A.2 was opened to vacuum the mercury came to rest below the start electrode; as shown in Figure A.3, the digital count display was automatically reset to zero, the oscilloscope lit-up and the aperture current was initiated. When the tap was closed the instrument started to count as soon as the mercury touched the start electrode and stopped when it encountered one of the other electrodes, dependent upon the setting of the manometer volume switch. The count

obtained represented the total number of particles in the blank electrolyte above a size level approximately 2% of the orifice diameter. For the desired accuracy this had to be within an acceptable range, e.g. for a one hundred and forty micrometre aperture tube at 0.5×10^{-6} m^3 manometer volume, the maximum blank count needed to be 150, although a lower count gave a better accuracy. If a higher count was obtained the beaker was rinsed and a fresh sample analysed. If it was still unacceptable the electrolyte was re-filtered. If the count continued to be high the possibility of external 'noise', interference, or a blocked orifice, was considered. Once acceptable, t_L, I and A were set to 20, 8 and 32 respectively, a size level 40% of the orifice diameter, and a count taken. One or two pulses generally appeared.

A.3.2 Calibration

Calibration was performed using Lycopodium 'monosized' particles of twenty eight micrometres in diameter lying between 5% and 20% of the orifice diameter by the Half Count Technique.

A small sample of Lycopodium powder was dispersed in a few drops of alcohol on a watch glass. Two hundred millilitres of electrolyte in a two hundred and fifty millilitre beaker was placed on the sample stand, the sample added and the stirrer started.

t_L, t_u, A and I were set to 1, 110, 1 and 1 respectively, and tap T opened. Pulses appeared on the oscilloscope screen; A and I were then adjusted until the majority of these were about one and a half to two centimetres high. t_L was then increased until the shadow line coincided with the maximum height of the majority of the pulses. This was designated T. The control t_L was decreased to $\frac{T}{2}$, 2 to 4

counts taken, and the average designated N_1. t_L was then increased to $\frac{3T}{2}$ and the same procedure repeated to give N_2. N_3 was given by:

$$N_3 = \frac{N_1 + N_2}{2} \quad \text{.....A.3.2.1}$$

t_L was set back to T and a count taken. The setting was raised or lowered, to decrease or increase the count, until count N_3 was obtained as closely as possible. The final setting was designated t'. If this value was more than 1 or 2 threshold divisions from T, the calibration procedure was repeated using t' as T. k, the calibration constant was calculated from:

$$k = \frac{d}{\sqrt[3]{t' \times I \times A}} \quad \text{.....A.3.2.2}$$

Example: For a one hundred and forty micrometre orifice tube, 0.5 x 10^{-6} m^3 manometer volume, 0.9% sodium chloride solution and twenty eight micrometre diameter Lycopodium powder.

$I = 4 \qquad A = 8 \qquad T = 24$

$\frac{T}{2} = 12 \qquad N = 495, 473, 485. \qquad N_1 = 484$

$\frac{3T}{2} = 36 \qquad N = 9, 12, 13, 10. \qquad N_2 = 11$

$\therefore \quad N_3 = \frac{484 + 11}{2} = 248$

At $t' = 22 \qquad N = 245, 256, 238 \qquad N_{av} = 246$

$\therefore \quad I = 4, \quad A = 8, \quad t' = 22$ and $d = 28$

$\therefore \quad k = \frac{28}{\sqrt[3]{22 \times 4 \times 8}} = 3.2$

A.3.3 Analysis Technique

A sample of the dispersion was transferred to the electrolyte beaker as discussed in Section 7.9, the beaker placed on the platform

and the stirrer started. t_L, I and A were set to 10, ¼, and 1/8 respectively, as discussed in Sections A.3 and A.3.1, and a count taken. The count had to be near to that donated 10% 'coincidence' for the particular orifice tube and manometer volume. If a higher count was obtained, the dispersion was diluted with electrolyte; if it was lower a fresh, more concentrated supension was prepared. When a satisfactory value had been achieved, t_L, I and A were set to 20, 8 and 32 respectively as discussed in Section A.3.1, and the count was arranged to be less than two as before. The intervals at which counts were taken depended upon the size range to be covered, but a full range of 16 points analysis was generally adopted with counts being taken at the levels shown in Table A.1.

A.4 MODEL M2 VOLUME CONVERTER CONTROLS

These are shown in Figure A.4.

(a) Off: Disconnected the M2 allowing the ZB to operate conventionally by manometer volume selection.

(b) Int. and Dif: Determined whether the ZB readout would be integral (cumulative) or differential (frequency) volume values.

(c) Stop: Cancelled the timer and prevented the pulses from feeding to the readout. In the event of an orifice blockage, it was pressed, the blockage removed and the cycle recommenced in the Dif. mode.

(d) Start: Initiated the count cycle which switched on the count indicator light.

(e) Time Factor T: Set the sample analysis time from 128 to 2 seconds, over-riding the ZB manometer volume contacts.

(f) Division Factor U: Determined the computer division factor as part of volume conversion. 4 generated four pulses for each particle-generated pulse and $\frac{1}{128}$ generated one pulse for each 128 particle-generated pulses.

(g) Resultant: Confirmed the value used for computed volume conversion.

A.5 COMPLETE ANALYSIS USING M2 VOLUME CONVERTOR

A beaker filled with the electrolyte and sample was placed in counting position. The ZB controls were set to $t_L = 20$, $t_u = 40$, I = 8, A = 32, M2 controls to INT., T = 128, U = 4, and tap T opened. Reset on the M2 was pressed; pulse patterns appeared on the oscilloscope and the digital readout fell to zero. Start was pressed, the counting continued until the count indicator light went out. The readout value was then recorded on the data sheet shown in Table A.1. The settings were then altered and start pressed until all the settings shown had been scanned. A blank count was then taken of the prefiltered electrolyte in a clean beaker using the same settings as the sample. Data handling is also shown in Table A.1.

A.6 COMMON SOURCES OF ERROR

Even with the established procedures just described there were practical sources of error. These could be identified and eliminated as follows:

(a) A high blank count could be eliminated by proper electrolyte filtration as discussed in Section A.2.

(b) Orifice blockage would result in an increase in pulse height

and counting time. These could be detected by a change in oscilloscope pattern and orifice observation through the microscope.

(c) Air bubbles in the sample and inside the orifice tube due to vigorous mixing. Slow mixing was used throughout to avoid vortex formation.

(d) Air leaks, breaks in the mercury column or dirty manometer.

(e) Cracked or damaged orifice tube.

(f) External interference from flickering or humming fluorescent lights, thermostats, motor brushes or power line noise.

In the early part of this work, use was made of an obsolete Coulter Counter Model A, fitted with a two hundred and eighty micrometre orifice tube. The results were calculated using a computer program shown in Figure A.5 and a typical type out is shown in Figure A.6.

TABLE A.1

COULTER COUNTER DATA AND WEIGHT CONVERSION

INDUSTRIAL MODEL ZB + VOLUME CONVERTER MODEL M2

Phase Ratio: 3%

Pump Speed: 86.7 revs s^{-1}

Electrolyte: 0.9% Sodium Chloride

Date: 10.6.1974

Aperture Diameter: 140 x 10^{-6} m

Manometer Volume: 0.5 x 10^{-6} m^3

Calibration Data: I = 4, A = 8, t = 22

Calibration Factor, k 3.2

Model ZB				Model M2			Model M2 Int. Mode			Cum. Wt. %
tL	tu	I	A	T	U	$d=k.\sqrt[3]{tL.I.A}$	Raw $\sum(\Delta n)\overline{V}$	B	$\sum(\Delta n)\overline{V}$-B	Oversize
20	40	8	32	128	4	55.2	996	0	996	3.3
20	40	8	16	64	4	43.8	1332	0	1332	4.5
20	40	8	8	32	4	34.8	4236	0	4236	14.2
20	40	8	4	16	4	27.6	9080	0	9080	30.5
20	40	8	2	8	4	21.9	15331	0	15331	51.5
20	40	8	1	8	2	17.4	20881	0	20881	70.2
20	40	4	1	8	1	13.8	25234	0	25234	84.8
20	40	2	1	8	½	11.0	27641	1	27640	92.9
20	40	1	1	8	¼	8.7	28751	3	28748	96.6
20	40	1	½	8	1/8	6.9	29221	6	29215	98.2
20	40	1	¼	8	1/16	5.5	29431	10	29421	98.9
20	40	1	1/8	8	1/32	4.3	29518	15	29503	99.1
20	40	½	1/8	8	1/64	3.4	29576	21	29555	99.3
20	40	¼	1/8	8	1/128	2.7	29650	30	29620	99.5
20	40	1/8	1/8	4	1/128	2.2	29738	32	29706	99.8
10	20	1/16	1/8	2	1/128	1.4	29783	36	29757	100.0

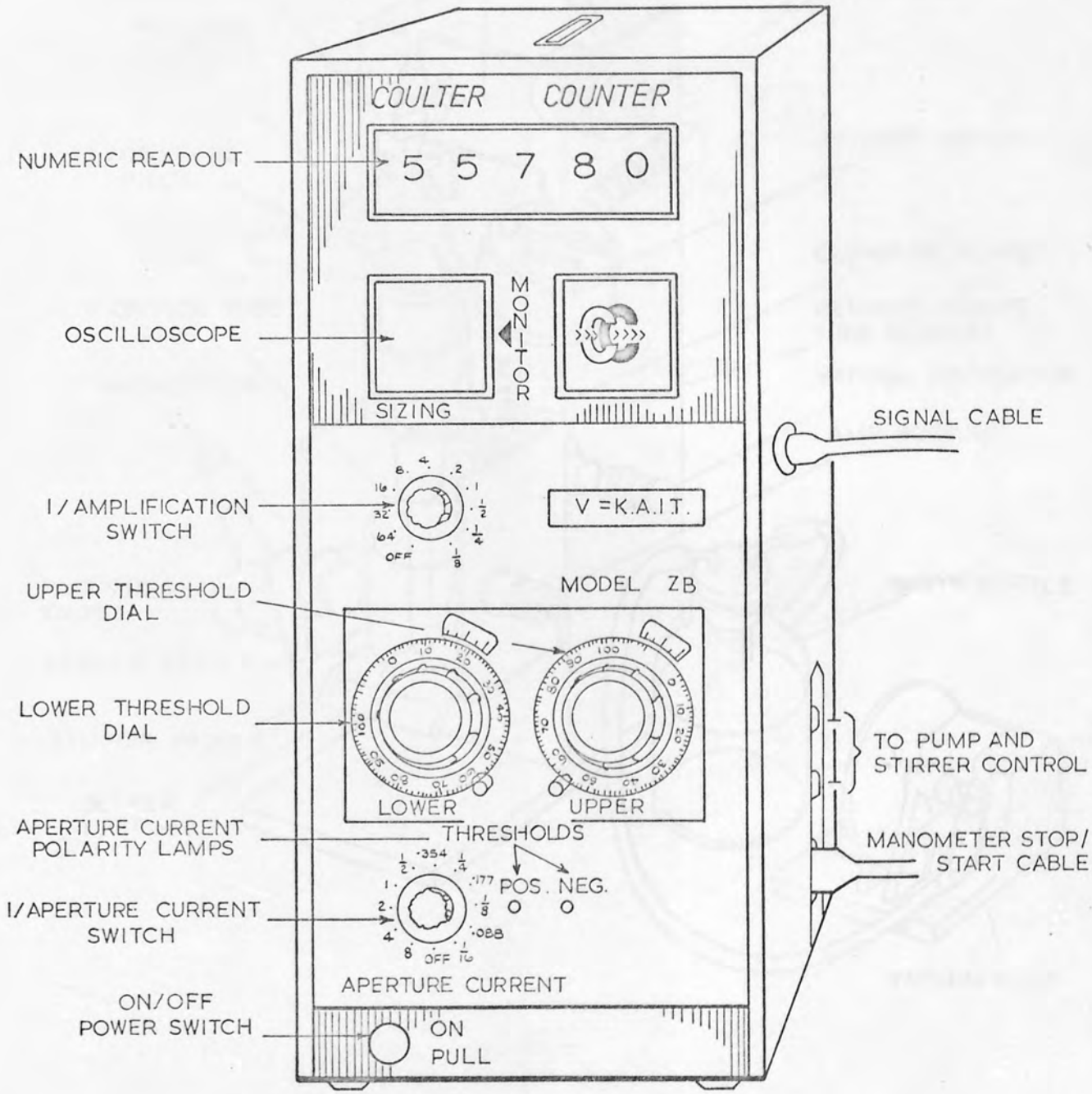

Fig. A.1 Coulter counter model Z_B front panel

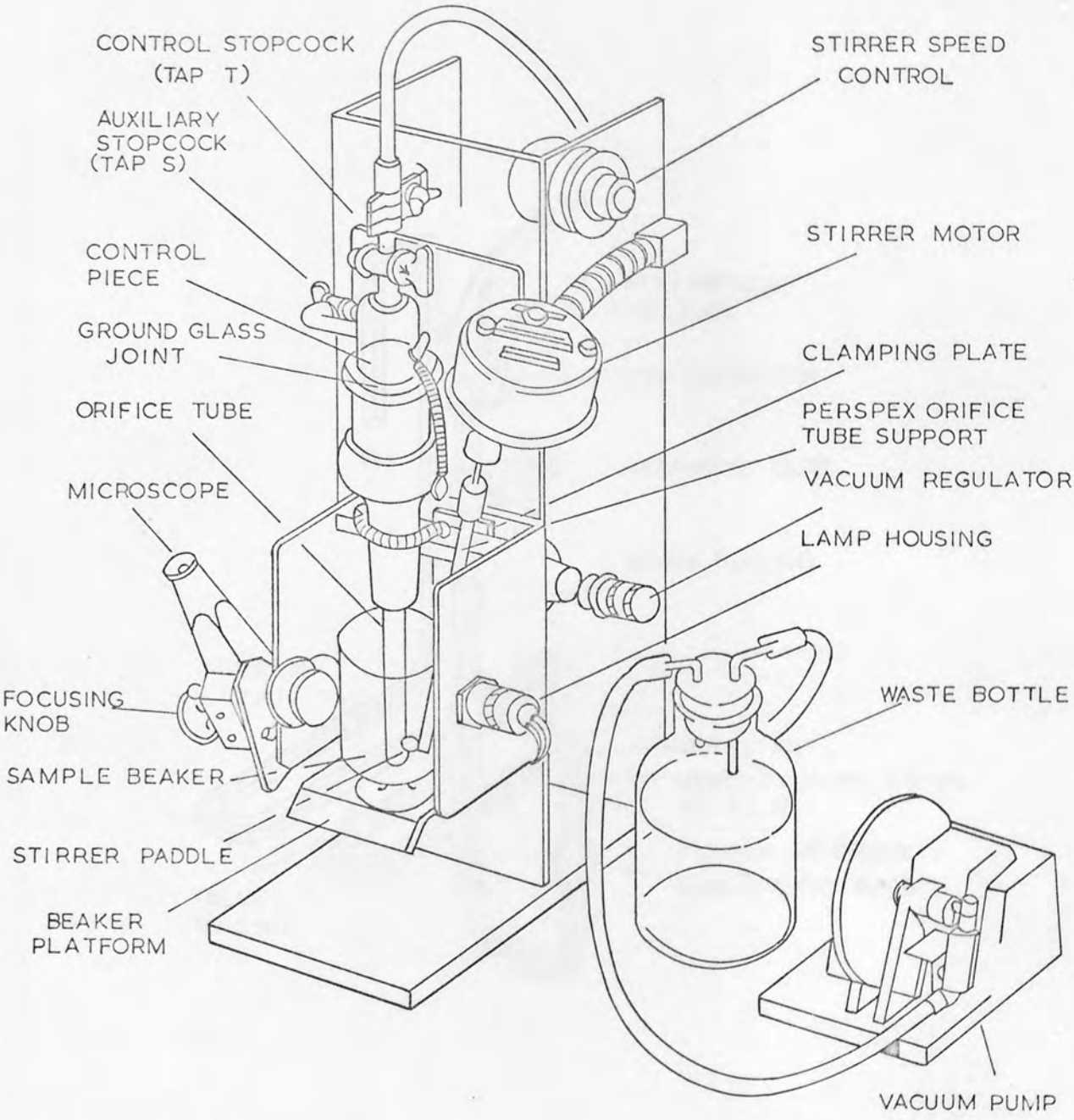

Fig. A.2. Glassware stand assembly

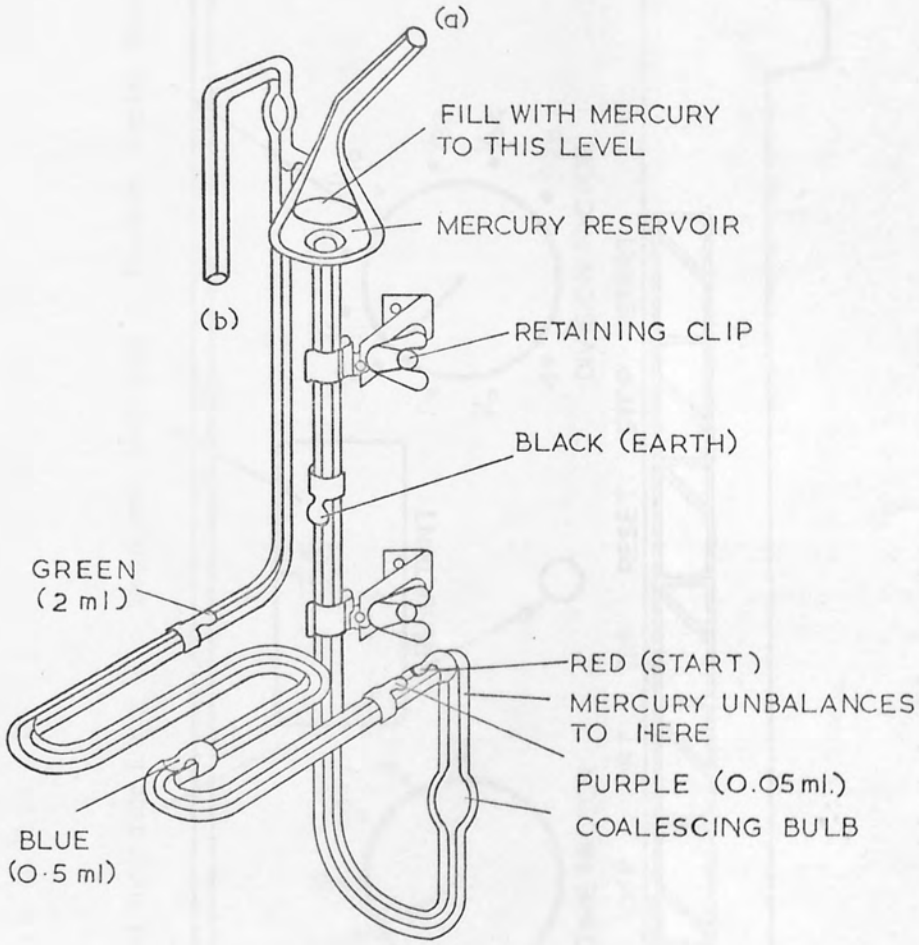

Fig. A. 3. Mercury manometer

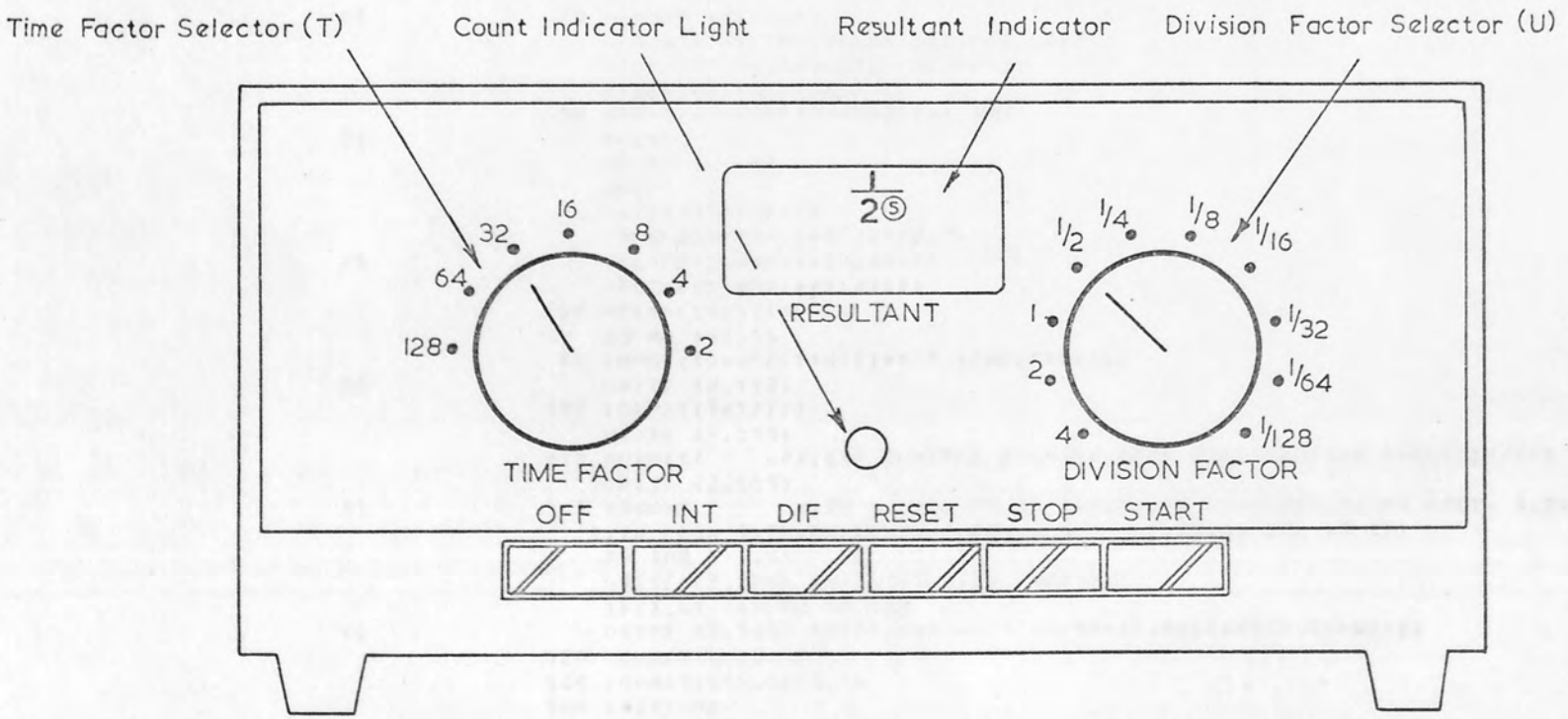

Fig. A.4 Model M_2 volume converter

```
      PROGRAM NAME(INPUT,OUTPUT,TAPE1=INPUT,TAPE2=OUTPUT)
      DIMENSION NMEAN(15),BLANK(15),TDASH(15),F(15),NDD(15),N(15),T(15),
     1  DELTAN(15),DELNT(15),DN(15),TMEAN(15),DPART(15),CUMWT(15)
      REAL KFACTR,NMEAN,NDD,N
      READ(1,10) VOLUM,APERD,KFACTR
   10 FORMAT (3F15.6)
      KFACTR=2.5*(APERD/100.)**3*500./VOLUM
      READ (1,12) TDASH
   12 FORMAT (4F15.6/4F15.6/4F15.6/3F15.6)
      READ (1,14) F
   14 FORMAT (4F15.6/4F15.6/4F15.6/3F15.6)
      DO 100 L=1,9
      DO 30 J=1,15
      READ(1,20) NMEAN(J),BLANK(J)
   20 FORMAT (2F15.6)
      NDD(J)=KFACTR*(NMEAN(J)/1000.)**2
      N(J)=NMEAN(J)+NDD(J)-BLANK(J)
      T(J)=TDASH(J)*F(J)
   30 DPART(J)=KFACTR*(T(J))**.333
      DEL=0.
      DO 60 I=1,14
      J=I+1
      DN(I)=N(J)-N(I)
      TMEAN(I)=(T(I)+T(J))/2.
      DELNT(I)=DN(I)*TMEAN(I)
      DELTAN(I)=DEL+DELNT(I)
   60 DEL=DELTAN(I)
      DO 80 I=1,14
   80 CUMWT(I)=(DELTAN(I)*100.)/DELTAN(14)
      WRITE (2,112)
  112 FORMAT(1H1///)
      WRITE (2,113)
  113 FORMAT(    40X,43H COULTER COUNTER SIZE DISTRIBUTION ANALYSIS///)
      WRITE (2,115)
  115 FORMAT (    5X,7H N MEAN,9X,4H T*F,7X,9H DIAMETER,7X,8H DELTA N,7X
     1,7H MEAN T,7X,8H DELTA*T,7X,8H SUM D*T,7X,9H CUM WT %/)
      DO 100 I=1,15
      WRITE (2,120) NMEAN(I),T(I),DPART(I)
      IF(I.GT.14) GO TO 100
      WRITE (2,140) DN(I),TMEAN(I),DELNT(I),DELTAN(I),CUMWT(I)
  120 FORMAT(3F15.5)
  140 FORMAT(45X,5F15.5)
  100 CONTINUE
      STOP
      END
```

Fig. A.5. Computer program for drop size analysis using model A coulter counter

COULTER COUNTER SIZE DISTRIBUTION ANALYSIS

N MEAN	T*F	DIAMETER	DELTA N	MEAN T	DELTA*T	SUM D*T	CUM WT %
0.20000E 01	0.50000E 03	0.10497E 03	0.00000E 00	0.25500E 03	0.00000E 00	0.00000E 00	0.00000E 00
0.20000E 01	0.41000E 03	0.95215E 02	0.00000E 00	0.18000E 03	0.00000E 00	0.00000E 00	0.00000E 00
0.20000E 01	0.15000E 03	0.85333E 02	0.00000E 00	0.12000E 03	0.00000E 00	0.00000E 00	0.00000E 00
0.20000E 01	0.90000E 02	0.70297E 02	0.00000E 00	0.75000E 02	0.00000E 00	0.00000E 00	0.00000E 00
0.20000E 01	0.60000E 02	0.61419E 02	0.30870E-04	0.45030E 02	0.13901E-02	0.13901E-02	0.21893E-03
0.25000E 01	0.50360E 02	0.48792E 02	0.25003E 01	0.22560E 02	0.56406E 02	0.56407E 02	0.88837E 01
0.50000E 01	0.15060E 02	0.38761E 02	0.30005E 01	0.11313E 02	0.33945E 02	0.90352E 02	0.14230E 02
0.80000E 01	0.75660E 01	0.30820E 02	0.27016E 02	0.56910E 01	0.15375E 03	0.24410E 03	0.38444E 02
0.35000E 02	0.58160E 01	0.24539E 02	0.19525E 02	0.28800E 01	0.56231E 02	0.30033E 03	0.47300E 02
0.55000E 02	0.19440E 01	0.19605E 02	0.66163E 02	0.14763E 01	0.97676E 02	0.39801E 03	0.62683E 02
0.12200E 03	0.10086E 01	0.15755E 02	0.12867E 03	0.77520E 00	0.99748E 02	0.49776E 03	0.78392E 02
0.25300E 03	0.54180E 00	0.14810E 02	0.13164E 03	0.42570E 00	0.56041E 02	0.55380E 03	0.87218E 02
0.38400E 03	0.30960E 00	0.10632E 02	0.20027E 03	0.25320E 00	0.50708E 02	0.60450E 03	0.95204E 02
0.59100E 03	0.19680E 00	0.91430E 01	0.20630E 03	0.14760E 00	0.30450E 02	0.63495E 03	0.10000E 03
0.81400E 03	0.98400E-01	0.72584E 01					

Fig. A.6. Typical output from computer program

APPENDIX B

EXIT DROP SIZE ANALYSIS

```
10  PRINT "EXIT DROP SIZE ANALYSIS"
20  DIM D(43),N(43),B(43)
25  READ F
26  F=F*3
30  DIM M(6),S(6),C(6),V(6)
31  FOR C=1,6
35  B(1)=1.49:B(2)=2.04:B(3)=2.59:B(4)=3.14:B(5)=3.7
40  B(6)=4.25:B(7)=4.3:B(8)=5.35:B(9)=5.9:B(10)=6.46
45  B(11)=7.01:B(12)=7.56:B(13)=8.11:B(14)=8.66:B(15)=9.22
50  B(16)=9.77:B(17)=10.32:B(18)=10.87:B(19)=11.42:B(20)=11.98
55  B(21)=12.53:B(22)=13.08:B(23)=13.63:B(24)=14.18:B(25)=14.74
60  B(26)=15.29:B(27)=15.84:B(28)=16.39:B(29)=16.94:B(30)=17.5
65  B(31)=18.05:B(32)=18.6:B(33)=19.15:B(34)=19.7:B(35)=20.26
70  B(36)=20.81:B(37)=21.36:B(38)=21.91:B(39)=22.46:B(40)=23.02
75  B(41)=23.57:B(42)=24.12:B(43)=24.67:B(44)=25.22:B(45)=25.73
80  B(46)=26.33:B(47)=26.33:B(48)=27.43
85  L1=0:L2=0:L3=0:L4=0
90  T=0
105  FOR J=1,43
110  READ N(J)
120  T=N(J)+T
130  D(J)=B(J)/F
140  L1=L1+N(J)*D(J)
150  L2=L2+N(J)*(D(J))↑2
160  L3=L3+N(J)*(D(J))↑3
170  L4=L4+N(J)*(D(J))↑4
180  NEXT J
185  PRINT L1,L2,L3,L4
186  I1=L1
187  I2=L2
188  I3=L3
189  I4=L4
190  M1=I1/T
200  M2=SQR(I2/T)
210  M3=(I3/T)↑.3333
220  M4=I2/I1
230  M5=I3/I2
240  M6=I4/I3
250  FOR K=1,6
260  S(K)=0
270  FOR J=1,43
280  S(K)=S(K)+(D(J)-M(K))↑2
290  NEXT J
300  S(K)=S(K)/T
310  IF S(K)<.1E-31 THEN S(K)=0
320  NEXT K
330  PRINT "MAGNIFICATION FACTOR",F
340  FOR J=1,43
350  PRINT D(J),N(J)
360  NEXT J
370  PRINT "TOTAL NUMBER OF DROPS IS",T
380  PRINT "MEAN",TAB(18),"VALUE","STD. DEV."
390  PRINT "MLD",M1,S(1)
400  PRINT "MSD",M2,S(2)
410  PRINT "MVD",M3,S(3)
420  PRINT "LMD",M4,S(4)
430  PRINT "SMD",M5,S(5)
440  PRINT "VMD",M6,S(6)
450  NEXT C
460  STOP
500  DATA 3.5
510  DATA 5,13,19,23,35,39,36,21,23,20,17,27,15,9,9,3,1,3,1,4
520  DATA 3,1,1,0,1,0,1,0,1,0,0,0,0,0,0,0,0,0,0,0
530  DATA 0,0,0,0,0,0,0,3
540  DATA 7,29,45,52,63,41,32,24,23,17,19,7,5,3,6,3,3,1,2,1
550  DATA 0,1,0,0,0,0,0,0,0,0,0,0,0,0,0,0,0,0,0,0
560  DATA 0,0,0,0,0,0,0,3
570  DATA 14,34,46,66,74,47,22,20,12,5,5,6,9,1,4,5,0,2,2,0
580  DATA 0,0,1,0,0,0,0,0,0,0,0,0,0,0,0,0,0,0,0,0
590  DATA 0,0,0,0,0,0,0,3
600  DATA 15,53,63,65,33,23,20,16,6,7,4,4,5,2,5,0,0,1,1,0
610  DATA 0,0,0,0,0,0,0,0,0,0,0,0,0,0,0,0,0,0,0,0
620  DATA 0,0,0,0,0,0,1,2
630  DATA 40,77,62,53,41,12,15,6,12,6,7,4,2,4,1,2,1,0,0,0
640  DATA 0,0,0,0,0,0,0,0,0,0,0,0,0,0,0,0,0,0,0,0
650  DATA 1,0,0,1,0,2,0,0
660  DATA 58,38,31,34,24,11,16,3,11,7,5,6,2,2,2,1,0,0,0,0
670  DATA 0,1,0,0,0,0,0,0,0,0,0,0,0,0,0,0,0,0,0,0
680  DATA 0,0,1,0,0,0,0,0
```

```
?RUN
EXIT DROP SIZE ANALYSIS
  133.329        135.953        141.319        217.729
MAGNIFICATION FACTOR              10.5
      .141905       5
      .194236      13
      .246667      19
      .299048      23
      .352381      35
      .404762      39
      .457143      36
      .509524      21
      .561905      23
      .615238      20
      .667619      17
      .72          27
      .772381      15
      .824762       9
      .878095       9
      .930476       3
      .982857       1
     1.03524        3
     1.08762        1
     1.14095        4
     1.19333        3
     1.24571        1
     1.2931         1
     1.35048        0
     1.40381        1
     1.45619        0
     1.50857        1
     1.56095        0
     1.61333        1
     1.66667        0
     1.71905        0
     1.77143        0
     1.82381        0
     1.87619        0
     1.92952        0
     1.9819         0
     2.03429        0
     2.08667        0
     2.13905        0
     2.19238        0
     2.24476        0
     2.29714        0
     2.34952        0
     2.4019         0
     2.45524        0
     2.50762        0
     2.56           0
     2.61238        3
TOTAL NUMBER OF DROPS IS      344
MEAN                VALUE     STD. DEV.
MLD                  .547467      .333642
MSD                  .823367      .333642
MVD                  .743433      .333642
LMD                  .721917      .333642
SMD                 1.03943       .333642
VMD                 1.5467        .333642
```

A typical exit drop size analysis

APPENDIX C

VOIDAGE DETERMINATION BY DISPLACEMENT METHOD

Packing Thickness = 2.6×10^{-2} m

Datum Reading = 81.32×10^{-2} m

Volume Collected $m^3 \times 10^{-6}$	New Reading $m \times 10^{-2}$	Distance Drop $m \times 10^{-2}$
20	79.60	1.72
20	77.87	1.73
20	76.10	1.77
20	74.25	1.85
20	69.97	4.28

$\therefore$ Distance drop per 20×10^{-6} m^3 above the packing =

$$\frac{1.72 + 1.73 + 1.77 + 1.85}{4} = 1.78 \times 10^{-2} \text{ m}$$

$4.28 \times 10^{-2} - 2.6 \times 10^{-2} = 1.48 \times 10^{-2}$ m. This contains 16.63×10^{-6} m^3 water.

But water collected = 20×10^{-6} m^3

$\therefore$ Hold up of water = $20 \times 10^{-6} - 16.63 \times 10^{-6} = 3.37 \times 10^{-6}$ m^3.

Volume of packing = 30.77×10^{-6} m^3

$\therefore$ Packing Voidage $\varepsilon_1 = \frac{30.77 - 3.37}{30.77} = 0.891$

This was repeated three more times with the following results:

$\varepsilon_1 = 0.894$

$\varepsilon_1 = 0.888$

$\varepsilon_1 = 0.897$

$\therefore$ Average value of ε_1 was = 0.892.

APPENDIX D

PHYSICAL PROPERTIES OF LIQUID-LIQUID SYSTEM

The following physical properties have been taken from International Critical Tables, except interfacial tension which has been measured with a Du Nouy Tensiometer.

Interfacial Tension	Dynes cm^{-1}	Temperature ^{o}C
Toluene-Water	34.5	23
Viscosity	**Centipoise**	
Toluene	0.58	20.6
Density	**g cm^{-3}**	
Toluene	0.864	20

APPENDIX E

TYPICAL EXPERIMENTAL AND CALCULATED DATA

```
5   REM              " VOIDAGE CALCN. FROM KOZENY EQN."
6   DIM P(20),V(20),A(20),X(20),E(20),F(20)
10   READ L
15   M=.1E-01
20   G=980
30   D=.7E-03
40   K=(150*M*L)/(G*(D↑2))
50   FOR I=1,7
60   READ P(I),V(I)
70   P(I)=1033*P(I)/14.7
80   A(I)=P(I)/(K*V(I))
90   X(I)=.5
100   E(I)=.5*(1+X(I)↑2-(A(I)*X(I)↑3))
110   F(I)=E(I)-X(I)
120   IF F(I)<.1E-04 THEN 150
130   X(I)=E(I)
140   GOTO 100
150   NEXT I
152   PRINT TAB(1);"P.D.G/CM.SQ";TAB(14);"VEL.CM/SEC";TAB(33);"VOIDAGE"
154   FOR I=1,7
155   PRINT P(I),V(I),E(I)
160   NEXT I
170   STOP
180   DATA 2.6
190   DATA 2.9,1.023,3.7,1.25,4.5,1.477,5.5,1.833,6.7,2.23
200   DATA 7.5,2.5,8.3,2.77
```

Voidage determination using Blake - Kozeny equation

EFFECT OF SUPERFICIAL VELOCITY, INLET DROP SIZE AND PHASE RATIO ON TWO PHASE FLOW PRESSURE DROP

Packing Thickness = 4.4×10^{-2} m

Initial Voidage $\varepsilon_1 = 0.917$

Inlet Drop Size	26×10^{-6} m	27×10^{-6} m	38×10^{-6} m
Phase Ratio	3%	7%	3%
Superficial Velocity ms^{-1} $(\times 10^{-2})$	Pressure Drop $Nm^{-2} \times 10^{3}$		
1.023	34.47	34.13	34.20
1.25	43.44	43.09	43.09
1.477	53.78	53.22	53.36
1.833	67.57	67.22	67.22
2.23	80.67	80.67	80.67
2.5	91.70	91.01	91.36
2.77	99.97	97.90	99.63

EFFECT OF SUPERFICIAL VELOCITY ON HOLD-UP AND SATURATION DETERMINATIONS

Packing Thickness = 4.4×10^{-2} m

Initial Voidage ε_1 = 0.917

Phase Ratio = 3%

Superficial Velocity $ms^{-1}(\times 10^{-2})$	Calculated Voidage ε_a Kozeny	Hold-Up ϕ_H	Saturation S
1.023	0.870	0.566	0.051
1.250	0.867	0.602	0.054
1.477	0.866	0.614	0.056
1.833	0.866	0.614	0.056
2.230	0.867	0.602	0.054
2.500	0.866	0.614	0.056
2.770	0.868	0.590	0.053

$\therefore$ Average Hold-up = 0.600

$\therefore$ Average Saturation = 0.054

TYPICAL SINGLE PHASE FLOW CONDUCTIVITY VALUES AT DIFFERENT SUPERFICIAL VELOCITIES

Packing Thickness = 2.8×10^{-2} m

Initial Voidage ε_1 = 0.926

Superficial Velocity $ms^{-1}(\times 10^{-2})$	Conductivity Data at different planes in the bed $ohm^{-1} \times 10^{-6}$				
	1-2	2-3	3-4	4-5	5-6
0.599	6.3	6.0	6.0	6.8	6.9
0.994	6.3	6.0	6.0	6.7	6.8
1.667	6.3	6.0	5.9	6.8	6.9
2.164	6.3	6.0	6.0	6.8	6.9
2.982	6.3	6.0	6.0	6.8	6.9

VARIATION OF TWO PHASE FLOW CONDUCTIVITY VALUES WITH SUPERFICIAL VELOCITY

Packing Thickness = 2.8×10^{-2} m

Initial Voidage ε_1 = 0.926

Phase Ratio = 3%

Superficial Velocity $ms^{-1}\left(\times 10^{-2}\right)$	Conductivity Data at different planes in the bed $ohm^{-1} \times 10^{-6}$				
	1-2	2-3	3-4	4-5	5-6
1.023	3.9	4.0	4.0	4.5	4.2
1.477	4.1	4.4	4.4	4.8	4.4
1.833	4.4	4.6	4.6	5.1	4.5
2.23	4.5	4.7	4.7	5.2	4.6
2.77	4.9	5.0	5.0	5.6	4.8

APPENDIX F

ROTAMETER CALIBRATION CHARTS

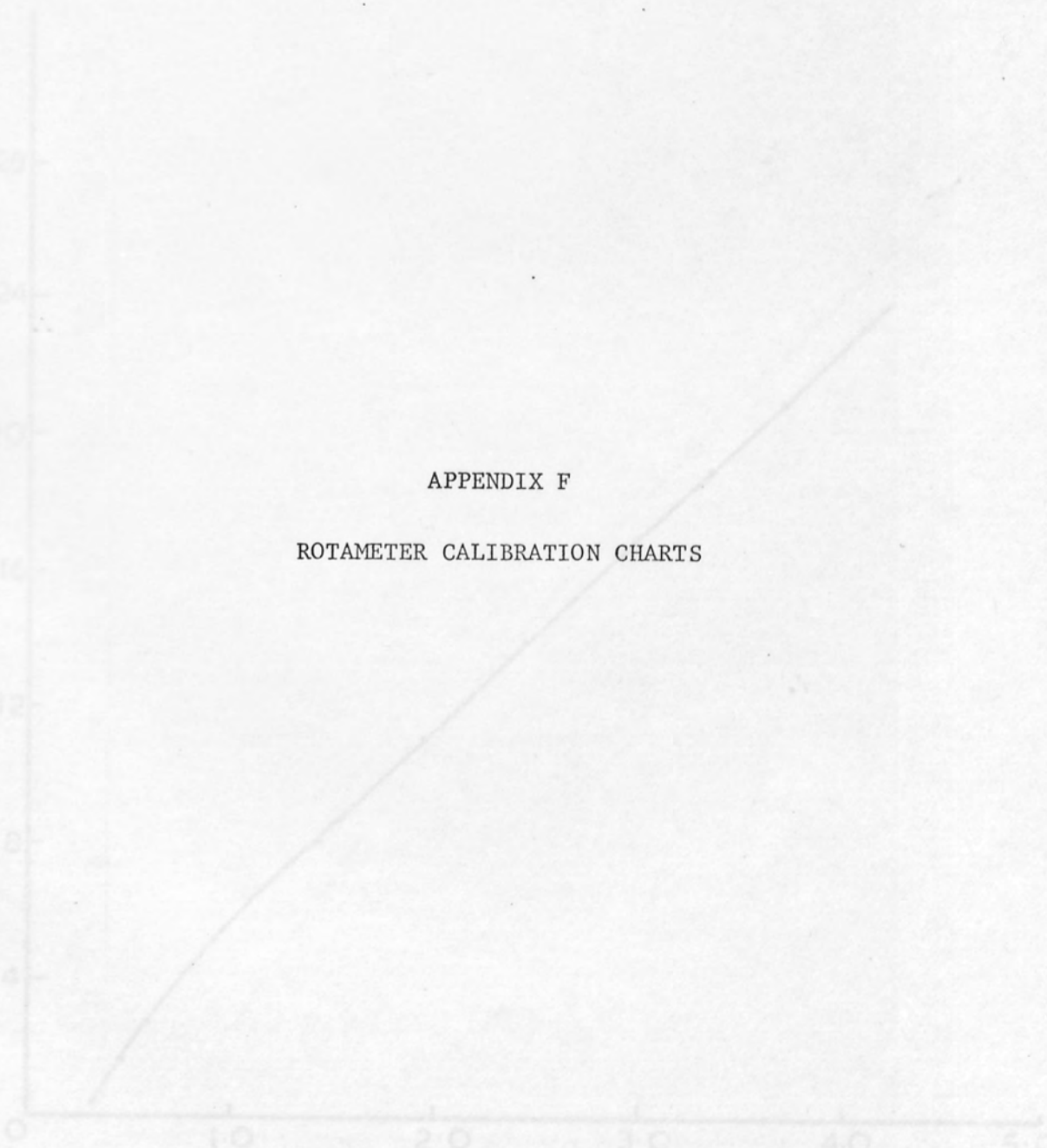

7A Calibration curve for toluene

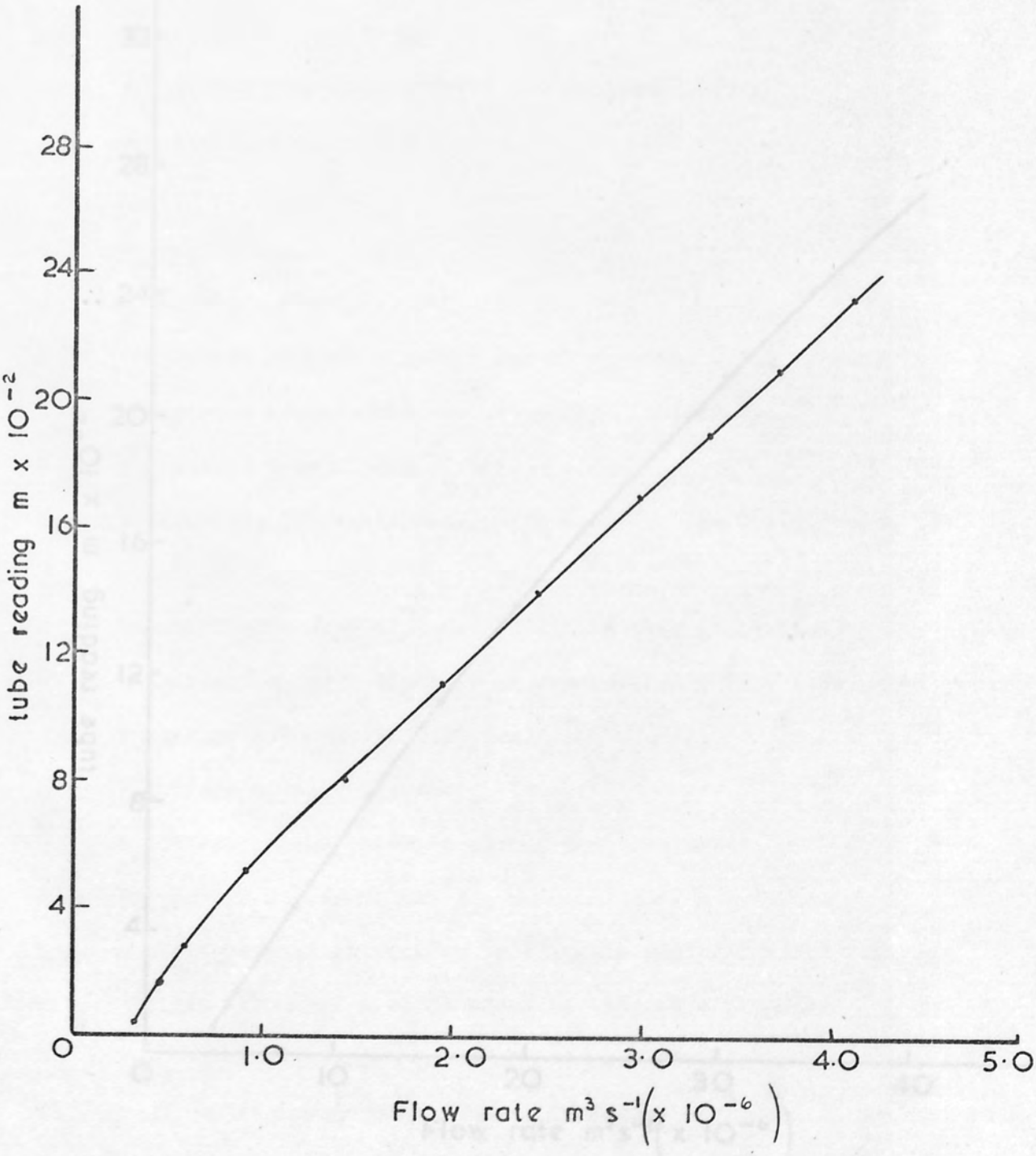

Fig. F.1

14 K Calibration curve for water

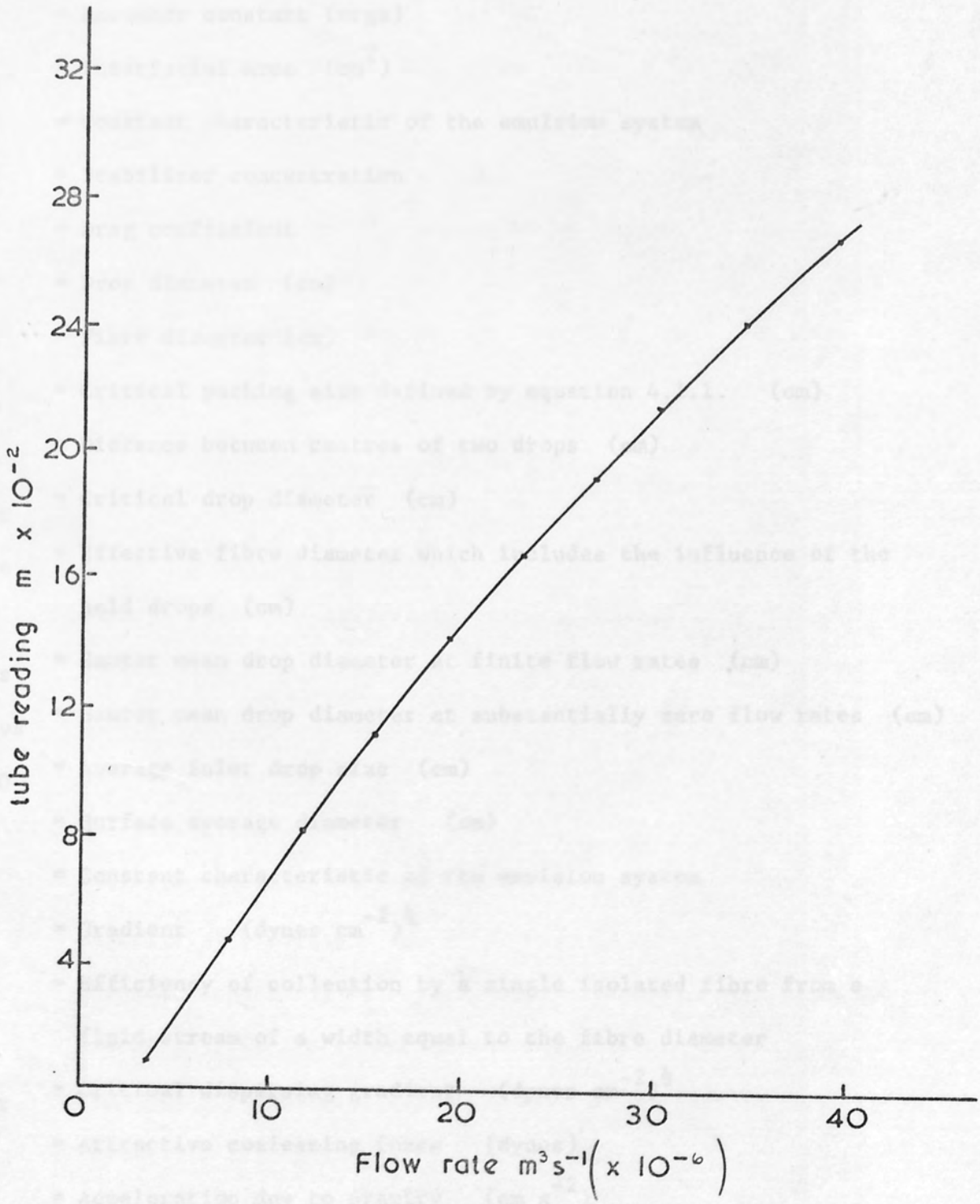

Fig. F. 2

NOMENCLATURE

Symbols have the following meanings except where specifically indicated in the text.

a = Orifice radius at the exit of a dispersed phase channel through the fibrous bed (cm)

A = Hammaker constant (ergs)

A_s = Interfacial area (cm^2)

b = Constant characteristic of the emulsion system

c_1 = Stabilizer concentration

C = Drag coefficient

d = Drop diameter (cm)

d_f = Fibre diameter (cm)

d_p = Critical packing size defined by equation 4.1.1. (cm)

d_o = Distance between centres of two drops (cm)

d_{cr} = Critical drop diameter (cm)

d_{fe} = Effective fibre diameter which includes the influence of the held drops (cm)

d_{vs} = Sauter mean drop diameter at finite flow rates (cm)

d^o_{vs} = Sauter mean drop diameter at substantially zero flow rates (cm)

d_{10} = Average inlet drop size (cm)

D_s = Surface average diameter (cm)

e = Constant characteristic of the emulsion system

E = Gradient $(\text{dynes cm}^{-2})^{\frac{1}{2}}$

E_s = Efficiency of collection by a single isolated fibre from a fluid stream of a width equal to the fibre diameter

E_{cr} = Critical dispersing gradient $(\text{dynes cm}^{-2})^{\frac{1}{2}}$

F' = Attractive coalescing force (dynes)

g = Acceleration due to gravity (cm s^{-2})

G = Shear rate (s^{-1})

h = Height of a packed section (cm)

H = Distance of rise or fall of the drop to the interface (cm)

k = Proportionality constant

k_B = Brownian diffusion coefficient ($cm^3\ s^{-1}$)

k_I = Interception coefficient ($cm^3\ s^{-1}$)

k_T = Turbulent coagulation coefficient ($cm^3\ s^{-1}$)

k' = Constant dependent upon packing material

K = Boltzman constant ($g\ cm\ s^{-2}\ ^oK$)

K' = Dielectric constant of the continuous phase

L = Fibrous bed thickness (cm)

n_i = Number of drops of diameter d_i

Δp = Pressure drop ($g\ cm^{-2}$)

r = Drop radius (cm)

R = Interception parameter $\frac{d}{d_f}$

Re = Reynolds number $\frac{\rho V' d_f}{\mu}$

S = Average degree of saturation (dimensionless)

t = Coalescence time (s)

t_m = Mean coalescence time (s)

$t_{\frac{1}{2}}$ = Half-life rest time (s)

T = System temperature (^oC)

U_o = Interstitial velocity ($cm\ s^{-1}$)

V = Superficial velocity ($cm\ s^{-1}$)

V'_{cr} = Critical separating velocity. The velocity at which the filter coefficient begins to decrease ($cm\ s^{-1}$)

V' = Dispersion superficial velocity ($cm\ s^{-1}$)

V_t = Terminal velocity in finite medium ($cm\ s^{-1}$)

V_o = Velocity of the dispersed phase relative to the continuous phase at substantially zero flow rates ($cm\ s^{-1}$)

X = Fractional hold up of dispersed phase (dimensionless)

GREEK LETTERS

α = Ratio of total number of particles striking a fibre to the total number approaching it

β = Fraction of collisions between drops that resulted in coalescence

λ = Filter coefficient (cm^{-1})

τ_d = Hydraulic diameter $\frac{\varepsilon d_f}{4(1-\varepsilon)}$ (cm)

σ = Interfacial tension (dynes cm^{-1})

σ_{12} = Interfacial tension between liquid 1 and liquid 2 (dynes cm^{-1})

σ_{13} = Surface tension of liquid 1 on solid 3 (dynes cm^{-1})

σ_{23} = Surface tension of liquid 2 on solid 3 (dynes cm^{-1})

ρ = Density $(g\ cm^{-3})$

$\Delta\rho$ = Density difference between the two phases $(g\ cm^{-3})$

μ = Viscosity $(g\ cm^{-1}\ s^{-1})$

ε = Packing voidage (dimensionless)

η_c = Overall coalescence efficiency

θ = Contact angle

ϕ_H = Dispersed phase hold up in a fibrous bed

ϕ' = Volume fraction of dispersed phase

ν = Kinematic viscosity $\frac{\mu_c}{\rho_c}$ $(cm^2\ s^{-1})$

SUBSCRIPTS

1 = Single phase flow

2 = Two phase flow

c = Continuous phase

d = Dispersed phase

REFERENCES

1. HAYES, J.H., HAYS, L.A. and WOOD, H.S. - Chem. Eng. Prog. - 45 (4) - 235 - (1949).

2. REDMON, O.C. - Chem. Eng. Prog. - 59 (9) - 87 - (1963).

3. PURCHAS, D.B., - 'Industrial Filtration of Liquids', - 2nd Edition - Leonard Hill - London (1971).

4. OSTERMAN, J.W., - Filt. and Sep. - March/April - 127 - (1966).

5. HILL, J.B., Ind. Eng. Chem. - 31 , 1361 - (1939).

6. MEISSNER, H.P. and CHERTOW, B. - Ind. Eng. Chem. 38 (8) - 856 -(1946).

7. WATERMAN, L.C. - Hydrocarbon Processing and Pet. Refiner - 44 (2) - 133 - (1965).

8. FARLEY, R. and VALENTIN, F.H.H., - A.I.Ch.E. Symp. Ser. No.1-39-(1965)

9. ATKINSON, E. and FRESHWATER, D.C. - Brit. Chem. Engrg. - Oct. - 554 - (1958).

10. SULLIVAN, F.E. - Chem. Eng. Prog. - 52 (2) - 83F - (1956).

11. WATERMAN, L.C. - Chem. Eng. Prog. - 61 (10) - 51 - (1965).

12. PHILLIPS, R.J. and NAPIER, H.G. - Pet. Refiner - 38 (2) - 151 -(1959).

13. PHILOON, W.C., KNEBEL, H.A., SOUKUP, J.A. and FAIN, P. - U.S. Atomic Energy Comm. MCW - 1461 - (1961).

14. DOYLE, A., MOFFETT, D.R. and VONNEGUT, B. - J. Coll. Sci. - 19 - 136 - (1964).

15. PEARCE, C.A.R. - Brit. J. Appl. Phys. - 5 - 136 - (1954).

16. LOWES, L. and TANNER, M.C., - Brit. Patent - 909, 485 - (1962).

17. JORDAN, G.V., Trans. A.S.M.E. - 77, 393 - (1955).

18. JORDAN, G.V. - Chem. Eng. Prog. - 61 (10) - 64 - (1965).

19. BURTIS, T.A. and KIRKBRIDE, C.G. - Trans. A.I.Ch.E. - 42 (3) - 413 - (1946).

20. SAREEN, S.S., et al - A.I.Ch.E.J. - 12 (6) - 1045 - (1966).

21. SHERONY, D.F., et al - Can.J. Chem. Engng. - 49 - 321 - (1971).

22. DOUGLAS, E. and ELLIOTT, I.G. - Trans. Inst. Marine Eng. 74 (5) - 164 - (1962).

23. DOUGLAS, E. - Brit. Patent - 972, 286 - (1960).

24. ZWICK, B.J. - The Oil Weekly - 101 - 107 - May 12th (1941).

25. GARRISON, M. and VAN LOENEN, W.F. - U.S. Patent - 1,947,709 -(1934).

26. BORDER, L.E. - Chem. Met. Eng. - 47 - 776 - (1940).

27. BARTLE, J.W. - Filt. and Sep.- 3 (5) - 404 - (1966).

28. GAMMON, H.M. - Filt and Sep.-July/Aug. - 409 - (1973).

29. KAISER, R., COLTON, C.K., MISKOLCZY, G. and MIR, L. - A.I.Ch.E. Symp., Series No.124 - 68 - 115 - (1971).

30. EUZEN, J.P. et al - I.S.E.C. - Lyon, France - Sept. (1974), - Session 5 - Paper 130.

31. FOWKES, F.M., ANDERSON, F.W. and BERGER, J.E. - Env. Sci. and Tech. - 4 (6) - 510 - (1970).

32. DAVIES, G.A. and JEFFREYS, G.V. - Filt. and Sep. - Sept/Oct. - 546 - (1970).

33. GILLESPIE, T. and RIDEAL, E.K. - Trans. Far. Soc. - 52 - 137 - (1956).

34. JEFFREYS, G.V. and HAWKSLEY, J.L. - J.Appl. Chem. - 12 - 329 - (1962).

35. HODGSON, T.D. - Ph.D. Thesis - Univ. Coll. of Wales - (1966).

36. LAWSON, G.B. - Ph.D. Thesis - Univ. of Manchester - (1967).

37. CHARLES, G.E. and MASON, S.G. - J. Coll.Sci. - 15 - 105 - (1960).

38. WARD, J.W. and COX, A.B. - Nature - 136 - 182 - (1935).

39. JEFFREYS, G.V. and HAWKSLEY, J.L. - A.I.Ch.E.J. - 11 - 413 -(1965).

40. COCKBAIN, E.G. and Mc ROBERTS, T.S. - J. Coll. Sci. - 8 - 440 - (1953).

41. WATANABE, T. and KUSUI, M. - Bull. Chem. Soc. Japan - 31 - 236 - (1958).

42. ELTON, G.A. and PICKNETT, R.G. - Proceedings of the 2nd International Congress on Surface Activity - Vol.1 - 288 - Butterworths - London - (1957).

43. NEILSON, L.E., WALL, R. and ADAMS, G. - J. Coll. Sci. - 13 - 441 - (1958).

44. KONNECKI, H.G. - Z. Phys. Chem. - 211 - 208 - (1959).

45. JEFFREYS, G.V. and LAWSON, G.B. - Trans. Inst. Chem. Eng. - 43 - T294 - (1965).

46. DAVIES, G.A., JEFFREYS, G.V. and SMITH, D.V. - I.S.E.C. - Hague - (1971).

47. SHEDULKO, A. - Z. Electrochem - 61 - 222 - (1957).

48. EDGE, R.M. and GREAVES, M. - I.Ch.E. Symp. Series No.26 -63 - (1967)

49. SMITH, D.V. - Ph.D. Thesis - University of Manchester - (1969).

50. CHAPPELEAR, D.C. - J. Coll. Sci. - 16 - 186 - (1961).

51. FRANKEL S.P. and MYSELS, K.S. - J.Phys. Chem. - 66 - 190 - (1962).

52. PRINCEN, H.M. - J. Coll. Sci. - 18 - 178 - (1963).

53. HARTLAND, S. - Chem. Eng. Sci. - 22 - 1675 - (1967).

54. CHARLES, G.E. and MASON, S.G. - J. Coll. Sci. - 15 - 236 - (1960).

55. ALLAK, A.M.A. - Ph.D. Thesis - Univ. of Aston in Birmingham - (1973).

56. SMITH, D.V. - M.Sc. Thesis - University of Manchester - (1966).

57. LANG, S.B. - Ph.D. Thesis - University of California - (1962).

58. LANG, S.B. and WILKE, G.R. - Ind. Eng. Chem. Fund. - 10 - 329 - (1971).

59. JEFFREYS, G.V. and DAVIES, G.A. - 'Recent Advances in Liquid-Liquid Extraction'. Edited by C. Hanson, Pergamon Press-Oxford, N.Y. etc. (1971).

60. ALLAN, R.S. and MASON, S.G. - Trans. Far. Soc. - 57 - 2027 - (1961).

61. BROWN, A.H. and HANSON, C. - Trans. Far. Soc. - 61 - 1754 - (1965).

62. HARTLAND, S. - Trans. Inst. Chem. Eng. - 46 - T275 - (1968).

63. HITIT, H.A. - Ph.D. Thesis - Univ. of Aston in Birmingham - (1972).

64. MAC CAY, G.D.M. and MASON, S.G. - J. Coll. Sci. 18 - 674 - (1963).

65. GROOTHIUS, H. and ZWIDERWEG, F.J. - Chem. Eng. Sci. - 12 - 288 - (1960).

66. MATEJICEK, J. et al - Coll. of Czechoslav. Chem. Commun. - 36 - 35 - (1971).

67. MATEJICEK, J. et al - Ibid - 36 - 1347 - (1971).

68. SCHEELE, G.F. and LENG, D.E. - Chem. Eng. Sci. - 26 - 1867 - (1971).

69. KINTNER, R.C. - Adv. in Chem. Eng. - 4 - 87 - (1968).

70. MAC CAY, G. and MASON, S.G. - Can. J. Chem. Eng. - 41 - 203 - (1963).

71. ROBINSON, J. and HARTLAND, S. - I.S.E.C. - Hague - (1971).

72. Mc AVOY, R.M. and KINTNER, R.C. - J. Coll. Sci. - 20 - 188 - (1965).

73. MURDOCH, P.G. and LENG, D.E. - Chem. Eng. Sci. - 26 - 1881 - (1971).

74. OSIPOW, L.I. - 'Surface Chemistry' - Reinhold Pub. Corp. - N.Y. -(1962).

75. BIKERMAN, J.J. - 'Physical Surfaces' - Academic Press - N.Y. -(1970).

76. HARKINS, W.D. - 'The Physical Chemistry of Surface Films' - Reinhold Pub. Corp. - New York - N.Y. - (1952).

77. BIKERMAN, J.J. - 'Proc. 2nd Int. Cong. Surface Activity' - Vol. 3 - Butterworth - London - (1957).

78. ZISMAN, W.A.- 'Contact Angle, Wettability and Adhesion' - Advances in Chem. Services - 43 - 1 - (1964).

79. PETHICA,B.A. and PETHICA, T.J.P. - 'Proc. 2nd Int. Cong. Surface Activity' - Vol. 3 - Butterworth - London (1957).

80. JOHNSON, R.E. - J. Phys. Chem. - 63 - 1655 - (1959).

81. LESTER, G.R. - J. Coll. Sci. - 16 - 315 - (1961).

82. ELLIOT, G.E.P. and RIDIFORD, A.C. - 'Contact Angles' - Recent Progress in Surface Science - Vol. 2 - (1964).

83. WENZEL, R.N. - Ind. Eng. Chem. - 28 - 988 - (1936).

84. WENZEL, R.N. - J. Phys. Chem. - 53 - 1466 - (1949).

85. BARTELL, F.E. and SHEPHARD, J.W. - J. Phys. Chem. - 57 - 455 - (1953).

86. BARTELL, F.E. and SHEPHARD, J.W. - Ibid - 57 - 458 - (1953).

87. FOX, H.W. and ZISMAN, W.A. - J. Coll. Sci. - 7 - 109 - (1952).

88. DAVIES, J.T. and RIDEAL, E.K. - 'Interfacial Phenomena' - Academic Press - New York - N.Y. - (1961).

89. FAWKES, F.M. and HARKINS, W.D. - J. Am. Chem. Soc. - 62 - 3372 - (1940).

90. PONTER, A.B. et al - Int. J. Heat Mass Transfer - 10 - 1633 - (1967).

91. BORGIN, K. - Norsk Skogind - 13 - 429 - (1959).

92. ELLIOT, T.A. and LEESE, L. - J. Chem. Soc. - 22 - 22 - (1957).

93. YARNOLD, G.D. and MASON, B.J. - Proc. Phys. Soc. - B62 - 125 - (1949).

94. ABLETT, R. - Phil. Mag. - 46 - 244 - (1923).

95. RAY, B.R. and BARTELL, F.E. - J. Phys. Chem. - 57 - 49 - (1953).

96. BASCOM, W.D. and SINGLETERRY, C.R. - J. Phys. Chem. 66 - 236 - (1962).

97. PEPER, H. and BERCH, J. - J. Phys. Chem. - 68 - 1586 - (1964).

98. JUMA, S.M. - M.Sc.Thesis - University of Manchester - (1969).

99. LEWIS, J.B., JONES I. and PRATT, H.R.C. - Trans. Inst. Chem. Eng. - 29 - 126 - (1951).

100. GAYLER, R. and PRATT, H.R.C. - Ibid - 31 - 69 - (1953).

101. GAYLER, R. and PRATT, H.R.C. - Ibid - 29 - 110 - (1951).

102. GAYLER, R., ROBERTS, N.W. and PRATT, H.R.C. - Ibid - 31 - 57 - (1953).

103. DELL, F.R. and PRATT, H.R.C. - Ibid - 29 - 270 - (1951).

104. DELL, F.R. and PRATT, H.R.C. - Ibid - 29 - 89 - (1951).

105. VOYUTSKII, S.S. et al - Dokl. Akad. Nauk. SSSR - 91 - 1155 - (1953) CA - 49 - 12053d - (1955).

106. VOYUTSKII, S.S. et al - Izv. Vyssk. Ucked Zaved. Khim. Technol - 2 - 1970 - (1958). CA - 52 - 19266a - (1958).

107. GUDSEN, R.C. - M.Sc. Thesis - I.I.T. - Chicago - (1964).

108. GRAHAM, R.J. - M.Sc. Thesis - University of California - Lawrence Radiation Laboratory - Berkeley - (1962).

109. THORNTON, J.D. and RAMSHAW, C. - Inst. Chem. Eng. Symp. Ser. - No. 26 - 80 - (1967).

110. THOMAS, R.J. and MUMFORD, C.J. - I.S.E.C. - Hague - Vol.1 - 400 - (1971).

111. THORNTON, J.D. - Ind. Chem. - Dec. - 632 - (1963).

112. THORNTON, J.D. and RAMSHAW, C. - Inst. Chem. Eng. Symp. Ser. - No. 26. - 73 - (1967).

113. LANGDON, W.M. et al - Environmental Sci. and Technology - 6 (10) - 905 - (1972).

114. BRECKENFIELD, R.R. and WILKE, C.R. - Chem. Eng. Prog. - 46 - 187 - (1950).

115. BLANDING, F.H. and ELGIN, J.C. - Trans. A.I. Ch.E. - 38 - 305 - (1942).

116. CRAWFORD, R. and WILKE, C.R. - Chem. Eng. Prog. -47 - 423 - (1951).

117. VINSON, C.G. and CHURCHILL, S.W. - The Chem. Eng. J. - 1 - 110 - (1970).

118. HONEYKAMP, J.R. and BURKHART, L.E. - Ind. Eng. Chem. Proc. Des. Dev. - 1 - 177 - (1962).

119. SLATTER M.A. - M.Sc. Thesis - University of Aston in Birmingham - (1968).

120. PIPPER, H. - Ph.D. Thesis - Univ. of Manchester (1965).

121. DAVIES, G.A. and JEFFREYS, G.V. - Filt. & Sep. - July/Aug. - 349 - (1969).

122. DAVIES, G.A., JEFFREYS, G.V. and AFZAL, M. - Brit. Chem. Eng. and Proc. Tech. - 17 (9) - 709 - (1972).

123. DAVIES, G.A., JEFFREYS, G.V., ALI, F. and AFZAL, M. - The Chem. Eng.- Oct. - 392 - (1972).

124. ALI, F. - Ph.D. Thesis - University of Manchester (1971).

125. DAVIES, G.A., JEFFREYS, G.V. and BAYLEY, D.P. - 'A New Packing For Gas - Liquid and Liquid-Liquid Separation Processes' - Knitmesh, Ltd. - (1971).

126. JACKSON, I.D. et al - Proc. ISEC - 1 - 567 - (1974).

127. WILKINSON, D. - Ph.D. Thesis - University of Aston in Birmingham - (1974).

128. HAZLETT, R.N. - I.E.C. Fund - 8 (4) - 625 - (1969).

129. LANGDON, W.M. et al - Petro/Chem. Engng. - Nov. - 34 - (1963).

130. LINDENHOFEN, H.E. - Filt. and Sep. - July/Aug. - 317 - (1968).

131. LINDENHOFEN, H.E. - Filt. and Sep. - Sept/Oct. - 567 - (1969).

132. HAZLETT, R.N. - I.E.C. Fund - 8 (4) - 633 - (1969).

133. CURTIS, B.G. - Filt. and Sep. - Jan/Feb. - 35 - (1964).

134. HAZLETT, R.N. et al - Filt. and Sep. - July/Aug. - 456 - (1972).

135. BITTEN, J.F. et al - J. Coll. Int. Sci. - 37 (2) - 312 - (1971).

136. BROWN, R. - 'A Microphotographic Study of Water Coalescence' - U.S. Army Film RF 1916 - Mobility Eng. Research and Development Command - Fort Belvoir - Virginia - (1966).

137. SHERONY, D.F. - M.Sc. Thesis - I.I.T. - Chicago - (1967).

138. LANGMUIR, I. - OSRD Rept 865 - Sept. - (1942).

139. SPIELMAN, L.A. - Ph.D. Thesis - Univ. of California- Berkeley - California - (1968).

140. BITTEN, J.F. - J. Coll. Int. Sci. - 33 (2) - 265 - (1970).

141. SPIELMAN, L.A. and GOREN, S.L. - Ind. Eng. Chem. - 62 (10) - 10 - (1970).

142. SPIELMAN, L.A. and GOREN, S.L. - Ind. Eng. Chem. Fund - 11 (1) - 66 - (1972).

143. SPIELMAN, L.A. and GOREN, S.L. - Ind. Eng. Chem. Fund - 11 (1) - 73 - (1972).

144. SHERONY, D.F. et al - Can. J. Chem. Eng. - 49 - 314 - (1971).

145. ROSENFELD, J.I. and WASAN, D.T. - Can. J. Chem. Eng. - 52 - 3 - (1974).

146. ROSENFELD, J.I. - Ph.D. Thesis - I.I.T. - Chicago - (1973).

147. SPIELMAN, L.A. and GOREN, S.L. - Env. Sci. Tech. - 4 (2) - 135 - (1970).

148. WASAN, D.T. et al - I.S.E.C. - Lyon - France - (1974).

149. CORDES, R.A. - Ph.D. Thesis - University of California - Berkely - (1972).

150. VINSON, C.G. - Ph.D. Thesis - University of Michigan - Ann Arbor - (1965).

151. SHERONY, D.F. - Ph.D. Thesis - I.I.T. - Chicago - (1969).

152. ROSE, P.R. - M.Sc. Thesis - I.I.T. - Chicago - (1963).

153. HUANG, W.S. - Ph.D. Thesis - I.I.T. - Chicago - (1968).

154. POLICHRONAKIS, C. - M.Sc. Thesis - University of Aston in Birmingham - (1972).

155. DAVIES, R. - Ind. Eng. Chem. - 62 (12) - 87 - (1970).

156. LLOYD, N.E. - J. Coll. Sci. - 14 - 441 - (1959).

157. WEISSBERGER, A. - 'Techniques of Chemistry' - Vol.1 - Pt. IIIA - (Wiley Interscience - (1972).

158. COULTER ELECTRONICS, LTD. - Coulter Counter Model ZB - Instruction Manual - (1975) - Coulter Electronics Ltd., Dunstable, England.

159. ZINKY, W.R. - Ann. N.Y. Acad. Sci. - 158 - 741 - (1969).

160. IRANI, R.R. and CALLIS, C.F. - 'Particle Size : Measurement, Interpretation and Application' - John Wiley - (1963).

161. KAHN, A. and LEWIS, D.R. - J. Phys. Chem. - 58 - 801 - (1954).

162. BENOIT, H. - Ann. Phys. - 6 - 561 - (1951).

163. O'KONSKI, C.T. and ZIMM, B. - Science - 11 - 113 - (1950).

164. MATTHEWS, B.A. - Can. J. Phar. Soc. - 6 (2) - 89 - (1971).

165. KUBITCHEK, H.E. - Research (London) - 13 - 128 - (1960).

166. ALLEN, T. - Proc. Particle Size Analysis Conf. - Loughborough - Society for Analytical Chem. - London - p.110 - (1967).

167. AUSTIN, D. - Unpublished Work - University of Aston in Birmingham.

168. BRUSSET, H. and DONATI, J.R. - J.Appl. Crystallogr. - 2 - 55 - (1969).

169. PILKINGTON RESEARCH AND DEVELOPMENT (Glass Fibre Technology) - Private Communication - (1973).

170. MUMFORD, C.J. - Ph.D. Thesis - University of Aston in Birmingham - (1970).

171. BIRD, R., STEWART, W. and LIGHTFOOT, E.N. - 'Transport Phenomena' - J. Wiley and Sons - New York - (1960).

172. CHIU, K.F. - Chemical Engineering Report - University of Aston in Birmingham - (1975).

173. CARMEN, P.C. - 'Flow of Gases Through Porous Media' - Butterworth Scientific Pub. - London - (1956).

174. RIDGWAY, K. and TARBUCK, K.J. - Brit. Chem. Eng - 12 - 385 - (1967).

175. CORDES, R.A. - M.Sc. Thesis - University of California - Berkeley - Calif. - (1968).

176. MARTIN, M. et al - Geophysics - 3 - 258 - (1938).

177. CHUNG, W.O. - Chemical Engineering Report - University of Aston in Birmingham - (1975).

178. BEAR, J. - 'Dynamics of Fluids in Porous Media' - American Elsevier Environmental Science Series - N.Y. - (1972).

179. VAN MEURS, P. - I. Petrol Technol. - 210 - 295 - (1957).

180. LEVICK, V.G. - 'Physicochemical Hydrodynamics' - Prentice Hall - Englewood Cliffs - N.J. - (1962).

181. HELLER, J.P. - Rev. Sci. Instrum. - 30 - 1056 - (1959).

182. RYAN, J.T. - Ph.D. Thesis - University of Missouri - (1966).

183. SCHEELE, G.F. and MEISTER, B.J. - A.I. Ch.E. J. - 14 (1) -9 - (1968).